

Optimising Light Source Spectrum to Reduce the Energy Absorbed by Objects

Dorukalp Durmus

A thesis submitted in fulfilment of the requirements for the degree of Doctor of Philosophy

Sydney School of Architecture, Design and Planning

The University of Sydney

2018

I certify that the intellectual content of this thesis is the product of my own work, that all sources and assistance received in its preparation have been acknowledged and that the thesis has not been submitted for any other degree or purpose.

.....
Dorukalp Durmus

Abstract

Light is used to illuminate objects in the built environment. Humans can only observe light reflected from an object. However, light absorbed by an object turns into heat and does not contribute to visibility. Since the spectral output of the new lighting technologies can be tuned, it is possible to imagine a lighting system that detects the colours of objects and emits customised light to minimise the absorbed energy. Several previous optimisation studies investigated the use of narrowband light sources to maximise the luminous efficacy and colour quality of a light source. While these studies aimed to tune a white light source for general use, the lighting system proposed here minimises the energy consumed by lighting by detecting the individual colours of objects and emitting customised light onto each coloured part of the object. This thesis investigates the feasibility of absorption-minimising light source spectra and their impact on the colour appearance of objects and energy consumption.

Two computational studies (papers 1 and 2) were undertaken to form the theoretical basis of the absorption-minimising light source spectra. Computational simulations show that the theoretical single-peak test light sources can lower the energy consumption up to around 38 % to 62 %, and double-peak test light sources can result in energy savings of up to 71 %, without causing colour shifts in the appearance of test samples. In these studies, standardised reference illuminants, theoretical test spectra and coloured test samples were used. These studies are followed by the empirical evidence collected from two psychophysical experiments. Data from the experiments show that observers find the colour appearance of objects equally natural and attractive under spectrally optimised test light sources and reference white light sources. An increased colour difference, to a certain extent, is found acceptable, which allows even higher energy savings. However, the translucent nature of some objects may negatively affect the results. Future studies will investigate the spatial resolution needed to implement such a lighting system and employ object colour hue groupings, instead of single colours.

“Making workable choices occurs in a crucible of informative mistakes. Thus Intelligence accepts fallibility. And when absolute (infallible) choices are not known, Intelligence takes chance with limited data in an arena where mistakes are not only possible but also necessary.”

Darwi Odrade – Dune

∞

“The more we learn about the world, and the deeper our learning, the more conscious, specific, and articulate will be our knowledge of what we do not know, our knowledge of our ignorance.”

Karl Popper

Acknowledgments

I am greatly indebted to my supervisor Wendy Davis for her guidance, support, patience and kindness. She is an exceptional mentor and a true inspiration.

I would also like to thank John Attlesey, Violeta Birks, Densil Cabrera, Catherine Donnelley, Bettina Easton, Jo Elliot, Shayani Fernando, Wenye Hu, Paul Jones, Martyna Mokrzecka, and Dean Scott. I am also grateful to Cherry Russell, who provided proofreading services.

This PhD was partially supported by an Australian Postgraduate Award, administered by The University of Sydney on behalf of the Department of Education and Training.

Table of contents

Abstract	I
Acknowledgments	III
List of figures	V
List of publications	VI
Authorship attribution statement	VI
1 INTRODUCTION	1
2 BACKGROUND	4
2.1 Colour	5
2.1.1 Light	5
2.1.2 Optical properties of surfaces	15
2.1.3 Colour vision	16
2.2 Colorimetry	25
2.2.1 Tristimulus values	25
2.2.2 Chromaticity	26
2.2.3 Object colorimetry	28
2.2.4 Colour rendering	29
3 LITERATURE REVIEW	31
3.1 Colour quality metrics	32
3.2 Spectral design	34
3.2.1 Efficacy and colour rendering	34
3.2.2 Spectral optimisation	35
3.2.3 Application specific optimisation	36
3.3 Energy efficiency in the built environment	40
3.4 Sensors and projection systems	41
3.4.1 Reflectance estimation	41
3.4.2 Projection systems	42
4 OPTIMISING LIGHT SOURCE SPECTRUM FOR OBJECT REFLECTANCE	44
5 COLOUR DIFFERENCE AND ENERGY CONSUMPTION OF ABSORPTION-MINIMIZING SPECTRAL POWER DISTRIBUTIONS	54
6 OBJECT COLOUR NATURALNESS AND ATTRACTIVENESS WITH SPECTRALLY OPTIMIZED ILLUMINATION	59
7 CONCLUSIONS	72
REFERENCES	74
APPENDICES	87
Appendix A: Ethics approval	88
Appendix B: Conference paper	91

List of figures

Fig. 1. The concept drawing of the absorption minimising lighting system.....	2
Fig. 2. The electromagnetic spectrum.....	5
Fig. 3. The spectral power distribution of Planckian radiators at various temperatures.....	9
Fig. 4. The spectral power distribution of an incandescent lamp.....	9
Fig. 5. The spectral power distribution of a tri-phosphor fluorescent lamp.....	10
Fig. 6. The spectral power distribution of a high-pressure sodium lamp.....	11
Fig. 7. The spectral power distribution of a low-pressure sodium lamp.....	11
Fig. 8. The spectral power distribution of a metal halide lamp.....	12
Fig. 9. Light emission mechanism of p-n junction diode.....	12
Fig. 10. The spectral power distribution of a RGB and phosphor-coated LED.....	13
Fig. 11. The spectral power distribution of daylight at 5700 K and a blackbody radiator at the same temperature.....	14
Fig. 12. The CIE illuminants.....	15
Fig. 13. The spectral reflectance factor of lemon and a Nivea Creme container.....	16
Fig. 14. The layers of the retina.....	17
Fig. 15. The distribution of rods and cones as a function of angle from fovea.....	18
Fig. 16. The cross-section of the human eye.....	18
Fig. 17. The spectral luminous efficiency functions.....	19
Fig. 18. Modern colour vision theory.....	21
Fig. 19. Additive colour mixing.....	22
Fig. 20. Additive and subtractive colour mixing.....	22
Fig. 21. Subtractive colour mixing.....	23
Fig. 22. Perceptual attributes of colour represented in a three-dimensional space.....	24
Fig. 23. The CIE colour matching functions for the 2° standard observer.....	26
Fig. 24. The CIE 1931 (x, y) chromaticity diagram.....	27
Fig. 25. The CRI colour samples.....	30

List of publications

Chapter 4

Durmus, D., & Davis, W. (2015b). Optimising light source spectrum for object reflectance. *Optics Express*, 23(11), A456-A464.

Chapter 5

Durmus, D., & Davis, W. (2015a). *Colour difference and energy consumption of absorption-minimizing spectral power distributions*. Presented at Asia-Pacific Lighting Systems Workshop. Sydney, Australia.

Chapter 6

Durmus, D., & Davis, W. (2017). Object color naturalness and attractiveness with spectrally optimized illumination. *Optics Express*, 25(11), 12839-12850.

Authorship attribution statement

As the co-author of the papers mentioned above, I confirm that Dorukalp Durmus's contribution to these papers is consistent with him being named first author. The candidate's contributions include the design and execution of the experiments, data collection and analysis, and drafting of manuscripts. As the co-author, I contributed to the experimental design and concept, as well as the review and editing of the manuscripts.

.....
Wendy Davis

1 INTRODUCTION

Electric lighting significantly contributes to the energy consumption in buildings. According to the International Energy Agency (IEA), around 18 % of the total electricity consumption in the world is accounted for by lighting (2014). The energy used for illuminating objects costs around USD 455 billion a year worldwide (S. T. Tan, Sun, Demir, & DenBaars, 2012). The high costs of lighting and increasing need for sustainable design practices have encouraged the investigation of new technologies to reduce the energy consumed by lighting products. One of the key developments in the lighting industry was the introduction of solid-state lighting (SSL) devices. These light generating semiconductors offer unprecedented control over the output of a light source, which enables higher efficiency and lighting quality.

Light is used in architectural spaces to allow occupants to see illuminated objects. Although higher efficiency is desirable for a lighting product, the parameters affecting the perception of the built environment, in particular the colour appearance of objects under a light source, is crucial for long-term user acceptance and success of a lighting technology. For example, conventional fluorescent lamps, first introduced in the 1930s, and compact fluorescent lamps, introduced in the 1970s, did not gain widespread public acceptance due to the poor colour quality of the earlier products (Sandahl, Gilbride, Ledbetter, Steward, & Calwell, 2006). The association of earlier fluorescent lamps with poor visual performance caused user dissatisfaction and some lamps were even removed, even though fluorescent lamps were almost four times more efficient than the incandescent bulbs they were replacing (Sandahl et al., 2006). Today, it is widely accepted that energy efficiency alone is not sufficient for the successful adoption of a lighting technology.

New lighting technologies, such as the SSL, can be tuned to achieve increased light output, high efficiency or good colour quality. Computational and experimental techniques have been extensively applied to the study of light source optimisation, especially in regards to colour quality and energy efficiency. However, these studies were largely concerned with the properties of light sources rather than the perception of individual objects. Most of the previous optimisation studies used a set of colour samples to represent objects in the real world and optimised the light source spectrum for that specific colour set. Since the efficacy of a light source is inversely related to its colour quality (Davis & Ohno, 2009), in these studies, the efficacy was increased at the expense of the lighting quality, or vice versa.

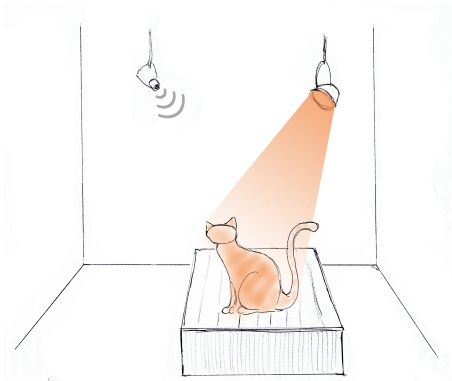


Fig. 1. A concept drawing of the proposed absorption-minimising lighting system is shown in the figure. The sensor (left upper corner) detects the colour(s) of the orange cat and the projection system (right upper corner) emits spectrally optimised light onto the cat.

In contrast, this thesis investigates the optimisation of the light source spectrum for object reflectance, which enables a reduction in energy consumption while maintaining the colour appearance of objects. This reduction is possible due to the principles that govern the optical surface properties of objects and human colour vision. Objects reflect, transmit or absorb the incident light on their surface. While the light reflected from the surface of an object is perceived by the observer, the absorbed light turns into heat and does not contribute to visibility. The absorbed light can be considered wasted for illumination purposes. Since the spectral output of SSL devices can be tuned, it is plausible to imagine a lighting system where sensors detect the colour of objects in the built environment and luminaires emit customised light to each distinct coloured part of the object. A possible implementation of this lighting system is shown in Fig. 1. An orange cat predominantly reflects middle and long wavelengths and absorbs most of the energy

emitted in the short wavelengths. The proposed lighting system first detects the optical surface properties of the cat through sensors and then emits customised light to the orange cat to reduce the absorption, while maintaining her colour appearance.

This thesis aims to quantify reductions in energy consumption that can be achieved when light absorption is minimised without causing deterioration of the colour appearance of objects. Chapter 2 summarises existing knowledge relevant to this thesis. In particular, it describes the relevant optical principles and human colour vision.

Chapter 3 systemically reviews the literature that considers the colour quality and optimisation of light sources, lighting and energy efficiency in buildings, and the current state of sensing and projection technologies. Since the quantitative analysis of absorption minimisation through optimisation has not been investigated previously, the thesis then introduces two computational simulations underpinning the theoretical framework (Chapters 4 and 5), followed by two psychophysical experiments testing the feasibility of the proposed lighting system (Chapter 6). The papers in Chapters 4 and 6 were published in *Optics Express*, while the study in Chapter 5 is a peer-reviewed conference paper.

The paper in Chapter 4 presents the analysis of the spectral properties of the absorption-minimising spectra when the appearance of predefined colour samples under standard illuminants and theoretical test light spectra were investigated. During the analysis of the computational simulations, which involved iteratively developed theoretical spectra, only the single-peak test light sources that resulted in the highest energy savings and lowest colour shifts were investigated.

A logical extension of the research was testing other spectral characteristics, such as an additional peak in the spectrum. In Chapter 5, the characteristics of double-peak test spectra and relative energy consumptions are shown.

Chapter 6 describes the real-life implementation of the proposed lighting system, which includes real objects and commercially available light sources. The published findings from the analysis of two psychophysical experiments are presented in this chapter. Participants' judgments of the colour appearance of the real objects with regards to their naturalness and attractiveness under the optimised test spectra and reference white light sources are also discussed. The optimised test sources were taken from the previous computational simulations and generated in the lighting lab, while the reference light source was a commercially available white light emitting diode (LED).

Chapter 7 summarises the results, discusses the limitations of the thesis and makes recommendations for future research.

2 BACKGROUND

This chapter summarises the background knowledge on which this thesis is based. This is drawn from the disciplines of physics (optics), physiology (human vision) and psychology. The themes discussed here, such as the spectral properties of light sources, human colour vision and colorimetry, are particularly relevant to the proposed lighting system discussed in this thesis.

2.1 Colour

2.1.1 Light

An electromagnetic wave is a form of electromagnetic radiation that propagates radiant energy from a source through space. Electromagnetic waves can be described by their frequency f or wavelength λ . The unit of frequency in the International System of Units (SI, abbreviated from its French name *Le Système International d'Unités*) is hertz (Hz) and the unit of wavelength is the metre (m). The frequency of a wave, the number of waveforms passing a fixed position in one second, is inversely related to its wavelength

$$f = \frac{c}{\lambda} \quad (1)$$

where $c = 299,792,458$ m/s, which is the speed of light in the vacuum (P. J. Mohr, Taylor, & Newell, 2012) and considered a universal physical constant (DeCusatis, 1997). The electromagnetic spectrum consists of many wavelengths, ranging from very low-frequency radio waves to high-frequency X-rays, as shown in Fig. 2 (Reitz, Milford, & Christy, 2008). Visible electromagnetic radiation includes all the radiation that falls within the detection limit of the human visual system, regardless of its effect on the visibility of a stimulus (Agoston, 1979). Distinctively, light is the visible radiant power that causes awareness in the observer by means of visual perception (Agoston, 1979).

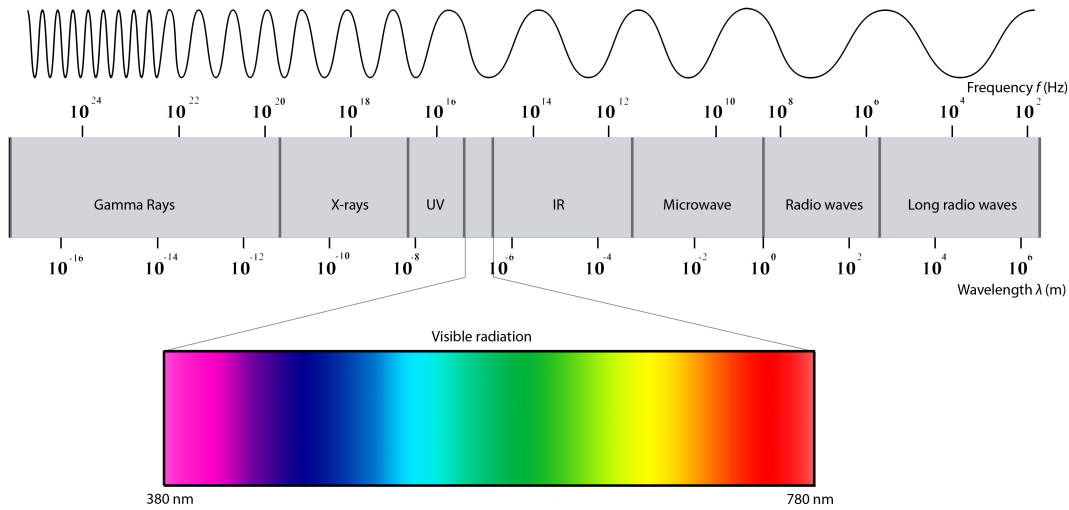


Fig. 2. Visible radiation, which ranges approximately between 380 nm and 780 nm, is part of the electromagnetic spectrum. The colours of the spectrum shown in this figure do not align perfectly with the defined borders presented in Table 1.

The spectral range of visible radiation, which is approximately between 380 nm and 780 nm, and the adjacent regions, ultraviolet (UV) and infrared (IR) radiation, are given in Table 1. The precise boundaries of visible radiation are not completely established due to variations in the impact of the radiant power at the edges and observers' responsivity in the visibility range (Sloney, 2016). The lower limit of visible radiation is considered to be between 360 nm and 400 nm and the upper limit is around 760 nm to 830 nm (Sloney, 2016). However, under laboratory conditions, the human eye can detect even longer wavelengths, up to 1064 nm (Sloney, Wangemann, Franks, & Wolbarsht, 1976). The range of visible radiation in the shorter wavelengths can extend to 310 nm for young

observers (Dash & Dash, 2011; Lynch & Livingston, 2001) and aphakic observers, who have increased sensitivity in the UV region due to the surgical removal of their lens (K. E. W. P. Tan, 1971).

Table 1. Spectral Range of Visible Electromagnetic Radiation and Adjacent Regions, between 100 nm and 10,000 nm (DeCusatis, 1997; Malacara, 2011).

Spectral Region	Subregion	Wavelength range (nm)
Ultraviolet	UV-C	100 to 280
	UV-B	280 to 315
	UV-A	315 to 380
Visible	Violet	380 to 430
	Blue	430 to 500
	Cyan	500 to 520
	Green	520 to 565
	Yellow	565 to 580
	Orange	580 to 625
	Red	625 to 780
	IR-A, Near IR (NIR)	780 to 1,400
Infrared	IR-B	1,400 to 3,000
	IR-C, Far IR	3,000 to 10,000

Traditionally, visible radiation is divided into seven regions, as shown in Table 1. In 1666, Isaac Newton used a glass prism to diffract white light into its components. Newton called this band of continuous colours the *spectrum*, meaning “appearance” or “apparition” in Latin (Hunt & Pointer, 2011). He acknowledged that there was a gradual transition of colours, but nonetheless divided the spectrum into seven parts (red, orange, yellow, green, blue, indigo and violet), linking it to the seven notes of the major musical scale and the mystical power of the number seven in Ancient Greece (McLaren, 1985; Newton, 1704). In modern representations of the spectrum, however, indigo is often omitted due to its indistinguishability from blue and violet (Hunt & Pointer, 2011). The spectrally pure colours (or monochromatic colours), which can be produced by a single wavelength only, are not distributed homogeneously along the visible spectrum as they are often graphically depicted. For example, red and blue each covers a wider range than yellow, due to the lack of homogeneity in the sensitivity of the human visual system.

The spectrally pure colours are not the only colours that exist. Newton’s colour wheel included secondary and complementary colours, as well as the pure spectral colours. Newton obtained new colours by diluting pure colours with white, increasing or reducing their intensity, or by mixing two colours (Malacara, 2011). In addition, a mixture of two spectral colours can match the appearance of another spectrally pure colour due to the overlapping nature of the sensitivity of the three types of cone cells, which are responsible for colour vision. For example, monochromatic orange light of 600 nm can be produced by mixing monochromatic yellow light of a 580 nm and monochromatic red light of a 700 nm, although neither yellow nor red monochromatic light contains an orange component (Malacara, 2011). Consequently, the spectral components of the light source can be measured and defined mathematically to allow precise colour communication.

2.1.1.1 Radiometric and photometric units

Radiometry is the measurement of electromagnetic radiation, which characterises the radiant power and the geometry of its propagation through space. Similarly, photometry is the measurement of the electromagnetic radiation, which takes only the visible radiation into account. While radiometry quantifies the absolute power, photometry weighs the radiant power with the *luminous efficiency function*, the spectral sensitivity of the human visual system.

The radiant flux (radiant power), Φ_e , is the radiant energy \mathcal{E}_e per unit time t propagated from a source,

$$\Phi_e = \frac{d\mathcal{E}_e}{dt} \quad (\text{DeCusatis, 1997}). \quad (2)$$

The unit of radiant flux is the watt (W). The photometric unit corresponding to the radiant flux is the luminous flux Φ_v . It has the unit of lumen (lm),

$$\Phi_v = K_m \int_{380}^{830} \Phi_{e,\lambda} V(\lambda) d\lambda \quad (3)$$

where the spectral luminous efficiency function $V(\lambda)$ represents the human visual response to light intensity under photopic conditions (DeCusatis, 1997). The constant $K_m = 683 \text{ lm/W}$ links radiometric and physiological quantities, so that a monochromatic light source of 555 nm, the wavelength at which $V(\lambda)$ peaks, with 1 W radiant flux has a luminous flux of 683 lm (DeCusatis, 1997).

Radiant intensity, I_e , is the radiant flux per unit solid angle Ω in a given direction,

$$I_e = \frac{d\Phi_e}{d\Omega} \quad (4)$$

where the solid angle is the ratio of a portion of the surface area of a sphere to the square of the radius of the same sphere (DeCusatis, 1997). The solid angle is dimensionless, and its unit is steradian (sr). Luminous intensity, I_v , is the photometric quantity for intensity

$$I_v = K_m \int_{380}^{830} I_{e,\lambda} V(\lambda) d\lambda \quad (5)$$

and its unit, candela (cd), is one of the base SI units (DeCusatis, 1997). In 1979, candela was redefined by *Conférence Générale des Poids et Mesures* (CGPM) as “the luminous intensity, in a given direction of a source that emits monochromatic radiation of frequency 540×10^{12} Hz, and that has a radiant intensity in that direction of $1/683 \text{ W/sr}$ ” (BIPM, 1979). The frequency of 540×10^{12} Hz corresponds to a wavelength of 555.016 nm in standard air (Ohno, 1999).

Radiance, L_e , is the radiant flux per unit solid angle per unit projected area of a surface in a given direction at a given point

$$L_e = \frac{d^2\Phi_e}{d\Omega_S dA_S \cos \theta} \quad (6)$$

where dA_S is the area of the source containing the point, $d\Omega_S$ is the solid angle, and θ is the angle between the normal of the surface dA_S and the direction of measurement (DeCusatis, 1997).

Luminance, L_v , is the photometric equivalent of radiance

$$L_v = K_m \int_{380}^{830} L_{e,\lambda} V(\lambda) d\lambda \quad (7)$$

where the SI unit for luminance is candela per square metre (cd/m^2) (DeCusatis, 1997).

The radiant flux received per unit area is called irradiance, E_e . Similarly, the luminous flux per unit area is called illuminance, E_v . Irradiance is given by

$$E_e = \frac{d\Phi_S}{dA_D} \quad (8)$$

where subscript S indicates the source, and subscript D denotes the detector, and the luminous flux incident on a surface is

$$E_v = \frac{\Phi}{A} = \frac{I\Omega}{r^2\Omega} = \frac{I}{r^2} \quad (9)$$

where $\Phi = \Omega I$ from Eq. (4), and r is the distance between the point and the surface (DeCusatis, 1997). The unit for illuminance is lux (lx).

2.1.1.2 Luminous efficacy

The ratio of the luminous flux emitted by a light source to the power consumed by the source is called the luminous efficacy of a source (or luminous efficacy), η_v (CIE, 2011). Luminous efficacy

$$\eta_v = \eta_e K \quad (10)$$

is the product of the radiant efficiency of the source η_e and the luminous efficacy of radiation (LER), K (CIE, 2011; Ohno, 2004). The radiant efficiency of a source is “the ratio of the radiant flux of the emitted radiation to the power consumed by the source” (CIE, 2011), and the LER is the ratio of luminous flux to radiant flux

$$K = \frac{K_m \int_{\lambda} V(\lambda) S(\lambda) d\lambda}{\int_{\lambda} S(\lambda) d\lambda} \quad (11)$$

with a unit of lumens per watt (lm/W) and $S(\lambda)$ is the spectral power emitted by a light source (CIE, 2011; Ohno, 2004).

2.1.1.3 Spectral power distribution

A spectral power distribution (SPD) is the power emitted by a light source per unit wavelength. It is also referred to as the relative spectral distribution $S(\lambda)$,

$$S(\lambda) = \frac{X_{\lambda}(\lambda)}{R} \quad (12)$$

where $X_{\lambda}(\lambda)$ is the radiant flux per wavelength, and R is “a fixed reference value which can be an average value, a maximum value or an arbitrarily chosen value of this distribution” (CIE, 2011).

2.1.1.4 Light sources

2.1.1.4.1 Blackbody radiation

A blackbody is an ideal object that perfectly absorbs all the radiation incident on its surface and does not transmit or reflect any. The absorbed radiation causes the body to heat and glow. In thermal equilibrium, a blackbody radiates the same amount of energy it receives. According to Planck’s law, the spectral exitance, the radiant flux emitted by a surface per unit area per wavelength, of blackbody radiation, $M_{e\lambda}$, is given by,

$$M_{e\lambda} = \frac{2\pi hc^2}{\lambda^5} \left(\frac{1}{e^{hc/\lambda kT} - 1} \right) \quad (13)$$

where T is the temperature in units of kelvin (K), h is Planck’s constant $(6.6256 \pm 0.0005) \times 10^{-34}$ joule second (Js), and k is the Boltzmann’s constant 1.3807×10^{-23} J/K (DeCusatis, 1997). A blackbody radiator, also known as the Planckian radiator, emits more power when its temperature increases. The power emitted from a Planckian radiator as a function of wavelength at various temperatures is shown in Fig. 3. The physical temperature of the Planckian radiator is often used to name the spectral power distribution of blackbody radiation.

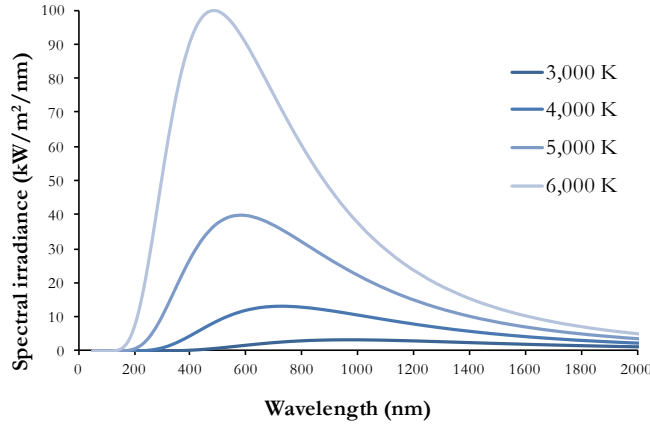


Fig. 3. The spectral power distribution of Planckian radiators at 3000 K, 4000 K, 5000 K, and 6000 K. Increase in temperature causes the spectral peak of the spectrum to shift to the shorter wavelengths, resulting in a bluish colour appearance. Lower temperature Planckian radiators, such as 3000 K, have a yellowish colour appearance.

“The temperature of a Planckian radiator whose radiation has the same chromaticity as that of a given stimulus” is called the colour temperature, T_c , where chromaticity is the property of a colour stimulus defined in a two-dimensional (plane) diagram (CIE, 2011). The term correlated colour temperature (CCT), T_{cp} , is used when the light source emits light of a chromaticity that is close, but not identical, to the chromaticity of the Planckian radiator at the same brightness and under specified viewing conditions (CIE, 2011).

2.1.1.4.2 Incandescent lamps

Although Planckian radiators are theoretical bodies, there are physical light sources that have similar spectral compositions. For example, the phenomenon of incandescence, the emission of electromagnetic radiation by thermal radiation, indicates that a blackbody radiates visible light at 798 K (Draper, 1847). In an incandescent lamp, a filament is heated by passing an electric current through the wire until it starts glowing. A glass envelope, which contains a vacuum or inert gases, encapsulates the filament to protect it from oxidation. The spectral emission of an incandescent lamp, shown in Fig. 4, is very close to a blackbody radiator of the same temperature.

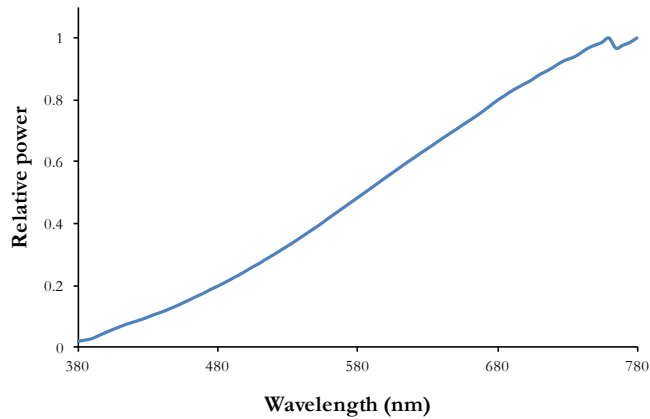


Fig. 4. The spectral power distribution of an incandescent lamp, at a colour temperature of approximately 2856 K, has spectral emission that is continuous across the visible spectrum. The incandescent lamp mostly emits light at the long wavelengths; thus, it appears yellowish in colour.

Tungsten is a commonly used filament material due to its constant spectral emissivity and high melting point (3683 K) (Hunt & Pointer, 2011). Evaporated tungsten, however, causes the filament to deteriorate and shortens the lifetime of the lamp, while deposits on the glass envelope cause a

reduction in light output. Additionally, an incandescent lamp emits mostly infrared radiation, which is heat, and it has a very low luminous efficacy. An ideal blackbody produces visible radiation most efficiently at 6600 K, for which the LER is 95 lm/W (Klipstein, 1996), but this temperature is above the melting point of tungsten. A tungsten filament lamp at 3200 K has a luminous efficacy around 25 lm/W operating at 3200 K, and 10 lm/W at 2650 K (Hunt & Pointer, 2011).

A halogen lamp is a tungsten incandescent lamp whose envelope contains small amounts of halogens, such as iodine or bromine. The halogen gas combines with the evaporated tungsten and migrates back toward the centre of the lamp, depositing the tungsten back onto the filament. This continuous cycle is called the halogen cycle, and it increases the lifetime of the lamp while preventing dark deposits on the glass envelope. As a result, halogen lamps can be run at higher temperatures (around 2850 K to 3300 K) with higher efficacies, around 15 lm/W to 35 lm/W (Hunt & Pointer, 2011), than standard incandescent lamps. Historically, tungsten lamps have been widely used in commercial and residential lighting. However, due to their low efficacy, governments around the world are phasing them out for general purposes, banning their manufacture, importation and sale (Waide, 2010).

2.1.1.4.3 Gas discharge lamps

A gas discharge lamp consists of a glass tube containing electrodes and gases, in which an electrical current is applied. An electrical discharge through an ionised gas excites atoms to a higher energy state, and the excited atoms emit photons to return to a more stable lower energy state. A high starting voltage and a current limiting device, usually a ballast, is needed to start and maintain the current flow.

Noble gases (argon, neon, krypton, and xenon) and metals, such as mercury, sodium, and metal halides, are commonly used in gas discharge lamps. The spectral power distribution of these light sources depends on the emission spectra of the atoms in the gas, the pressure of the gas and the amount of current. Unlike incandescent lamps, most gas discharge lamps emit discontinuous spectral power.

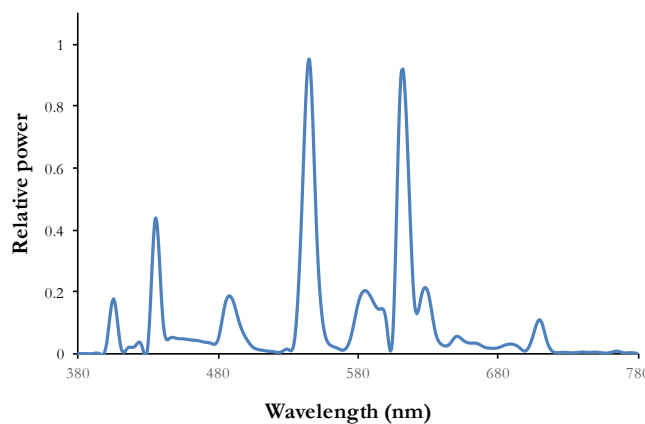


Fig. 5. The spectral power distribution of a tri-phosphor fluorescent lamp, with three spectral peaks at 435 nm, 545 nm, and 612 nm.

A fluorescent lamp is a glass tube containing low-pressure mercury vapour, which produces radiation at the short wavelengths when ignited, particularly at 253.7 nm, as well as argon, xenon, neon, or krypton (Hunt & Pointer, 2011). The phosphor-coated inner surface of the glass tube converts the UV into visible radiation. The composition of the phosphor coating determines the spectral emission of the lamp. Figure 5 shows a fluorescent lamp SPD with the spectral emission concentrated in three bands of the spectrum. Fluorescent lamps are widely used in the built environment due to their long life and high luminous efficacy, typically ranging from 45 lm/W to 110 lm/W (EMSD, 2016).

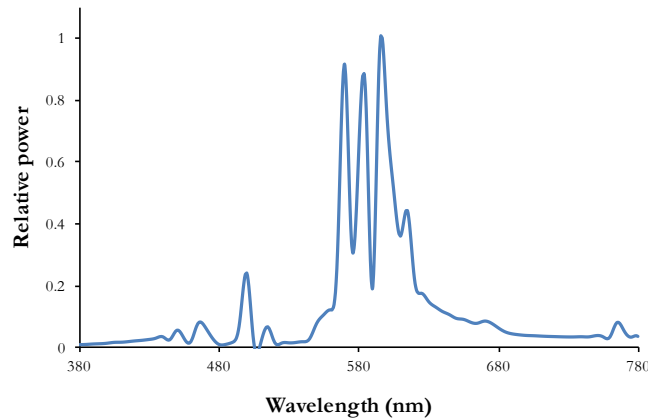


Fig. 6. The spectral power distribution of a high-pressure sodium lamp has a spiky shape. Although they do not exhibit high colour quality, high-pressure sodium lamps typically have high luminous efficacies.

Low-pressure sodium vapour lamps emit light mostly at two wavelengths, 589.0 nm and 589.6 nm, and have luminous efficacies up to 200 lm/W (Sprengers, Campbell, & Kostlin, 1985). Their high efficacy and almost monochromatic yellow appearance restrict their usage to roadway and security lighting, where distinguishing colours is not considered to be of prime importance. When the pressure of the sodium gas is increased, the emission of power becomes broader due to the change in the energy levels of the gas atoms. The spectral power distributions of a high-pressure and low-pressure sodium lamp are shown in Fig. 6, and Fig. 7, respectively. High-pressure sodium lamps have luminous efficacies around 100 lm/W to 150 lm/W; they are mostly used for outdoor lighting (Hunt & Pointer, 2011).

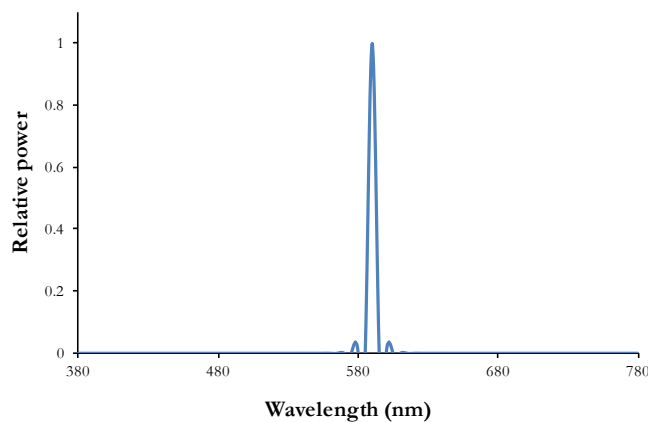


Fig. 7. The low-pressure sodium lamp has a very narrowband spectral power distribution, which results in very poor colour quality and high luminous efficacy.

A high-pressure mercury vapour lamp emits light by passing an electric arc through vaporised mercury. The SPD of the mercury lamp has several peaks, prominently at 253.7 nm, 365 nm, 404.8 nm, 435.8 nm, 546.1 nm, and 579.1 nm (Sansonetti, Salit, & Reader, 1996). The absence of power in the longer wavelengths results in a bluish-green colour appearance. A phosphor coating is then applied to the glass envelope to convert UV radiation to visible light of longer wavelengths. The luminous efficacy of mercury lamps ranges from around 35 lm/W to 65 lm/W (Schiler, 1997), and they are used as overhead outdoor area lights.

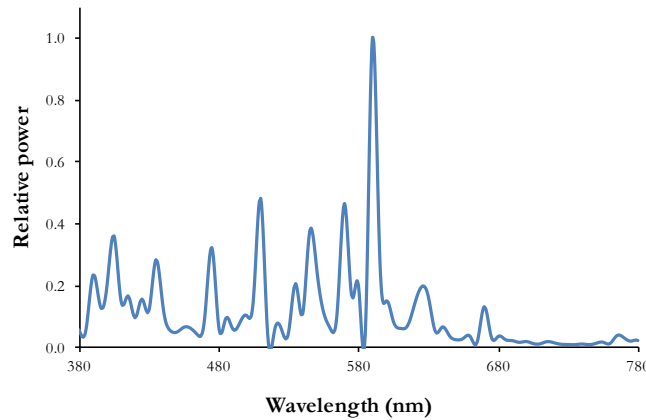


Fig. 8. The spectral power distribution of a metal halide lamp consists of several spikes throughout the visible spectrum. This spectral composition enables metal halide lamps to have high colour quality.

Similarly, metal halide lamps generate light by passing an electric arc through vaporised mercury and metal halide compounds such as sodium iodide, resulting in additional spectral lines in its emission, as shown in Fig. 8. Metal halide lamps have higher luminous efficacies, around 75 lm/W to 100 lm/W (Grondzik, Kwok, Stein, & Reynolds, 2009), and are used for both indoor and outdoor lighting, such as sports arenas, retail and industrial spaces.

2.1.1.4.4 Solid-state lighting

SSL devices generate visible, UV and IR radiation from semiconductors by means of *electroluminescence*, the emission of photons from a material in response to an electric current. When a semiconductor diode (p-n junction) is powered, electrons flow from the cathode (n-type semiconductor) to the anode (p-type semiconductor) and recombine with a hole, as shown in Fig. 9. When a free electron from the conduction band combines with the hole in the valence band, it drops to a lower energy state and releases energy in the form of a photon (National Research Council, 2013). LEDs are the most common type of SSL device, and they can be divided into two groups, depending on the characteristics of the semiconductor compounds. Typically, LEDs are made of inorganic semiconductor materials, such as gallium phosphide (GaP) and indium gallium nitride (InGaN). However, organic compounds, such as indium tin oxide (ITO) and tris (8-hydroxyquinolino) aluminium (Alq₃), can be used to manufacture other types of LEDs, such as the small molecule based LEDs (SMLEDs), also known as organic LEDs (OLEDs), and polymer LEDs (PLEDs) (Geffroy, Le Roy, & Prat, 2006).

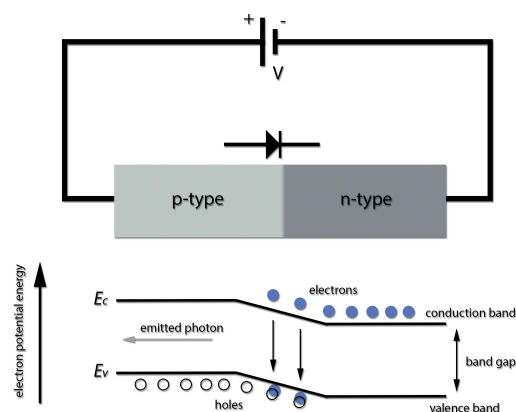


Fig. 9. When a semiconductor device is powered, electrons flow from the cathode (n-type) to the anode (p-type) and recombine with the holes. When the electrons drop from a higher energy state (the conduction band) to a lower energy state (the valence band), they emit photons (light) as a form of energy.

The spectral emission of an LED is usually narrowband, and its spectrum depends on the semiconductor materials used and the band gap. White LEDs can be manufactured by mixing multi-colour LEDs, coating a blue LED with yellow phosphor, or converting UV to visible radiation with blue and yellow (or red, green and blue) phosphors (National Research Council, 2013). The spectral power distributions of a phosphor-coated LED (pcLED) and a red green blue (RGB) LED are shown in Fig. 10.

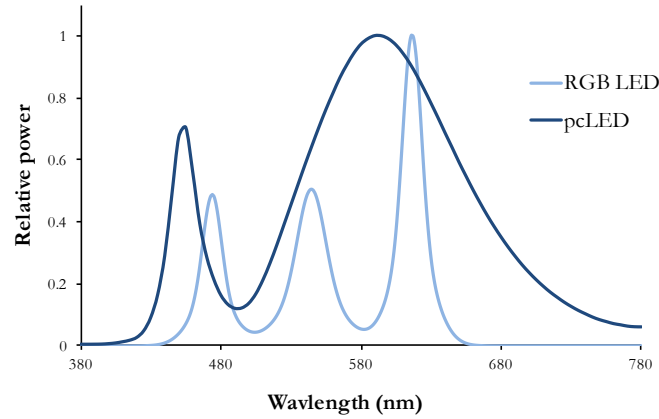


Fig. 10. The spectral power distribution of a phosphor-coated LED (darker blue line) and a three colour LED with peak wavelengths at 473 nm, 544 nm, and 616 nm (lighter blue line).

The ease with which researchers can control the light output of LEDs encouraged the expansion of research focusing on the optimisation of the spectral output of SSL devices. As a result, there is considerable variability in the luminous efficacy and spectral composition of LED products. While the luminous efficacies for commercialised white LEDs are generally between 60 lm/W and 188 lm/W, the highest luminous efficacy recorded for a white LED is 303 lm/W (Casey, 2014; National Research Council, 2013). The rapid expansion of manufacturing capabilities, reduced costs and government incentives allowed LEDs to be commonly available in most lighting market segments, including residential and commercial, theatrical, automotive, signalling and outdoor applications.

2.1.1.4.5 Daylight

Direct and indirect light coming from the sun during the day, except for the scattered light from celestial objects, such as the moon, is called *daylight*. Daylight consists of three components: direct sunlight, diffuse sky radiation (or *skylight*), and reflection of sunlight and skylight from Earth or objects on earth (Hernández-Andrés, Romero, Nieves, & Lee, 2001). While direct sunlight is consistent in terms of its spectral output, the spectral composition of diffuse sky radiation varies with the state of the sky (i.e. the altitude of the sun, cloud formation, and atmospheric conditions). The spectrum of the solar radiation also includes radiation beyond visible light (i.e. X-rays, UV, IR, and radio waves) (Iqbal, 1983).

According to the National Aeronautics and Space Administration (NASA), the *effective temperature* of the sun, the temperature of a blackbody that would emit the same total amount of electromagnetic radiation (Roy & Clarke, 2003), is approximately 5777 K (NASA, 2016). However, several studies, undertaken in different parts of the world, have shown that the spectral distribution, therefore CCT, of *natural light* varies between 3000 K and 10⁶ K (Dixon, 1978; Hernández-Andrés, Romero, García-Beltrán, & Nieves, 1998; Judd, MacAdam, & Wyszecki, 1964; Romero, García-Beltrán, & Hernández-Andrés, 1997; Sastri & Das, 1968; Tarrant, 1968; Winch, Boshoff, Kok, & Du Toit, 1966). The similarities in these spectral measurements formed the foundations of a set of representative daylight spectra, E_{λ} , corresponding to different CCTs, ranging from 4000 K to 25000 K (CIE, 2004c; Hernández-Andrés et al., 2001). Figure 11 shows the normalised spectral power distribution of daylight at 5700 K and a blackbody radiator of the same temperature. As shown in Fig. 11, daylight does not have a smooth power distribution, due to the selective absorption of the

light by the atmosphere of the earth and the sun. The magnitude of this absorption depends on the day and the time of day (Hernández-Andrés, Nieves, Valero, & Romero, 2004).

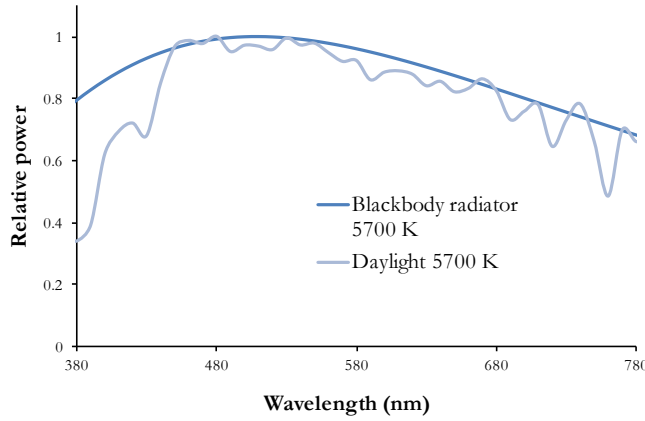


Fig. 11. The spectral power distribution of daylight at 5700 K has small spikes, due to variations in the sky (i.e. the altitude of the sun, cloud formation, and atmospheric conditions). A blackbody radiator of the same temperature has a smooth spectrum.

Daylight is used in architectural spaces to reduce the energy consumed by electric lighting, to stimulate circadian rhythm and to improve visual comfort (Ochoa, Aries, van Loenen, & Hensen, 2012). Incorporating daylight in buildings involves several design challenges, such as excessive heat, glare, and lack of uniformity and consistency in illumination levels.

2.1.1.4.6 Standard illuminants

The CIE (the International Commission on Illumination, abbreviated from its French name, *Commission Internationale de l'Eclairage*) has established standard illuminants with defined spectral power distributions to reduce complexities and introduce standardisation in the field of colour measurement (2006). The CIE defines an *illuminant* as a light-radiating body with spectral distributions specified (published) by the CIE, in contrast to a *light source*, which is a physical object that produces radiant power (2010). Standard illuminants are mathematical constructs that are published to provide a basis for comparison of object colour appearances under different light sources.

The spectrum of a tungsten filament incandescent lamp has been adopted as the CIE standard illuminant A. The CIE standard illuminant A has the same relative spectral power distribution as a Planckian radiator at a temperature of 2856 K (CIE, 2011). The relative spectral power distribution of illuminant A is $S_A(\lambda)$,

$$S_A(\lambda) = 100 \left(\frac{560}{\lambda} \right)^5 \times \frac{\exp \frac{1,435 \times 10^7}{2848 \times 560} - 1}{\exp \frac{1,435 \times 10^7}{2848 \lambda} - 1} \quad (14)$$

where the two exponential terms are wavelength-dependant constants (CIE, 2004a). The standard illuminant D₆₅ is recommended by the CIE to represent average daylight with a correlated colour temperature of 6500 K (2004a). The relative spectral power distributions of some of the CIE illuminants are shown in Fig. 12. The CIE also defines other supplementary daylight illuminants, such as D₅₀, D₅₅ and D₇₅, with CCTs of 5000 K, 5500 K and 7500 K, respectively. The illuminant D₅₀ is used as a reference SPD in printing, graphic design and colour management profiles in displays (Hunt & Pointer, 2011; International Color Consortium, 2004). The standard illuminant D₆₅ is the reference illuminant in various fields, including display colorimetry and the dyeing industry (ASTM, 1989; Hunt & Pointer, 2011; ISO, 1998).

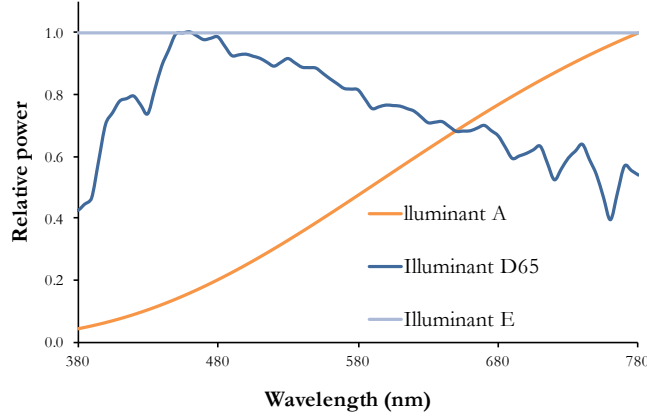


Fig. 12. The CIE standard illuminant A represents the incandescent lamp at a temperature of 2856 K. The illuminant D₆₅ represents daylight at 6500 K and illuminant E is an equal-energy radiator, which emits the same amount of power at each wavelength along the visible spectrum. The CIE standard illuminants are commonly used in colorimetric research as reference light SPDs.

The illuminant E, also known as the equal-energy radiator, is a theoretical light source with a constant spectral emission along the spectrum. The equal-energy radiator emits the same amount of power at each wavelength, as shown in Fig. 12.

2.1.2 Optical properties of surfaces

Light that strikes the surface of an object is transmitted, absorbed or reflected. The law of conservation of energy indicates that the total power incident on the surface of an object is the sum of *absorptance*, α , “ratio of the absorbed radiant flux or luminous flux to the incident flux under specified conditions,” *reflectance*, ρ , “ratio of the reflected radiant flux or luminous flux to the incident flux in the given conditions,” and *transmittance*, τ , “ratio of the transmitted radiant flux or luminous flux to the incident flux in the given conditions.”

$$\alpha + \rho + \tau = 1 \quad (\text{CIE, 2011}). \quad (15)$$

The *reflectance factor*, R , is the “ratio of the radiant flux or luminous flux reflected in the directions delimited by the given cone to that reflected in the same directions by a perfect reflecting diffuser identically irradiated or illuminated” (CIE, 2011). The surface reflectance factor of an object can also be represented as a function of wavelength,

$$\rho(\lambda) = \frac{\Phi^r(\lambda)}{\Phi^i(\lambda)} \quad (16)$$

where $\rho(\lambda)$ is the spectral reflectance function (or factor), $\Phi^r(\lambda)$ is the reflected radiant or luminous flux, and $\Phi^i(\lambda)$ is the incident flux (CIE, 2011; DeCusatis, 1997). The spectral reflectance factor of an object is wavelength-dependent and is a value between 0 and 1, where $\rho(\lambda) = 1$ indicates that all the incident flux at each wavelength is reflected, with no transmission or absorption. Conversely, a spectral reflectance factor of $\rho(\lambda) = 0$ means that no radiation is reflected from the surface of the object. However, both of these cases are theoretical conditions, as objects in real life usually reflect some of the radiant energy incident on their surface and the rest of the incident radiation is either absorbed or transmitted. For an opaque object, the transmittance is considered $\tau = 0$, and the light incident on the surface of the object is either absorbed or reflected. The absorbed radiant energy is consequently transformed into heat or another form of internal energy.

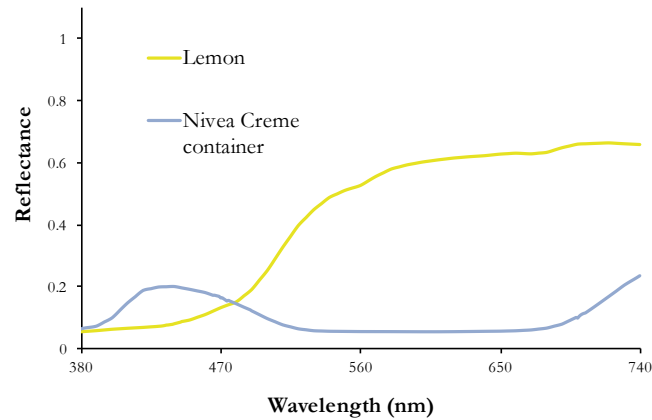


Fig. 13. The lemon reflects light mostly in the middle and long wavelengths, resulting in a yellowish colour appearance. The dark blue Nivea Creme container reflects only a small amount of light in the shorter wavelengths and very long wavelengths.

Figure 13 shows the spectral reflectance factors of a lemon and a Nivea Crème container. The lemon predominantly reflects light in the longer wavelengths and a small amount in the shorter wavelengths. The blue Nivea Creme container reflects some light in the shorter and longer wavelengths, but very little in the middle wavelengths. A lower reflectance denotes a darker colour appearance, while a higher reflectance factor indicates a lighter colour appearance.

2.1.3 Colour vision

2.1.3.1 Human visual response

The human visual response to light starts with visible radiation entering the eye. One of the most complex parts of the body, the human eye has evolved to capture light and enable human vision. The human eye consists of several components that collect and transmit light to the brain, where colour perception occurs. The transparent front part of the eye is called the cornea. The cornea contributes around two-thirds of the optical power of the eye (Goldstein & Brockmole, 2016). The cornea has a curved surface and it is the primary refractive element of the eye due to the difference of the index of refraction between the cornea and air. The change in the direction of light as it enters a medium is determined by the difference in the refractive indices of the media (Boynton, 1979). The indices of refraction of the ocular media are shown in Table 2.

Table 2. Indices of Refraction of the Ocular Media (Hecht 2002).

Medium	Indices of refraction
Air	1
Water	1.33
Aqueous Humour	1.336
Vitreous Humour	1.337
Cornea	1.376
Lens (cortex)	1.886
Lens (core)	1.406

The iris is the coloured part of the eye behind the cornea. The iris controls the amount of light entering the eye by varying the size of the pupil, the hole located in the centre of the iris. The pupil appears dark due to the transmittance of the light rays into the eye. Although the size of the pupil largely depends on the level of illumination on the retina, other factors, such as the spectral and temporal characteristics of the light, the size and region of the retina stimulated, and non-visual phenomena, such as emotional reactions, can play a part in the *pupillary response* (Boynton, 1979). The pupillary light reflex provides the optimum visual acuity at various illumination intensities. In lower lighting conditions, an increased iris aperture allows more light to enter the eye. In photopic

conditions, when the luminance of the visual field is higher, the pupil constricts to reduce the optical aberrations, diffraction and stray light, which may lead to a loss in image quality.

Accommodation is the process of maintaining a clear image by focusing on objects at varying distances from the eye by changing the shape of the lens (Boynton, 1979). The lens has a flexible structure with variable indices of refraction, higher in the centre, which reduces some of the aberrations that would occur in a normal optical system (Fairchild, 2013). Roughly one-third of the eye's total optical power comes from the lens, which is used to fine-tune the image formed on the retina. The lens loses its capacity to bend with age, resulting in an inability to focus on near objects. The hardening of the lens is almost concurrent with an increase in its optical density, where absorption and scattering of short wavelength radiation by the lens are increased. As a result, the lens becomes yellower with age, which influences human colour vision. After passing through the lens, light travels through a clear liquid fluid, the vitreous humour, and reaches the retina, the inner light-sensitive layer of the eye where the optical image is formed, at the back of the eye.

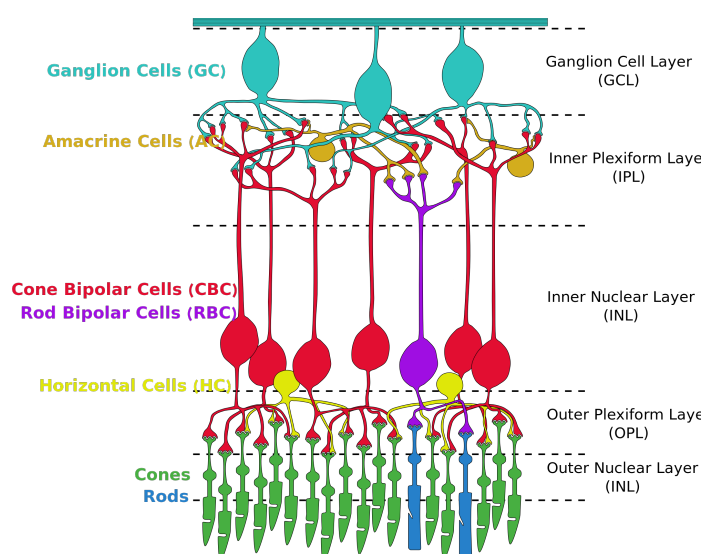


Fig. 14. A photon enters the retina from the ganglion cell layer side of the retina. It travels down until it reaches the photoreceptor cells, the cones and rods, where it is absorbed (Encke, 2014).

The neural retina consists of several layers of nerve cells, as shown in Fig. 14, that are essential for vision. In the retina, three types of photosensitive cells convert the photons into chemical and electrical signals through phototransduction. The rods and cones are the photosensitive cells responsible for vision, while the intrinsically photosensitive retinal ganglion cells (ipRGCs) contribute to non-image forming functions, such as synchronising circadian rhythms (Hattar, Liao, Takao, Berson, & Yau, 2002). The rods and cones contain different types of *photopigments*, light-sensitive proteins, such as the photopsins in the cones and the rhodopsins in the rods. When a photon passes through the transparent layers of the retina, it reaches the photoreceptors (i.e. rods and cones) in the interior end of the retina (Fairchild, 2013). The photopigments in a photoreceptor cell go through a chemical change when they detect a photon. The absorption of light triggers a photoreceptor's electrical potential to decrease (also called *hyperpolarisation*), causing a reduction in the amount of neurotransmitter released (the cell turns "off") (Lodish et al., 1995). Hyperpolarisation is a gradual response to light intensity. The rods and cones are connected to interneurons (horizontal, bipolar and amacrine cells) in various combinations, as shown in Fig. 14. The signals are transmitted to the ganglion cells through the middle layer of the retina. When the ganglion cells receive excitatory signals beyond a threshold level, they fire *action potentials* (nerve impulses) to transmit information to the brain along the optic nerve, exhibiting the all-or-none principle, as opposed to the gradual response of the photoreceptors (Lodish et al., 1995). The convergence of the photoreceptors to the optic nerve fibres impacts visual acuity. Greater convergence results in poor visual acuity (e.g. rods), while less convergence results in better visual acuity (e.g. cones in the fovea).

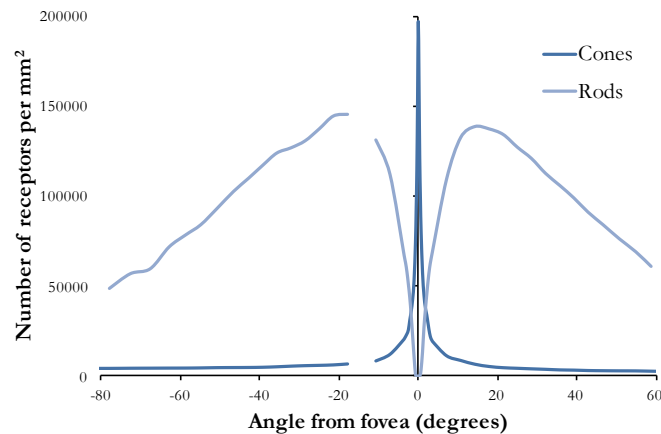


Fig. 15. A high number of cone cells are concentrated in the fovea. Although there are no rod cells in the centre of the fovea, the rods are more abundant and more uniformly distributed in the rest of the retina compared to the cones. In the blind spot, about 15° from the fovea, the optic nerve cells leave the eye, so light-detecting photoreceptor cells are absent. The data are taken from Curcio, Sloan, Kalina, & Hendrickson (1990).

The retina is not uniformly sensitive to visible radiation due to the distribution of the photoreceptor cells, as shown in Fig. 15. Colour vision is limited outside the 40° on either side of the eye's visual axis (Hurvich, 1981), while colour vision and fine detail gradually increase in the fovea. The sharpest image forms in the fovea, the small central zone near the optical axis that contains only cone cells, which is shown in Fig. 16. It is the area where the best spatial and colour vision forms, covering approximately 2° of visual angle in the central field of vision (Fairchild, 2013), where a 17 cm diameter at the distance of 2.5 m is considered 1° of the *visual field* (Agoston, 1979). The *blind spot* is positioned about 15° from the fovea (Tong & Engel, 2001), where the optic nerve cells leave the eye to connect to the brain. The blind spot has no photoreceptors, so an image cannot be formed in the optical disc where the nerve cells leave the eye. However, the blind spot does not necessarily cause a gap in visual perception. The missing information is compensated by a process called *filling-in*, where the surrounding retinal stimulation and information from the other eye are interpolated to fill the gap in vision (Ramachandran & Gregory, 1991).

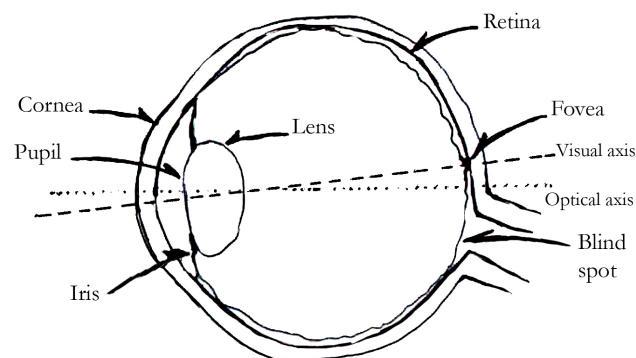


Fig. 16. The optical axis is a theoretical construct that goes through the centre of the cornea and lens and intersects the retina at an arbitrary point. However, the visual axis only goes through the centre of the lens, intersecting the retina at the fovea, where the sharpest image is formed.

The rods and cones, the two main classes of photoreceptors, vary in terms of their quantity and function. There are 90 million rods and four million cones in an average human retina (Curcio et al., 1990). Positioned outside the fovea, the rods are about 100 times more sensitive to brightness and enable vision at low luminance levels (less than around 10^{-3} cd/m²) (CIE, 1994). Rhodopsin pigments, the light-sensitive protein cells in the rods, are sensitive enough to detect a single photon (Okawa & Sampath, 2007). Rhodopsin pigments become bleached at higher luminance levels (i.e.

greater than 100 cd/m^2) before being regenerated after approximately 20 minutes (Lamb & Pugh, 2006). The rods are slow to respond to light, and they provide poor visual acuity due to the convergence of several signals from rods into a single neuron in the optic nerve fibres.

In intermediate light levels, also referred to as mesopic vision, approximately 10^{-3} cd/m^2 to 3 cd/m^2 , both the rods and cones are active (CIE, 1989). In photopic vision, where luminance levels are approximately 3 cd/m^2 to 10^8 cd/m^2 , only the cones operate, resulting in colour vision and higher spatial resolution. Unlike the rods, some cones have sole connections to the optic nerve, resulting in maximal visual acuity. The cones, concentrated in the fovea, are less abundant, but respond faster to changes in stimuli.

There are three different types of cones. L cones are maximally sensitive to long wavelengths, M cones to medium wavelengths, and S-cones to short wavelengths. These three types of cones are distinctive in terms of their distribution in the retina. The relative quantity of the L, M and S cones is approximately 40:20:1 (Fairchild, 2013). The spectral sensitivities of the three cone types, especially L and M cones, broadly overlap. This overlapping is critical to the perception of colour by the human visual system. The cone sensitivities are directly related to the spectral absorbance characteristics of the photopsins (Bowmaker & Dartnall, 1980; MacLeod & Hayhoe, 1974; MacNichol, 1964; Rushton, 1962, 1975).

Some spatial properties separate S cones from M and L cones. First, S cones do not exist in the fovea and are sparsely distributed in the retina (Hunt & Pointer, 2011). Additionally, S cones do not greatly contribute to contrast discrimination or perception of luminance, but they are critical for distinguishing the perceptual attributes of colour, such as hue and chroma (Eisner & MacLeod, 1980). While S cones are not as sensitive as L and M cones, all of the cone responses gradually reduce for wavelengths in both ends of the visible spectrum. The *principle of univariance* states that an individual photoreceptor cannot differentiate the spectral composition or the intensity of a stimulus (Rushton, 1972). Although the wavelength of the stimulus may affect the probability that a receptor cell absorbs a photon, the wavelength information can only be extracted by comparing the outputs of different cones. For example, an intense red light and a dimmer yellow light are indistinguishable for the M cones, as they both trigger moderate stimulation of the M cones. Red light, however, would trigger a stronger stimulation of the L cones than the M cones, while yellow light of medium intensity would trigger a stronger response in the M cones than the L cones. The visual system can differentiate between wavelengths by combining and comparing responses across the cone types. However, this means that different spectra can trigger undistinguishable patterns of cone activity and, therefore, percepts.

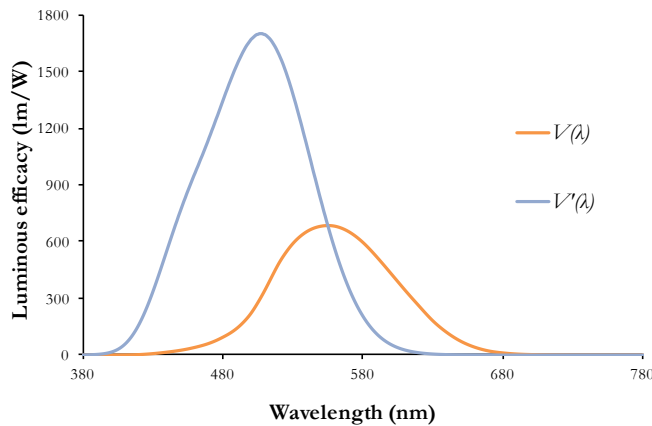


Fig. 17. The spectral luminous efficiency function for photopic vision, $V(\lambda)$, reaches its peak sensitivity (683 lm/W) at 555 nm (CIE, 2011). Visual sensitivity shifts toward the shorter wavelengths in scotopic vision, where $V'(\lambda)$ peaks (1700 lm/W) at 507 nm (DeCusatis, 1997).

In 1924, the CIE established the spectral luminous efficiency function ($V(\lambda)$), the human visual response to light intensity under photopic conditions. It numerically represents the average human observer in higher luminance environments. The luminous efficiency function corresponds to a weighted sum of the three cone responses, the only photoreceptors that contribute to photopic

vision. On the other hand, in scotopic conditions, when the luminance is less than around 10^{-3} cd/m², the rods are the only active photoreceptors (CIE, 2011). In contrast to photopic vision, there is no colour perception in scotopic vision, and visual sensitivity shifts towards the shorter wavelengths, as shown in Fig. 17. Similar to $V(\lambda)$, a spectral luminous efficiency function for the scotopic vision ($V'(\lambda)$) was defined by the CIE in 1951 (1951).

2.1.3.2 Colour vision theory

The fundamentals of colour processing in the visual system can be explained by two distinct mechanisms; the trichromatic theory at the photoreceptor level and opponency theory from the ganglion cell onwards. Trichromatic colour theory is usually attributed to Thomas Young, who proposed that colour vision might be the consequence of the signals from the three types of photoreceptor cells (1802). Building on Young's ideas, Helmholtz conducted colour-matching experiments to show that any light can be matched by a mixture of three different primary lights (von Helmholtz & Southall, 1962). In a colour-matching experiment, observers are asked to match the colours in two regions of a bipartite (split field) screen. A monochromatic light illuminates the reference field, and the participants tune the three monochromatic lights in the neighbouring field to match the reference stimulus. The amount of coloured light needed to match the reference light source for each wavelength is called the colour matching function (CMF). The amount of monochromatic red light needed for a match is represented by $\bar{r}(\lambda)$, while $\bar{g}(\lambda)$ represents the amount of monochromatic green light, and $\bar{b}(\lambda)$ represents the amount of monochromatic blue light needed for a match. The $\bar{r}(\lambda)$ function resulting from colour matching experiments has negative values, which means that the red primary should be added to the reference field for a match.

In the following decades, data from physiological studies supported the theory of trichromacy. Several researchers obtained the sensitivities of the L, M and S cones through physiological measurements (Dartnall, Bowmaker, & Mollon, 1983; Stockman, MacLeod, & Johnson, 1993; Svachkin, 1956). The spectral sensitivities of the S, M and L cones can be seen in Fig. 18a. Trichromacy is considered the dominant colour vision mode in humans, while only around 8 % of men and less than 1 % of women lack one or more types of cone cells (Sharpe, Stockman, Jägle, & Nathans, 1999). Although trichromacy largely explains colour discrimination, it does not account for the opponent colour perception, nor does it explain why dichromats (organisms with two types of cone cells) can perceive white and yellow (Kalloniatis & Luu, 2007).

The opponent-process theory, proposed by Ewald Hering as an alternative to trichromacy, argues that human vision is based on three channels (red-green, blue-yellow and black-white) working in an antagonistic manner (1868). According to the opponent theory of colour vision, the human visual system can perceive only one pole of a channel at a time (e.g. either blue or yellow). Therefore, objects (or light sources) do not appear bluish yellow or reddish green. A simplified graphical representation of the working mechanism of the opponent theory is given in Fig. 18b. Around a century after Hering first proposed his theory, the quantitative data from several physiological (De Valois, Smith, Kitai, & Karoly, 1958; Derrington, Krauskopf, & Lennie, 1984; Svachkin, 1956; Wiesel & Hubel, 1966) and psychophysical studies (Hurvich & Jameson, 1957; Jameson & Hurvich, 1955) indicated the existence of the opponent colour signals in the visual system.

One of the earliest pieces of evidence supporting the opponent theory was based on observations from behavioural experiments. Jameson and Hurvich developed a psychophysical method, *hue cancellation*, to isolate and quantify the individual opponent channels (Hurvich & Jameson, 1957; Jameson & Hurvich, 1955). In this classic experiment, the participants were asked to cancel out a primary colour (e.g. green) from the starting light condition (e.g. cyan, the mixture of blue and green) by adding a second light. The participants were able to remove the blue light from cyan, only by adding yellow light. The data from these experiments resulted in a graph similar to the one shown in Fig. 18c. The two opponent channels (i.e. red-green, yellow-blue) display an antagonistic relationship. An additional achromatic channel, which is not shown in the graph, is approximately equivalent to the spectral luminous efficiency function, $V(\lambda)$.

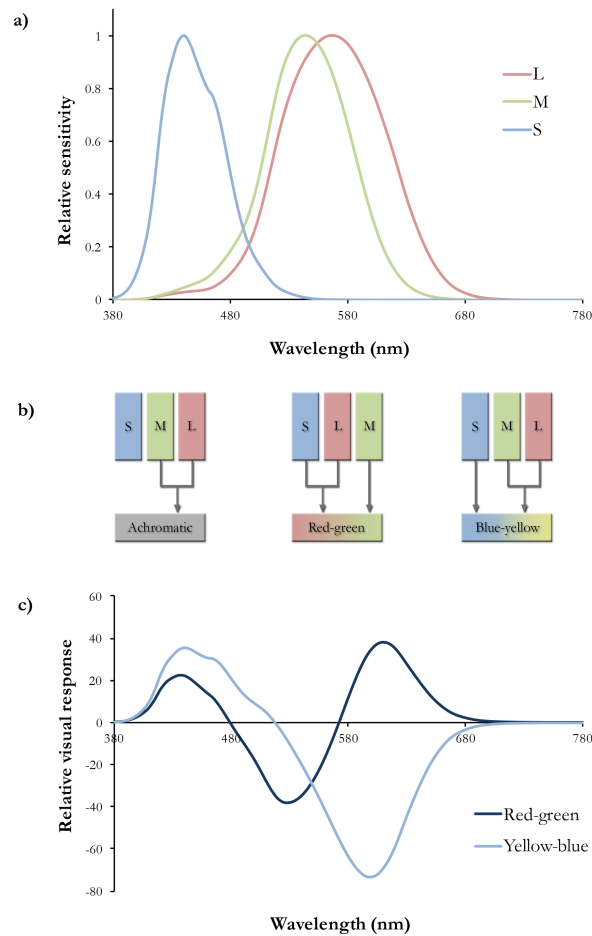


Fig. 18. Modern colour vision theory. a) normalised L, M and S cone sensitivities b) colour opponency at the neural processing stage c) the relative spectral sensitivities of chromatic opponent pathways underlying opponency (De Valois & De Valois, 1993).

Additional evidence supporting the opponent theory is the existence of chromatic *afterimages*. After adapting to a coloured stimulus for a period of time, the visual system becomes more sensitive to its opponent colour. For example, when observers fixate their vision on a green image for a minute or so, shifting their gaze to a white area produces a red afterimage. The trichromatic theory of colour vision fails to explain the complementary colours observed in these afterimages.

Today, it is commonly accepted that both of these opposing theories help explain how human colour vision occurs. Modern colour vision theory incorporates both trichromacy and opponency in different stages. Figure 18 shows a simplified representation of the modern understanding of the colour vision process. The first stage is the photoreceptor level, where three types of cones detect light and produce electrochemical signals. Later, in neural processing, rather than separate signals being sent to the brain, the outputs of three cone receptors are first compared and then transmitted to the visual cortex.

2.1.3.3 Colour mixing

The method of creating new colours by mixing individual colours of light is called additive colour mixing. Additive colour mixing applies to mixing light directly emitted from a light source. In additive mixing, a new colour can be achieved by superimposing different lights, by projecting them in succession at high frequency, or by viewing them in adjacent areas close enough to resolve (e.g. computer and television displays) (Hunt & Pointer, 2011). The final mixture in this process is the sum of the spectra of the individual lights. It results from the additive nature of visible radiation, as specified in Grassman's laws (Grassmann, 1854). For example, when a green light with a peak

wavelength of 525 nm is mixed with an amber light with a peak wavelength of 595 nm, the additive mixture becomes a two-peak spectrum, as shown in Fig. 19, which appears yellowish in colour.

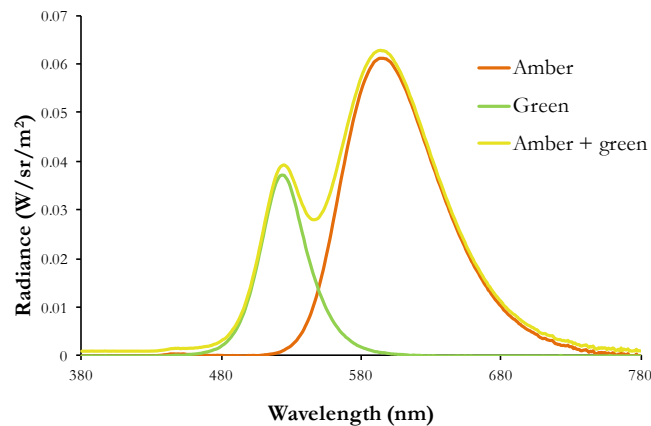


Fig. 19. In additive colour mixing, the combination of an amber light with a peak wavelength of 525 nm and a green light with a peak wavelength of 595 nm results in a two-peak spectrum, which appears yellowish in colour.

Primary colours, a set of three arbitrary colours, each of which cannot be created from a combination of the other two, constitute the basis of colour mixing in various media. Combining all of the primaries in additive mixing results in the appearance of white, while the absence of any colour results in the appearance of black. A set of arbitrary primary colours for additive and subtractive mixing is shown in Fig. 20.

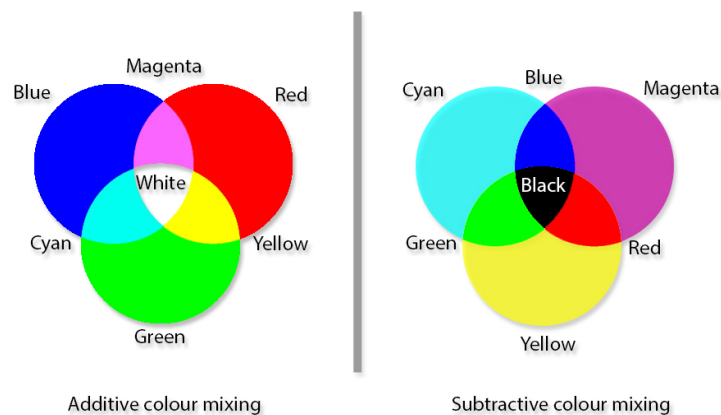


Fig. 20. The arbitrary primary colours in additive colour mixing (e.g. red, green and blue) are the secondary colours in subtractive colour mixing and vice versa.

Subtractive colour mixing occurs when light-reflecting (i.e. dyes, inks, paints) or light-transmitting (i.e. photographic filters) substances are mixed. The subtraction (of light) occurs due to the increased absorption that results when two or more coloured substances are mixed. When two or more coloured dyes, paints or inks are mixed, the mixture becomes darker. Subtractive colour mixing is used in print photography, printing, painting, and fabric dyeing. Subtractive colour mixing can be achieved by mixing pigments (e.g. in painting) or by superimposing different layers (e.g. in printing) (Hunt & Pointer, 2011).

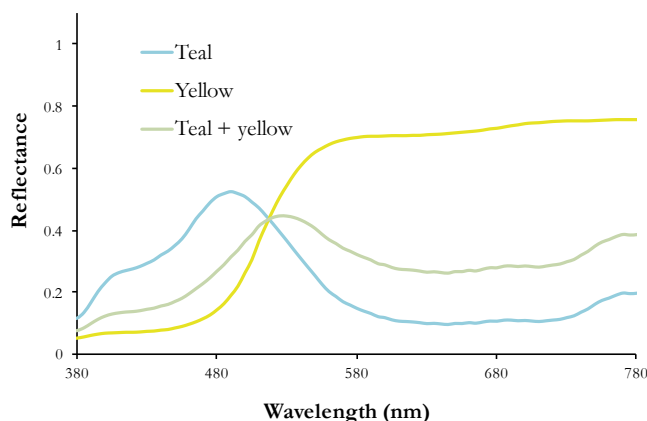


Fig. 21. In subtractive colour mixing, adding a teal paint to a yellow paint results in a green coloured paint. The reflectance factor of the teal and yellow mixture can be estimated by calculating the geometric mean of the individual paint reflectance factors. The mixture has low reflectance and it appears darker than either of its constituent colours.

The result of a subtractive mixture is often more difficult to predict and mathematically formulate than that of an additive mixture. The difficulty is caused by the uncertainties of dye interactions and the mixture's dependence on several characteristics of the individual substances, such as pigment particle size, density, refractive index, and transparency (MacEvoy, 2015). However, the reflectance function of paint or dye mixtures can be roughly calculated using the geometric mean of the individual reflectance functions, if the paints have equal tinting, opacity and dilution (MacEvoy, 2015). If the paints are not mixed in equal proportions, using a weighted geometric mean can provide a reasonably good prediction of the final mixture (Burns, 2015). Figure 21 shows the spectral reflectance factors of a subtractive mixture example when teal and yellow paints are equally mixed. The yellow paint has high reflectance in the longer wavelengths and low reflectance in the shorter wavelengths. On the other hand, the teal paint absorbs most light in the long wavelengths, while reflecting more light in the short wavelengths and some in the middle wavelengths. The paint mixture appears green and reflects most light of middle and long wavelengths. Since the geometric mean gives more weight to the smallest component (i.e. if one of the components were zero, the weighted sum would be zero), absorption is weighted more dominantly in the final mixture than reflectance. This mathematical function is consistent with the fact that the final mixture (i.e. green) has slightly lower reflectance than the mean of the two individual substances used for the mixture.

2.1.3.4 Perceptual attributes of colour

There are three basic perceptual attributes of colour: hue, brightness, and colourfulness. The CIE definitions of these attributes are given below.

Hue is the “attribute of a visual perception according to which an area appears to be similar to one of the colours – red, yellow, green, and blue – or to a combination of adjacent pairs of these colours considered in a closed ring” (CIE, 2011).

Brightness is the “attribute of a visual perception according to which an area appears to emit, or reflect, more or less light” (CIE, 2011). A related term, lightness, is defined as “the brightness of an area judged relative to the brightness of a similarly illuminated area that appears to be white or highly transmitting” (CIE, 2011). While brightness is an absolute level of perception, lightness is the relative brightness that changes with illumination and viewing conditions.

Colourfulness is the “attribute of a visual perception according to which the perceived colour of an area appears to be more or less chromatic” (CIE, 2011). Chroma is the “colourfulness of an area judged as a proportion of the brightness of a similarly illuminated area that appears white or highly transmitting” (CIE, 2011). A somewhat similar term, saturation, can be described as the “colourfulness of an area judged in proportion to its brightness” (CIE, 2011).

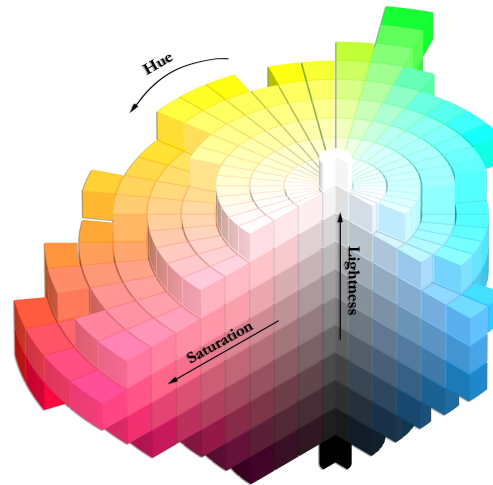


Fig. 22. The perceptual attributes of colours can be represented in a three-dimensional space. Hue varies along the circumference of the sphere, saturation increases with the radial distance, and lightness changes along the polar axis, reaching its maximum value at the zenith of the sphere. Adapted from the original image (SharkD, 2009).

The three attributes of colour are typically represented in a three-dimensional diagram, similar to the spherical structure shown in Fig. 22. The hue is usually denoted by the azimuthal angle of the sphere since there is no meaningful value of zero for the hue. The hue values (e.g. red, blue, green) change along the circumference of the three-dimensional shape. A perceived colour devoid of any hue (i.e. white, grey, black) is called an achromatic colour, and it is positioned along the polar axis. Colourfulness is represented by the distance from the centre of the sphere (the radius). A value of zero in colourfulness (zero radius) coincides with achromatic colours, and high colourfulness corresponds to a bigger radial distance. Brightness is represented by the vertical dimension of the sphere (the polar axis), ranging from the lowest brightness at the nadir point to the highest brightness at the zenith point.

2.1.3.5 Colour appearance phenomena

The perceptual attributes of colours are interconnected, and a change in one of the values impacts the others. Two luminance-based colour appearance phenomena are important for the visual experiments conducted in this project. The Bezold-Brücke hue shift, the change in hue that occurs when luminance is changed, describes the non-linear relationship between the stimulus intensity and wavelength of the monochromatic stimulus (Purdy, 1937). The data indicate that certain wavelengths (e.g. >600 nm) display greater variation in appearance with increasing luminance, while some of the wavelengths (i.e. 478 nm, 503 nm, and 572 nm) appear more consistent, despite changes in luminance (Purdy, 1937). Some researchers, however, suggest that the Bezold-Brücke hue shift is not relevant for related colours, that is, “colours perceived to belong to an area seen in relation to other colours” (CIE, 2011), which limits the impact of this phenomenon (Bartleson, 1979; Hunt, 1989). On the other hand, Pridmore argued that the Bezold-Brücke hue shift can also be observed for object colours that are seen in relation to other colours (1999, 2004).

Another colour appearance phenomenon, the Hunt effect, describes an increase in colourfulness with an increase in luminance. Research investigating colour perception with different levels of adaptation shows that colours in low luminance conditions appear to be less colourful (Hunt, 1952). These two phenomena may impact the perceived hue and saturation of the objects used in the experiments. Since the experiments were conducted in a lighting lab, where object colours were perceived to be unrelated, the careful adjustment of the luminance was necessary to avoid accidental hue and saturation shifts.

2.2 Colorimetry

Colorimetry is the science of colour measurement that aims to quantify and describe human colour perception. The textbook definition of colorimetry identifies several key points: “Colorimetry is that branch of colour science concerned with specifying numerically the colour of a physically defined visual stimulus in such a manner that:

- When viewed under the same conditions, stimuli with the same specification should look alike.
- Stimuli that look alike should have the same specification.
- The numbers comprising the specification are continuous functions of the physical parameters defining the spectral radiant power distribution of the stimulus” (Wyszecki & Stiles, 1982).

The definition of colorimetry makes it clear that it is a tool to make predictions about the colour appearance of objects under different light sources. The physical measurement of light sources and object reflectance factors are utilised to predict the human visual system’s response to coloured stimuli using quantitative methods.

2.2.1 Tristimulus values

The colour matching functions, $\bar{r}(\lambda)$, $\bar{g}(\lambda)$, and $\bar{b}(\lambda)$ were developed from two colour-matching experiments (Guild, 1931; Wright, 1929) and the data were combined to form the CIE 1931 RGB colour specification system with the monochromatic primaries of 700 nm, 546.1 nm, and 435.8 nm, respectively, for red, green and blue. The tristimulus values, R , G , and B , are “the amounts of the three reference matching stimuli required to give a match to the colour (or light) considered” and are obtained from the colour matching functions,

$$R = \int_{\lambda} \phi_{\lambda}(\lambda) \bar{r}(\lambda) d\lambda \quad (17)$$

$$G = \int_{\lambda} \phi_{\lambda}(\lambda) \bar{g}(\lambda) d\lambda \quad (18)$$

$$B = \int_{\lambda} \phi_{\lambda}(\lambda) \bar{b}(\lambda) d\lambda \quad (19)$$

where $\phi_{\lambda}(\lambda)$ is the colour stimulus function, “description of a colour stimulus by the spectral concentration of a radiometric quantity, such as radiance or radiant power, as a function of wavelength” (CIE, 2004a, 2011; Wyszecki & Stiles, 1982). However, to avoid negative values, $\bar{r}(\lambda)$, $\bar{g}(\lambda)$, and $\bar{b}(\lambda)$ colour matching functions were transformed into a new set of imaginary tristimulus values, $\bar{x}(\lambda)$, $\bar{y}(\lambda)$, and $\bar{z}(\lambda)$,

$$\bar{x}(\lambda) = 2.768892 \bar{r}(\lambda) + 1.751748 \bar{g}(\lambda) + 1.130160 \bar{b}(\lambda) \quad (20)$$

$$\bar{y}(\lambda) = 1.000000 \bar{r}(\lambda) + 4.590700 \bar{g}(\lambda) + 0.060100 \bar{b}(\lambda) \quad (21)$$

$$\bar{z}(\lambda) = 0 + 0.056508 \bar{g}(\lambda) + 5.594292 \bar{b}(\lambda) \quad (22)$$

where the tristimulus value $\bar{y}(\lambda)$ is equal to the luminous efficiency function $V(\lambda)$, so that the set of three linear equations links the colorimetric system to photometry (CIE, 2004a).

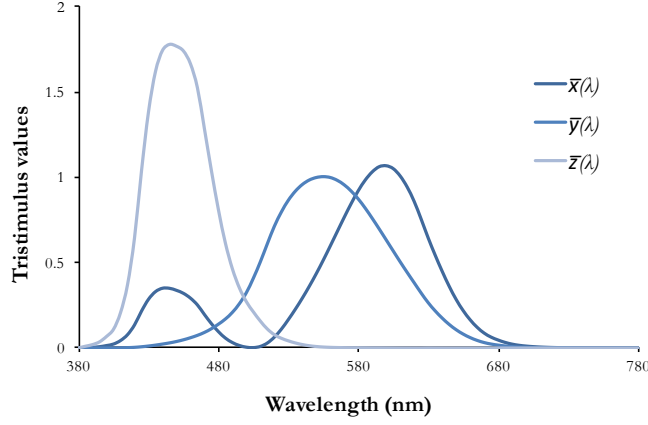


Fig. 23. The CIE 2° standard observer, the mathematical descriptors of the response to colour stimuli, is used when the viewing angle of the observer is between 1° and 4° (CIE, 2004a).

The \bar{x} , \bar{y} , and \bar{z} colour matching functions shown in Fig. 23 are called the CIE standard colorimetric observer, or the CIE standard 2° observer, referring to the field of view used in the experiments conducted to obtain these functions (CIE, 2004a). The CIE standard observer is commonly used in colorimetric calculations to represent the human visual response to coloured stimuli.

2.2.2 Chromaticity

The XYZ tristimulus values are calculated in a similar way to the RGB tristimulus values. Subsequently, the *chromaticity*, the colour of a light source independent of its luminance, can be derived from the tristimulus values,

$$X = \int_{\lambda} S(\lambda) \bar{x}(\lambda) d\lambda \quad (23)$$

$$Y = \int_{\lambda} S(\lambda) \bar{y}(\lambda) d\lambda \quad (24)$$

$$Z = \int_{\lambda} S(\lambda) \bar{z}(\lambda) d\lambda \quad (25)$$

$$x = \frac{X}{X + Y + Z} \quad (26)$$

$$y = \frac{Y}{X + Y + Z} \quad (27)$$

$$z = \frac{Z}{X + Y + Z} \quad (28)$$

where x , y , and z are the chromaticity coordinates (CIE, 2004a). Since $x+y+z = 1$, it is sufficient to report x , y , and Y (luminance) (CIE, 2004a). The two-dimensional plane diagram, shown in Fig. 24, is the CIE 1931 (x , y) chromaticity diagram. The outer line of the plane diagram is called the spectral locus, with wavelengths marked in nanometres, and the curved interior line is the blackbody locus (or Planckian locus), which indicates the chromaticity coordinates of a blackbody radiator at various temperatures. Colours outside of the chromaticity diagram are called imaginary colours (Agoston, 1979), because they cannot be physically realised. Chromaticity coordinates can be used to display gamut boundaries of a display, characterise colour mixing, and communicate precise colour information about light sources.

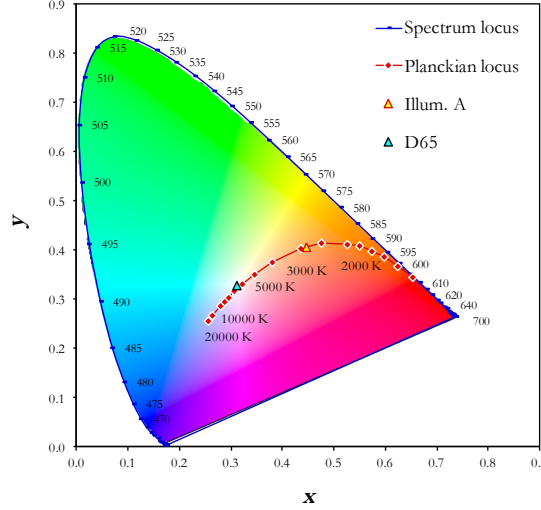


Fig. 24. The coordinates in the CIE 1931 (x , y) chromaticity diagram represent the chromaticity of light stimuli. The spectrum locus (blue line) is the boundary of the diagram where the monochromatic stimuli are represented. The Planckian locus (red line) represents the chromaticities of Planckian radiators at various temperatures. Illuminant A (red triangle) has a relatively low CCT and is positioned near the orange-red region. Illuminant D₆₅ (green triangle) has a higher CCT and neighbours the green-blue region. The coloured background image is for indicative purposes only.

The chromaticity diagram can be used to show colour mixing of light sources. Grassmann's laws provide the mathematical foundations of additive colour mixing, stating the symmetrical, additive and proportional qualities of colour mixing (Grassmann, 1854). The revised Grassmann laws specify the properties of additive colour mixing:

- “To specify a colour match, three independent variables are necessary and sufficient.
- For an additive mixture of colour stimuli, only their tristimulus values are relevant, not their spectral compositions.
- In additive mixtures of colour stimuli, if one or more components of the mixture are gradually changed, the resulting tristimulus values also change gradually” (Hunt & Pointer, 2011).

The tristimulus value of a colour mixture, X_T , Y_T , and Z_T , can be calculated by adding a_1 amount of the first colour stimulus (X_1 , Y_1 , and Z_1) to a_2 amount of the second colour stimulus (X_2 , Y_2 , and Z_2),

$$X_T = a_1 \int_{\lambda} S_1(\lambda) \bar{x}(\lambda) d\lambda + a_2 \int_{\lambda} S_2(\lambda) \bar{x}(\lambda) d\lambda \quad (29)$$

$$Y_T = a_1 \int_{\lambda} S_1(\lambda) \bar{y}(\lambda) d\lambda + a_2 \int_{\lambda} S_2(\lambda) \bar{y}(\lambda) d\lambda \quad (30)$$

$$Z_T = a_1 \int_{\lambda} S_1(\lambda) \bar{z}(\lambda) d\lambda + a_2 \int_{\lambda} S_2(\lambda) \bar{z}(\lambda) d\lambda \quad (31)$$

where S_1 is the spectral power distribution of the first light source and S_2 is the spectral power distribution of the second light source. Additive colour mixing forms the basis of light spectrum optimisation. The spectral properties of mixed light sources can be accurately predicted due to the reliability of these mathematical foundations.

2.2.3 Object colorimetry

While chromaticity and luminance define the colour appearance of a light source, they do not characterise the colour appearance of objects under a light source. The colour appearance of an object can be calculated with tristimulus values similar to those used to calculate chromaticity. For object colours, the colour stimulus function (or the colour signal), $\phi(\lambda)$, is given by

$$\phi(\lambda) = R(\lambda) S(\lambda) \quad (32)$$

where $R(\lambda)$ is the spectral reflectance factor of the object and $S(\lambda)$ is the spectral power distribution of the light source (CIE, 2004a). Therefore, the CIE XYZ tristimulus values can be calculated,

$$X = k \int_{\lambda} R(\lambda) S(\lambda) \bar{x}(\lambda) d\lambda \quad (33)$$

$$Y = k \int_{\lambda} R(\lambda) S(\lambda) \bar{y}(\lambda) d\lambda \quad (34)$$

$$Z = k \int_{\lambda} R(\lambda) S(\lambda) \bar{z}(\lambda) d\lambda \quad (35)$$

where k is a normalising constant,

$$k = \frac{100}{\int_{\lambda} S(\lambda) \bar{y}(\lambda) d\lambda} \quad (36)$$

so that $Y = 100$ for objects that reflect all the light at each wavelength (i.e. perfectly-reflecting white), when $R(\lambda) = 1$ (CIE, 2004a). The Y value provides a basis for correlating the colorimetric calculations with perceived brightness (Hunt & Pointer, 2011). The Y value is given as a percentage, which ranges from zero to 100, except for fluorescent objects (CIE, 2004a). A value of 100 corresponds to an object that reflects all the incident light on its surface and a value of zero means that the object absorbs all the light.

Tristimulus values are consequently extended to a three-dimensional colour space by incorporating chromatic adaptation and nonlinear visual responses (CIE, 2004a; Fairchild, 2013). The attributes of colour that correlate with the perceived hue, chroma and lightness are represented in a three-dimensional colour space, the CIE 1976 ($L^*a^*b^*$) (also known as CIELAB). Calculations of the coordinates for lightness, L^* ,

$$L^* = 116 \left(\frac{Y}{Y_n} \right)^{1/3} - 16 \quad (37)$$

redness-greenness, a^* ,

$$a^* = 500 \left[\left(\frac{X}{X_n} \right)^{1/3} - \left(\frac{Y}{Y_n} \right)^{1/3} \right] \quad (38)$$

and yellowness-blueness, b^* ,

$$b^* = 200 \left[\left(\frac{Y}{Y_n} \right)^{1/3} - \left(\frac{Z}{Z_n} \right)^{1/3} \right] \quad (39)$$

used X_n , Y_n , and Z_n as the tristimulus values of the reference white object, $R(\lambda) = 1$. The tristimulus values X_n , Y_n , and Z_n represent the white adaptation point (i.e. the chromaticity of the illuminant). CIELAB requires the use of a reference white point to account for the human visual system's adaptation to the brightest point in the visual field (Hunt & Pointer, 2011). The $L^*a^*b^*$ coordinates

can be displayed in a three-dimensional Cartesian space similar to Fig. 22. A positive a^* value corresponds to a reddish colour and negative a^* indicates a greenish colour. Similarly, a positive b^* value indicates yellowishness and a negative b^* value signifies bluishness.

The chroma, C_{ab}^* , is calculated by

$$C_{ab}^* = \sqrt{a^{*2} + b^{*2}} \quad (\text{CIE, 2004a}). \quad (40)$$

The colour difference between two stimuli is the Euclidian distance in the CIE 1976 ($L^*a^*b^*$) colour space. It is calculated with the CIE 1976 colour difference, ΔE_{ab}^* , formula,

$$\Delta E_{ab}^* = \sqrt{(\Delta L^*)^2 + (\Delta a^*)^2 + (\Delta b^*)^2} \quad (41)$$

where ΔL^* , Δa^* , and Δb^* are the differences between the coordinates of the two samples (denoted by subscripts 0 and 1), as

$$\Delta L^* = L_1^* - L_0^* \quad (42)$$

$$\Delta a^* = a_1^* - a_0^* \quad (43)$$

$$\Delta b^* = b_1^* - b_0^* \quad (\text{CIE, 2004a}). \quad (44)$$

The difference in chroma, ΔC_{ab}^* , is calculated by

$$\Delta C_{ab}^* = C_{ab,1}^* - C_{ab,0}^* \quad (45)$$

and $\Delta E_{ab}^* = 1$ is considered a just noticeable difference when the objects have the same size, shape, and background luminance (CIE, 2004a; Hunt & Pointer, 2011).

2.2.4 Colour rendering

The need for a quantitative description of the colour quality of a light source dates back to the introduction of specific electric light sources, particularly gas discharge lamps. Early gas discharge lamps had SPDs that were very different from the incandescent lamp spectrum. Some of these gas discharge lamps had CCTs, or even chromaticities, similar to incandescents, but the colour quality of these early gas discharge lamps was significantly different from the commonly used light sources of the day, incandescent and daylight (Schanda, 2007). Therefore, there was a need to quantify the colour quality of a light source with colorimetric tools.

The colour quality of a light source, as it relates to the appearance of illuminated objects, is commonly known as *colour rendering*. The CIE defines colour rendering as the “effect of an illuminant on the colour appearance of objects by conscious or subconscious comparison with their colour appearance under a reference illuminant” (2011). Recommended by the CIE, the colour rendering index (CRI) is a test-sample method that quantifies the magnitude of colour shifts for a set of pre-defined reflective samples when illuminated by a test light source relative to a reference illuminant (1995). The reference illuminants were selected to have an identical CCT to the light source being tested. A blackbody radiator was chosen as a reference when the test light source was under 5000 K and a daylight illuminant when it was at or above 5000 K. A set of eight reflective Munsell colour samples (Munsell, 1915), moderate in saturation and equal in lightness, was chosen for the first publication of the CRI (CIE, 1965; Wyszecki & Stiles, 1982). Another set of six samples, with higher saturation, was later added to the first set, giving a total of 14 samples, as shown in Fig. 25 (CIE, 1995; Schanda, 2007).

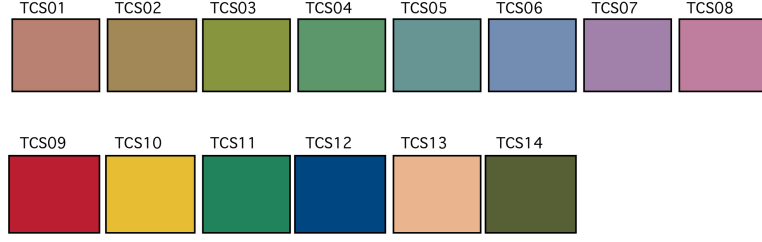


Fig. 25. The colour appearance of the CRI test samples under the D_{65} illuminant. The actual representation of the test samples is limited by the display's colour profile management properties.

After calculating the CIE 1931 XYZ tristimulus values of the test-colour samples, a simple chromatic adaptation transform (CAT) (von Kries, 1902) is applied to account for the observer's state of adaptation, which may differ between the reference illuminant and the test light source. A CIE special colour rendering index, R_i , quantifies the similarity in colour appearance of the test sample when illuminated by the two SPDs. It is computed in the CIE 1964 $W^*U^*V^*$ colour space,

$$R_i = 100 - 4.6 \Delta E_i \quad (46)$$

where i signifies the test-colour sample. The general colour rendering index, R_a , is the average of the special colour rendering indices for the first eight samples,

$$R_a = \frac{1}{8} \sum_{i=1}^8 R_i \quad (47)$$

where the coefficient (4.6) was chosen so that $R_a = 50$ for a warm white halophosphate fluorescent lamp (CIE, 1995; Davis & Ohno, 2009). The maximum value of the general colour rendering index is $R_a = 100$, which indicates that all eight samples appear identical when illuminated by the test source and the reference illuminant (i.e. daylight or Planckian radiator matched to the CCT of the test source).

The term colour rendering is widely used to describe the colour quality of a light source. By definition, however, it is limited to the metrics that employ a reference illuminant and a number of coloured objects. Recently, a broader meaning, *colour rendition*, “the effect of an illuminant (spectrum) on the colour appearance of objects” (CIE, 2017) has been defined, independent from colour rendering.

3 LITERATURE REVIEW

This chapter discusses recent progress in a wide range of topics relevant to this thesis, such as colour quality metrics, the spectral design of light source spectra, energy efficiency in the built environment, and technologies required for the proposed lighting system. The spectral design studies are investigated by focusing on three key aspects: colour quality, energy efficiency and special applications.

3.1 Colour quality metrics

Currently, the CRI is the most widely-used colour rendition metric in the world. However, it has several well-documented shortcomings. The CRI cannot predict visual colour differences accurately due to its outdated colorimetric foundations (i.e. the obsolete CIE 1960 $W^*U^*V^*$ colour space and the Von Kries chromatic adaptation formula) (C. Li, Luo, Cui, & Li, 2011). Negative R_a values (e.g. $R_a = -44$ for low-pressure sodium lamps) and the metric's poor performance for LEDs are among its other shortcomings (CIE, 2007; Narendran & Deng, 2002). Additionally, the CRI poorly predicts the colour rendition of highly saturated colours, due to the moderate lightness and chroma of the first eight reflective test samples, which are not representative of all the colours available in the environment (Davis & Ohno, 2010). Eight test colour samples are not sufficient to represent all the colours perceived by humans, and averaging the special colour rendering indices means that a lamp can be assigned a high R_a even when it renders one or two colours poorly (Davis & Ohno, 2005). Two light sources with identical R_a values can have very different colour rendering abilities. Moreover, the CRI does not consider luminance and ignores well-documented colour appearance phenomena, such as simultaneous contrast, successive contrast, hue changes with luminance, and colourfulness changes with luminance (Wyszecki & Stiles, 1982). The CRI method assumes complete chromatic adaptation, and it specifies a reference illuminant that matches the CCT of the test light source. Light sources with extreme CCTs (e.g. 2000 K blackbody radiator, which appears reddish, or 20000 K daylight illuminant, which appears blueish) can score $R_a = 100$, even though they distort colours significantly (Davis & Ohno, 2009). Another problem with the choice of the reference illuminants in the CRI method is the discontinuity at 5000 K, where the reference illuminant changes from a Planckian radiator to daylight, which implies that a test light source of 4999 K would receive a very different CRI R_a if its CCT was increased only 1.0 K, to 5000 K (Sándor & Schanda, 2006).

The fidelity of object colours is the only criterion embedded in the definition of colour rendering and any aberration of object colour appearance is penalised (Davis & Ohno, 2009). Visual clarity, the feeling of clear distinction between the surface colours of objects (Aston & Bellchamber, 1969), colour preference and colour discrimination are other important dimensions of colour quality. An increase in saturation may result in higher contrast, greater visual clarity (Hashimoto & Nayatani, 1994), improved colour discrimination (Thornton, 1972) and more preferred colour appearances (Camgöz, Yener, & Güvenç, 2002; Ohno, Fein, & Miller, 2015; Smets, 1982). The CRI, however, does not address preference and poorly predicts visual clarity (Hashimoto & Nayatani, 1994) and the colour discrimination capability of light sources (Royer, Houser, & Wilkerson, 2012). These shortcomings were acknowledged by the CIE and several metrics were proposed to replace or assist the CRI (2007). The proposed colour rendition metrics can be analysed in three groups: spectral band methods, gamut/discrimination methods, and test sample methods.

Spectral band methods are based on the similarity of a light source's spectrum to the spectrum of a reference illuminant that has good colour rendering characteristics, such as daylight. The first CIE colour rendering method was published in 1948. The eight spectral band method (Schanda, 2007) and the full spectrum index (FSI) (Rea, Deng, & Wolsey, 2003) compare the spectrum of a light source to a reference equal-energy radiator. However, spectral band methods have fundamental limitations. Although the reference illuminants, such as daylight and incandescent SPDs, have very good colour rendering properties, light sources do not need to have SPDs similar to those of the reference illuminants to achieve high colour rendering, due to the principle of univariance. These metrics also penalise light sources with narrowband emission that result in high efficiency and good colour rendering (Davis & Ohno, 2009).

Discrimination metrics are based on the notion that the number of colours able to be seen under a light source dictates observers' ability to distinguish colours. An increasing number of

colours in the *colour gamut*, “the volume in a colour space consisting of all the colours capable of being created using a particular output device and/or medium” (CIE, 2011), is associated with better discriminability (Thornton, 1972). Some of the gamut-based colour rendition metrics are the colour discrimination index (CDI) (Thornton, 1972), colour rendering capacity (CRC) (Xu, 1993), cone surface area (CSA) (Fotios & Levermore, 1997), categorical colour rendering index (CCRI) (Yaguchi, Takahashi, & Shioiri, 2001), feeling of contrast index (FCI) (Hashimoto, Yano, Shimizu, & Nayatani, 2007), gamut area index (GAI) (Rea & Freyssinier - Nova, 2008), and gamut area scale (GAS) (Žukauskas, Vaicekauskas, & Shur, 2010). In 2017, a new gamut-based method, the gamut volume index (GVI), was proposed to predict colour preferences, using the gamut area (Liu et al., 2017). Although gamut-based indices demonstrate a high correlation with preference, the size of the gamut area is not a perfect indicator of discrimination or object colour naturalness (Jost-Boissard, Avouac, & Fontoynt, 2015). A larger gamut area may cause hue shifts (which are not considered by gamut-based indices) or excessive increases in chroma. Neither of these effects is associated with natural or attractive appearances of objects (Davis & Ohno, 2009; Jost-Boissard et al., 2015; Ohno et al., 2015).

In test sample methods, the colour appearances of a set of predetermined test-samples illuminated by a reference illuminant and test source are compared. Since the CRI is the best-known and most widely accepted colour rendering metric, it is not surprising that several metrics use this approach. Although most of the test-band methods utilise fundamentally similar techniques, their evaluation of the magnitude of colour shifts can vary. Test sample method metrics, such as Pointer’s index (PI) (Pointer, 1986), colour rendering vectors (CRV) (van der Burgt & van Kemenade, 2006), rank-order based colour rendering index (RCRI) (Bodrogi, Brückner, & Khanh, 2011), Monte Carlo method of assessment (Whitehead & Mossman, 2012), CRI-CAM02UCS (C. Li, Luo, Li, & Cui, 2012), and CIE CRI2012 (nCRI) (Smet, Schanda, Whitehead, & Luo, 2013) measure only the fidelity of object colours. On the other hand, based on psychophysical studies (Newhall, Burnham, & Clark, 1957; Sanders, 1959; Siple & Springer, 1983; Yano & Hashimoto, 1997), some test-sample methods, such as the flattery index (Judd, 1967), colour preference index (CPI) (Thornton, 1974), preference index (PS) (Yano & Hashimoto, 1997), and harmony rendering index (HRI) (Szabo, Zilizi, Bodrogi, & Schanda, 2007) take preferred colour shifts into account. Similarly, the memory colour rendition index (MCRI) (Smet, Ryckaert, Pointer, Deconinck, & Hanselaer, 2010) uses objects familiar to the observers as test samples but, instead of a reference illuminant, the memories of colours are used as a reference point to quantify the colour rendition. Additionally, the CIE published the colour fidelity index (2017), which employs updated colorimetric calculations (i.e. CAM02-UCS colour space, a conversion formula to avoid negative values, and a linear transition between reference light sources) and 99 test samples.

These colour rendering metrics consider only one aspect of the colour quality of a light source (e.g. preference, naturalness). Although considering only a single attribute may facilitate the acceptance of a metric, this approach has several limitations, such as the oversimplification of colour rendering and the inability to account for fidelity and preference at the same time. Moreover, choosing a fidelity (naturalness) or preference metric may be problematic due to the trade-off between colour fidelity and preference. A larger gamut increases the object chroma and, thus, preferences to a certain extent, at the expense of fidelity (Houser, Wei, David, Krames, & Shen, 2013). Therefore, a light source with a larger gamut would render object colours differently from a reference illuminant, which may result in higher preference, but decreased fidelity.

Comparison studies suggest that colour fidelity or quality and relative gamut area should be included in a metric to convey enough information about the test light sources (Dangol et al., 2013; Houser et al., 2013; Smet, Ryckaert, Pointer, Deconinck, & Hanselaer, 2011). While some researchers have recommended combining existing metrics - e.g. CRI and CPI (Schanda, 1985), CRI and GAI (Rea & Freyssinier - Nova, 2008; Teunissen, van der Heijden, Poort, & de Beer, 2017), MCRI and GAI (Smet et al., 2011)) - others proposed new metrics to evaluate more than one dimension of the colour rendition, such as the colour fidelity index (CFI), colour-saturation index (CSI), hue distortion index (HDI) (Zukauskas et al., 2009), colour quality scale (CQS) (Davis & Ohno, 2010) and, more recently, TM-30-15 (IES, 2015).

The CQS, Q_a , proposed by Davis and Ohno attempts to address the shortcomings of the CRI by adopting a more uniform colour space (i.e. CIELAB) and CAT (i.e. CMCCAT2000), 15

saturated colour samples and root mean square (RMS) instead of averaging colour difference values, and a mathematical function to avoid negative metric output values (2010). The CQS does not penalise light sources for increasing object chroma when $dC_{ab}^* < 10$, but does penalise light sources with extremely low CCTs due to the reduced colour gamut (Davis & Ohno, 2010). The CQS addresses the three dimensions of colour rendition more specifically with additional scales: the colour fidelity scale (Q_f), the colour preference scale (Q_p) and the gamut area scale (Q_g) (Davis & Ohno, 2010).

Motivated by developments in colorimetry research and the problems associated with the CRI, the Illumination Engineering Society (IES) published TM-30-15 as an alternative to CIE's CRI. Similar to the CQS, TM-30-15 uses a uniform colour space (i.e. CIECAM02), an updated CAT (i.e. CIECAT02), and three metrics to quantify colour fidelity and changes related to saturation: average fidelity index (R_f), average gamut index (R_g), and a colour vector graphic (CVG) (IES, 2015). While R_f ranges between 0 and 100, and R_g ranges between 60 and 140 (when $R_f > 60$), CVG illustrates hue and saturation changes in an a^*b^* plot (IES, 2015). Some of the other improvements are unique to TM-30-15. These include the continuous reference illuminant (between 4500 K and 5500 K, the reference illuminant is a combination of a Planckian radiator and daylight) and a large set of spectrally uniform (equally sensitive to variations in the test SPD) colour samples (David et al., 2015). TM-30-15 offers several improvements to previous colour rendering metrics. However, it combines preference with a gamut measure and ignores the effects of CCT on discriminability.

An important limitation of all the colour rendering metrics is their low correlation with psychophysical data, especially when light sources are not limited to a specific CCT (i.e. multi-CCT scenarios) (Houser et al., 2013; Liu et al., 2017). The results of several metric comparison studies (Dangol et al., 2013; Fumagalli, Bonanomi, & Rizzi, 2015; Houser et al., 2013; Jost-Boissard et al., 2015; Jost-Boissard, Fontoynt, & Blanc-Gonnet, 2009; Khanh & Bodrogi, 2016; Smet et al., 2011) were inconsistent. Metrics that were well correlated with psychological data in some studies had low correlations with human judgments in other experiments. No single metric performed well in all studies. The metric comparison studies indicate that, even though new metrics have stronger theoretical foundations (i.e. updated colour spaces, CATs, the inclusion of visual phenomena), they do not perform significantly better than metrics based on simpler models (Houser et al., 2013). An underlying shortcoming could be the multi-dimensional nature of colour, as well as the ambiguity of lighting quality as opposed to colour quality. Light quality for white light sources is not well defined in the literature. Naturalness, preference, discrimination, vividness, visual clarity, brightness, harmony and border sharpness are some of the parameters that have been used to define the quality of a light source (Bodrogi, Brückner, Khanh, & Winkler, 2013; Vrabel, Bernecker, & Mistrick, 1998). This lack of consensus may be caused by the complexity of defining the context in which object colour appearance is judged.

Colour rendition metrics quantify the colour quality of white light sources by looking at a range of object colours possible in a space. These metrics are formalised to compare commercially available light sources in a practical manner. For example, a set of reflective test samples are chosen to represent the colour of objects in any given space, since the actual objects and their reflectance characteristics are usually unknown. However, if the reflectance characteristics of surfaces were known, the test samples and need for a wider gamut would be unnecessary. In such a case, it would be possible to calculate the particular hue, brightness and chroma shifts, which would quantify the quality of the object colours.

3.2 Spectral design

3.2.1 Efficacy and colour rendering

Both colour rendering and luminous efficacy of radiation are determined by the spectrum of a light source. A broad spectrum, similar to the reference illuminants of daylight and the incandescent lamp, can yield good colour rendering. However, several studies have demonstrated that a broadband spectrum is not necessary to achieve high colour rendering (Ohno, 2005; Ries, Leike, & Muschaweck, 2004; M. Zhang, Chen, & He, 2014; Žukauskas, Vaicekauskas, Ivanauskas, Gaska, & Shur, 2002). Furthermore, broadband light sources are typically not very efficient as a result of the relative insensitivity of the visual system to the very short and very long wavelengths of the visible spectrum.

On the other hand, the LER can reach a theoretical maximum of 683 lm/W for the monochromatic radiation of 555 nm. If a light source emits power mostly in the region of 555 nm, there will be an increased perception of light intensity. Such a light source (green light), however, would not be very useful in architectural spaces. This conundrum illustrates the inverse correlation between colour quality and energy efficiency. The inverse relationship between efficiency and colour quality is not linear, due to variations in spectral power distributions, differences in the cone cells' spectral sensitivities, and the complexity of signal transmission from the retina to the visual cortex.

Nonetheless, it is possible to design a spectrum with high luminous efficacy without sacrificing colour quality. As discussed, the principle of univariance states that the colour signal perceived by the visual system can be a result of various types of illumination. It is thus possible to design a spectrum composed of narrowband components that leads to a colour signal identical to one that is initiated by a broadband illuminant.

3.2.2 Spectral optimisation

The trade-off between colour quality and energy efficiency is an important criterion for spectral design. The wide adoption of SSL technologies and their increasing luminous efficacy led to several research projects concentrating on the optimisation of light sources to achieve both high luminous efficacy and high colour quality. Additive colour mixing of narrowband spectra (He & Yan, 2011; Oh, Oh, Park, Sung, & Do, 2011; Speier & Salsbury, 2006) and adjustment of peak wavelengths and bandwidths (Lu, Gao, Chen, & Chen, 2007) and lens design (Chien & Tien, 2011) are some of the techniques used in the optimisation processes. Colour rendering metrics, particularly the CRI, have been used as a benchmark to optimise the spectra of various lighting technologies, such as LEDs (Guo et al., 2013; Speier & Salsbury, 2006), lasers (Neumann et al., 2011), OLEDs (Shuming Chen, Tan, Wong, & Kwok, 2011) and quantum dots nanophosphors (Zhong, He, & Zhang, 2012a).

One of the simpler methods of optimisation is to target high colour rendering values without considering other parameters (e.g. LER). Earlier studies investigating the CRI claimed that some wavelengths were more significant than others. Thornton (1971) indicated that spectral power at 450 nm, 540 nm, and 610 nm was required to maximise CRI values, while spectral power in the regions of 500 nm and 580 nm were detrimental. Similarly, a computer-aided optimisation technique identified three key regions of spectral power (455 nm to 485 nm, 525 nm to 560 nm, and 595 nm to 620 nm) as necessary to achieve high colour rendering (Koedam & Opstelten, 1971). When the spectra consisted of power in these regions, the maximum R_a values ranged from 79 to 87 for CCTs between 2280 K and 6730 K (Koedam & Opstelten, 1971). In line with the earlier studies, a more recent mathematical model investigating the CRI has shown that R_a has sensitivities around the wavelengths of 444 nm, 480 nm, 564 nm and 622 nm, and R_g around 461 nm, 581 nm and 630 nm (Lin et al., 2014). In that study, the recorded maximum colour rendering values were $R_a = 94.4$ and $R_g = 97.2$ (Koedam & Opstelten, 1971). However, high colour rendering white light can also be generated by mixing wavelengths from different spectral regions. Psychophysical experiments have shown that a combination of four lasers at 457 nm, 532 nm, 589 nm and 635 nm can reach $R_g = 90$, and its light can be indistinguishable from reference white light sources (Neumann et al., 2011). Similarly, a study investigating the wavelength dependence of the colour rendering properties of a light source with CQS Q_a values, instead of CRI R_a , found that spectral power in the region of 580 nm was slightly detrimental to the CQS Q_a (H. Li, Mao, Han, & Luo, 2013), supporting previous claims by Thornton (1971). The same study also claimed that, to achieve high colour rendering, the SPD of a light source should be divided into three regions (380 nm to 495 nm, 495 nm to 595 nm, and 595 nm to 675 nm) (H. Li et al., 2013). It is not surprising that these three regions are close to the borders of the visible spectrum. It is important to note that a set of predetermined narrowband LEDs were optimised in this study. As a result, the optimal solutions were bound to be in a predetermined spectral shape (i.e. three peak spectrum). Although the data from these computational analyses may hold true, taking these values as a guideline may limit the possibilities of future light sources that are not bound to the incumbent spectral shapes.

The efficiency of a light source is another important consideration in spectral design. Several studies introduced luminous efficacy and LER to the optimisation process as a second parameter. A recent study showed that LER values of up to 360 lm/W for $R_a = 91$ at 3260 K and 313 lm/W

for $R_a = 95$ at 5490 K are achievable by creating a modified Planckian-like spectrum (Hertog, Llenas, Quintero, Hunt, & Carreras, 2014). In this study, the modified continuous spectra were created by mixing narrowband emitters to simulate spectra with reduced radiation in the short wavelengths, 380 nm to 550 nm, and long wavelengths, 560 nm to 730 nm (Hertog et al., 2014). Similarly, a computer simulation based on additive colour mixing led to R_a and R_9 values higher than 98, while the LER values ranged from 296 lm/W to 334 lm/W for CCTs between 2700 K and 6500 K (He & Yan, 2011). Other studies also demonstrated that good colour rendering can be achieved without sacrificing LER. Ohno (2004) performed calculations using three-band and four-band LEDs, where a four-band LED was optimised to $R_a = 97$, $R_9 = 96$, $R_{9-12} = 87$ and LER = 361 lm/W. Hung and Tsao (2013) developed SPDs with 396 lm/W and $R_a = 95$ at 2856 K, as well as 386 lm/W and $R_a = 97$ at 2856 K. However, high R_i values do not guarantee that the object colours that are not represented in the CRI sample set would be rendered well. The well-established shortcomings of the CRI signal the drawbacks of single degree of freedom optimisation techniques. Furthermore, optimising a spectrum for a single metric may lead to “gaming” the system. As Goodhart’s law states, “when a measure becomes a target, it ceases to be a good measure” (Strathern, 1997).

Several spectral optimisation studies took additional metrics into account to address the CRI’s shortcomings (Boissard & Fontoynont, 2009; Chien & Tien, 2012; Xiangfen Feng, Xu, Han, & Zhang, 2016). One of these studies employed a nonlinear program to achieve LER values up to 357 lm/W when CRI R_a values ranged from 90 to 96 and CQS Q_a values were between 90 and 95 (Zhong, He, & Zhang, 2012b). The same research group demonstrated even higher values using quantum dot white LEDs (QD-WLED) instead of pcLEDs. With the optimal values of the CRI $R_a = 95$, $R_9 = 95$, the CQS Q_a values ranged from 90 to 95 and the LER ranged from 327 lm/W to 371 lm/W using the QD-LEDs (Zhong et al., 2012a). Other parameters, such as D_{uv} (Guo et al., 2013), “the distance from the chromaticity coordinate of the source to the Planckian locus on the CIE 1960 $W^*U^*V^*$ chromaticity diagram, with polarity plus above the Planckian locus or minus below the Planckian locus” (Ohno, 2005), a similar measure, chromaticity distance (Thorseth, 2012), and junction temperature (Chhajed, Xi, Li, Gessmann, & Schubert, 2005) have also been used in optimisation studies in addition to colour rendering metrics and LER. A study simulated and realised three and four band LEDs that were optimised for MCRI, LER and chromaticity similarity to a set of reference illuminants (Smet, Ryckaert, Pointer, Deconinck, & Hanselaer, 2012). In visual appreciation experiments, the optimised LED (CRI $R_a = 79$, LER = 270 lm/W) was ranked higher than the reference incandescent illuminant (CRI $R_a = 100$, LER = 140 lm/W) when attractiveness, preference, naturalness, vividness and memory were considered (Smet et al., 2012).

3.2.3 Application specific optimisation

It is possible to adjust the spectral output of a light source for a range of parameters other than the colour quality of light sources. Various optimisation studies have been undertaken in the context of specific applications. These studies can be grouped into two main categories, visual and non-visual effects of lighting.

3.2.3.1 Visual effects of lighting

Several application-based optimisation studies have focused on various themes, such as mesopic lighting (Yao, 2016; Yao, Yuan, & Bian, 2016; Žukauskas, Vaicekauskas, & Vitta, 2012), retail lighting (XF Feng, Xu, Han, & Zhang, 2017), and lighting for clinical applications (Ito, Higashi, Ota, & Nakauchi, 2015; Wang, Cuijpers, Luo, Heynderickx, & Zheng, 2015). The completion of visual tasks, appreciation of the built environment and energy efficiency are common factors investigated in these types of studies. For example, a study investigating energy efficiency in buildings and visual comfort found that dynamic simulations of LEDs can reduce the energy consumption by 38 % without causing visual discomfort to the occupants (Yun, Jung, & Kim, 2013). In that study, LEDs that increase the chroma of blue and red objects were tested at different illuminance levels. The results showed that participants preferred the red-enhancing SPDs, which resulted in lower energy consumption than the blue-enhancing SPDs (Yun et al., 2013).

Museum lighting and conservation of illuminated artworks are themes highly relevant to the ideas proposed in this thesis (i.e. light absorption by objects and colour quality of light sources). Damage to artwork by visible and invisible radiation, as a function of time and illumination power, has been well documented (Beek & Heertjes, 1966; CIE, 2004b; Cuttle, 1996; Feller, 1964). Although lighting is needed for visibility, which leads to appreciation of the artwork, the radiation absorbed by the artwork causes damage. Studies have shown that tuning the spectral output of a light source may help address this challenge. A three-band spectrum that emits lower irradiance was found to be an acceptable alternative to the tungsten halogen lamp in terms of perceived brightness and overall appearance of the lit artworks, and it resulted in decreased energy absorption (Cuttle, 2000). In another study, a light source spectrum was customised by applying several filters to prevent the colourants from fading while maintaining the illuminance incident on the artworks (Delgado, Dirk, Druzik, & WestFall, 2011). Visual assessments showed that the appearance of the artwork under the three-band spectra and the reference light source was indistinguishable, although the statistical confidence for equality of perception of details and overall satisfaction were slightly reduced (Delgado et al., 2011). A common limitation of both of these studies was the use of filters to block out some of the spectral power. An improved solution would be to design spectra that do not emit power at certain wavelengths in the first place, rather than using bandpass filters. This would eliminate the problem of energy absorption by the filters, thus reducing the energy consumed by lighting.

The spectrum of a light source could also be adjusted to compensate for the desaturation of object colours caused by previous photochemical reactions, as well as preventing additional damage from the lighting. A recent study showed that the degradation of the colour of a work of art could be enhanced by chroma-increasing customised SPDs (Viénot, Coron, & Lavédrine, 2011). Other researchers used non-linear optimisation tools to reduce shifts in the colour appearance of 26 pigments in the frescoes of the Sistine Chapel by adjusting four LED channels (red, green, blue, warm white) relative to a reference daylight illuminant (Schanda, Csuti, & Szabo, 2016). Visual assessments by museum curators confirmed the acceptability of the optimised spectra, though green and blue pigments had lower lightness and red and yellow pigments had higher lightness under optimised spectra than reference spectra (Schanda et al., 2016). Similarly, Berns optimised three-band LEDs to minimise the colour difference between the colour appearance of 24 test samples under the test SPDs and reference D_{65} illuminant (2011). The optimisation parameters were the CRI R_a , LER and chroma values (to compensate for the loss of saturation in the paintings due to damage) (Berns, 2011). The results showed that the three-band light source could render materials similarly. The three-band LEDs had similar LERs and emitted less radiance, thereby reducing damage to the artwork. Berns stated that colour mismatches might occur under a triband light source, but added that these mismatches would occur significantly less than would be the case with a tungsten lamp (2011), which currently accounts for around 50 % of museum lighting (Perrin, Druzik, & Miller, 2014). In another study, researchers used damage factor as an optimisation parameter, in addition to chromaticity and colour quality (i.e. saturation), while maintaining a constant irradiance (Tuzikas, Žukauskas, Vaicekauskas, Petrulis, Vitta, & Shur, 2014). A relative damage factor (RDF) was defined to be equal to 1.0 for incandescent illuminant, where $RDF < 1.0$ indicated reduced damage. Optimised spectra resulted in reduced damage for low-grade paper (RDF between 0.23 and 0.43) and oil paintings (RDF between 0.77 and 0.89) (Tuzikas et al., 2014). However, the researchers reported colour quality using colour rendition metrics instead of quantifying the colour appearance of individual pigments. The optimised spectra had varying colour qualities (between $R_a = 16$ and $R_a = 96$, $Q_f = 35$ and $Q_f = 92$), which underscores the trade-off between damage and colour quality.

The results from several studies underscore the importance of spectrum optimisation in museum lighting. The optimisation of the spectrum has the potential to decrease the damage to artwork, which in turn increases the lifetime of fragile museum artefacts. The optimised spectra have the additional advantage of being free of UV and IR, which is damaging to art. However, the uniformity of the chroma shift, hue distortions, and overall change in the colour appearance of the artwork must be taken into account.

3.2.3.2 Non-visual effects of lighting

3.2.3.2.1 Circadian rhythm

Research investigating the non-visual biological effects of lighting on humans has increased in recent decades. The discovery of melanopsin, a light-sensitive photopigment (Provencio et al., 2000), an understanding of the ipRGCs' role in melanopsin suppression (Hattar et al., 2002), and knowledge of the impacts of illumination on circadian rhythms, mood, behaviour, alertness, and cognitive performance (Cajochen, 2007; Chellappa et al., 2011; Vandewalle, Maquet, & Dijk, 2009; Webb, 2006; Zaidi et al., 2007) added complexity to the consideration of the relationships between light and humans. New measurement quantities, such as the circadian efficiency function (or circadian action function), $\epsilon(\lambda)$, circadian efficacy of radiation, K_c , circadian action factor, a_{cr} (Gall & Lapuente, 2002), circadian efficiency, C_{VF} (Bellia, Bisegna, & Spada, 2011), melanopic spectral efficiency function, $V_{\epsilon}(\lambda)$ (Enezi et al., 2011), circadian illuminance (Oh, Yang, & Do, 2014), melatonin suppression index (MSI) (Aubé, Roby, & Kocifaj, 2013), and circadian light, CL_A (Rea, Figueiro, Bierman, & Hamner, 2012), have been proposed based on research investigating the wavelength dependency of the non-visual human response to visible radiation (Berson, Dunn, & Takao, 2002; Brainard et al., 2001; Dacey et al., 2005; Kozakov, Franke, & Schöpp, 2008; Thapan, Arendt, & Skene, 2001).

Researchers have started using the data from these studies to add additional parameters to optimisation processes. For example, in a recent study, 16 LEDs were optimised for six parameters: maximum and minimum impact on the ipRGCs, LER, colour gamut, damage to museum objects and minimum impact on *photoresists* (light-sensitive materials) (P. C. Hung & Papamichael, 2015). All of the optimised SDPs were noted to consist of spiky spectra, which indicated that a higher level of spectral controllability might improve these results in the future (P. C. Hung & Papamichael, 2015). Another study used a non-linear programming tool to optimise three-band LEDs for circadian action factor, LER, CCT and CRI (Kozakov, Franke, & Schöpp, 2008). However, an optimisation condition that required the spectrum to be similar to a Planckian radiator resulted in a forced reduction in LER values. Similarly, the customisation of four narrowband LEDs for circadian action factor, LER, and CQS Q_f revealed that, to achieve a high number of variations in the circadian function, which is important for an adaptive lighting system (i.e. a lighting system that impacts the circadian system differentially throughout the day), the constraints on LER and colour rendering should be loosened (Žukauskas & Vaicekauskas, 2015). Analogous limitations have been identified by another study that investigated energy efficiency (i.e. LER and luminous efficacy), colour quality (i.e. CRI R_a and CQS Q_a), circadian efficacy (i.e. K_c and a_{cr}), and circadian performance (i.e. MSI) of several existing light sources and optimised four-peak LEDs (Oh, Yang, & Do, 2014). Other studies have optimised the light source spectrum for mesopic vision, in addition to the energy efficiency, circadian and light quality metrics, and have reached similar conclusions (Yao, 2016; Yao, Yuan, & Bian, 2016; Žukauskas, Vaicekauskas, & Vitta, 2012). Unsurprisingly, the results from these studies reinforced the trade-off between energy efficiency and colour qualities of a light source (i.e. circadian function and colour rendering), adding more complexity to the optimisation process.

It is also important to note that the factors affecting circadian rhythm might be oversimplified. Although wavelength is a key component in the *entrainment* of the human non-visual system, intensity, timing, duration and spatial distribution of the light may also influence circadian rhythms (Rea, Figueiro, & Bullough, 2002). Furthermore, the body of current research is based on the assumption that the ipRGCs are solely responsible for the circadian rhythm entrainment through melatonin suppression and that ipRGCs are mainly sensitive to the shorter wavelengths. The discovery of additional factors influencing the human non-visual system may challenge the accuracy of the proposed circadian metrics.

3.2.3.2.2 Horticulture

Photosynthesis is the process by which plants convert carbon dioxide and water into oxygen and glucose. A green pigment, chlorophyll, allows plants to absorb electromagnetic radiation and convert it into chemical energy. The light absorption of two of the most common types of green pigments, chlorophyll-a and chlorophyll-b, peaks at around 429 nm and 660 nm, and at 454 nm and 643 nm, respectively (Porra, Thompson, & Kriedemann, 1989). Carotenoids, pigments found

in plants, algae, bacteria and fungi, also contribute to photosynthesis by absorbing radiation, mostly at short wavelengths (peaking at 449 nm and 488 nm), including UV-A and UV-B (De Fabo, Harding, & Shropshire, 1976). Photomorphogenesis refers to the light-aided growth and development of plants independent of photosynthesis (H. Mohr, 1972). In plants, the processes of seed germination and development and of *photoperiodism* (an organism's reaction to the daily cycle) are guided by photoreceptors, such as phytochromes, whose absorption spectra differ slightly from those of the chlorophylls (Sager, Smith, Edwards, & Cyr, 1988). Although their absorption spectra do not perfectly align, the photoreceptors absorb radiation mostly in short and long wavelengths (UV, blue light, red light, and far-red light), and reflect light in the middle wavelengths, thus resulting in the green appearance of plants. In summary, optimal plant growth requires a light source with emission in the spectral regions that correspond to the action spectra of the physiological activities of plants.

The rapid adoption of LEDs in horticultural research and applications was possible due to distinctive properties of the LEDs, such as their compact size, spectral flexibility, low radiant heat output, long operating lifetimes, and the potential cost savings from reduced energy consumption (Morrow, 2008). Early horticultural research on LEDs was undertaken by NASA “for the development of plant-based regenerative life-support systems for future Moon and Mars bases” (Morrow, 2008). Studies showed that narrowband LEDs can enhance photosynthesis and photomorphogenesis (Brown, Schuerger, & Sager, 1995; Goins, Yorio, Sanwo, & Brown, 1997; Stutte, 2009). Several studies showed that increased plant growth is possible with optimised spectra (Tamulaitis et al., 2005), even with additional parameters such as energy consumption (Poulet et al., 2014) and colour rendering (Oh, Kang, Park, & Do, 2015). Additionally, it has been proposed that customised lighting systems could initiate early and uniform flowering, reduce insects and diseases in certain crops, and generate crops enriched with vitamins or minerals (Massa, Kim, Wheeler, & Mitchell, 2008).

Optimising the spectral output of a light source might support the production of a healthy yield, especially in places where space and resources for growth are limited. However, several issues require further investigation and challenges need to be addressed to ensure the successful utilisation of spectrum optimisation. One of the limitations of narrowband visible LEDs is the lack of UV, which can be beneficial for certain crops (Massa, Kim, Wheeler, & Mitchell, 2008). Another potential problem is the absence of green light (removed by the optimisation process to reduce energy consumption), which can impact the colour appearance of the plants and obstruct the diagnosis of diseases and disorders by human observers (Massa et al., 2008). Adding colour rendering as a parameter to the spectrum optimisation would likely lower the energy efficiency of the light source. This problem could be addressed by limiting the spectra optimised for the colour appearance of the plants to the duration of the visual assessment of the crops.

Another issue is the slight variation in the absorption spectra of the chlorophylls, which depend on the solution used (e.g. chloroform, diethyl ether) in in-vitro studies (Porra, Thompson, & Kriedemann, 1989; Wellburn, 1994). Moreover, differences between in-vitro and in-vivo measurements of the absorption spectra of individual pigments indicate complexity in quantifying the action spectrum of plant physiological activity (Moss & Loomis, 1952). There might be other parameters relevant to plant growth that may not be directly related to the spectral properties of a light source. For example, light source position, intensity, and spatial distribution might impact plants' growth and life cycle. In short, more research is needed to clarify the precise spectral content required for different species before they can be introduced as parameters in the optimisation process.

Several studies have discussed the optimisation of light sources for increased light quality and energy efficiency and have focused on specific applications. Although some of these applications are beyond the scope of this project, it is worthwhile noting the range of themes to which spectral design could be applied. These studies have only used LEDs for spectral modelling, whereas a technology-independent optimisation process would enhance the usefulness of the research findings. Since SSL devices continue to progress rapidly, it is reasonable to expect increased precision in control of the light source spectrum in the future. It is also likely that lighting technologies beyond the SSL will emerge. Therefore, a theoretical, technology-independent approach to the optimisation process could be beneficial as a guide for the future studies.

3.3 Energy efficiency in the built environment

The International Energy Agency reported that the total electricity consumed by lighting was 3,418 terawatt hours (TWh) in 2006, representing 19 % of the total electricity consumption in the world (17,982 TWh) (Waide & Tanishima, 2006). While almost half of the lighting consumption (1,460 TWh) consisted of commercial lighting, residential and industrial lighting made a substantial contribution to total consumption, 1,045 TWh and 632 TWh, respectively (Waide & Tanishima, 2006). North America was found to have the highest per-capita light use with 101 megalumen hours (Mlmh), followed by Japan-Korea (72 Mlmh) and Australia-New Zealand (62 Mlmh) (Waide & Tanishima, 2006). In a more recent IEA publication, lighting accounted for 18 % of total electricity demand worldwide (2014). The financial ramifications of lighting consumption were estimated to be around USD 455 billion, 0.72 % of the world's gross domestic product (GDP) (S. T. Tan et al., 2012).

In the United States of America, one of the main consumers of energy in the world, 10 % of the total electricity consumed in commercial and residential buildings was used for lighting in 2016 (EIA, 2017). The U.S. Energy Information Administration (EIA) estimated electricity consumed by lighting to be around 279 TWh, which accounted for 7 % of total U.S. electricity consumption (2017). In Australia, lighting accounted for the consumption of around 27 petajoule (PJ) of energy in 2008, equivalent to 7.5 TWh (Harrington & Foster, 2008). This is nearly double the consumption levels of 1986, while a decrease of 25 PJ (approximately 6.9 TWh) in consumption is projected for 2020 (Harrington & Foster, 2008). Electricity use for lighting in commercial buildings varied according to the type of building. For example, electricity use by lighting accounted for 26 % in offices, 20 % in hotels, 17 % in other hospitality applications, 18 % in universities, and 28 % in courthouses in 2012 (Council of Australian Governments, 2012).

Electricity consumption contributes to greenhouse emissions, which have diverse effects on the environment. Many of the world's governments aim to reduce carbon emissions to limit long-term increase in average global temperature, which is critical to prevent extreme weather conditions and rising sea levels (IEA, 2013a). According to the World Energy Outlook, global carbon dioxide emission in 2014 was around 32.2 gigatonnes (Gt) (IEA, 2016). Along with the USA and Saudi Arabia, Australia has one of the highest carbon emissions per capita in the world, around 19 metric tonnes of equivalent carbon dioxide (Mt CO₂-e) per person, due to its dependency on coal to generate electricity (Perry, Henry, Perry, & MacArthur, 2015). In 2006, Australia's total emission was 576 million Mt CO₂-e (Council of Australian Governments, 2012), of which lighting contributed around 25 million Mt CO₂-e at a cost of approximately AUD 2 billion (Tilbury, Douglas, & Rowland, 2006). In 2015, Australia's greenhouse emission dropped to 527 million Mt CO₂-e, but it is projected to grow around 3 % by 2020 despite efforts to meet the Kyoto Protocol targets for 2020 and 2030 (Tilbury et al., 2006).

Several ways of reducing the amount of electricity consumed by lighting have been proposed and implemented. These include the use of various sensors, incorporating daylight in buildings, and the use of luminaires with higher luminous efficacies. The EIA predicts a decline in the energy consumed by lighting in 2040 due to the widespread adoption of LEDs and energy efficiency programs (2017). Similarly, the IEA foresees a 40 % reduction in electricity usage by lighting by 2050 resulting from the adoption of SSL devices, improved building design and incorporation of daylight into buildings (2013b).

On the other hand, the unpredictability of the future costs of producing energy, electricity consumption trends and sudden changes in political, economic and social factors could undermine energy consumption predictions (Paltsev, 2017). For example, a side effect of reductions in energy costs and lighting products is the rebound effect, the increase in energy consumption due to lowered prices (Herring & Roy, 2007). Herring and Roy identified three types of rebound effects: direct effects (increase in the consumption of the service due its lower price), indirect effects (spending the saved income on other services and products that consume energy), and economy-wide effects (changes in consumer preferences due to long-term changes in the economy) (2007). The increasing efficiency of lighting technologies, the decreased price of lighting services and the increase in lighting consumption are suggestive of the rebound effect. Indirect effects, such as the output of a service or a product acting as the input of another service or product, however, could be subtler and harder to track and record (Herring & Roy, 2007). For example, if the costs of steel

(output of a service) decrease, the costs for car manufacturing (another service) would decrease as well. This would lead to a higher demand for cars, which leads to an increase in overall production and consumption in the economy. It should be noted, however, that only 5 % of the income from these savings is estimated to be re-spent on services that use energy (Schipper & Grubb, 2000). The third type, economy-wide changes due to the rebound effect, is considered likely to have the greatest impact in the long term. An example of economy-wide effects is the drop in electricity and luminaire manufacturing costs, which encouraged the expansion of electric lighting in other markets, such as security and outdoor lighting (Herring & Roy, 2007). It is still debated whether energy use would have been higher if there had been no policies regulating lighting efficiency (Herring & Roy, 2007). Variation in the energy consumption data by economic sector and by country, level of response by micro-economic (consumers) and macro-economic (nationwide) elements, and the unfeasibility of running control experiments have posed a challenges to clarifying the impact of the rebound effect (Herring & Roy, 2007).

Consumer behaviour is a substantial factor in the success of lighting efficiency practices. Technological innovations and financial and regulatory incentives can shape consumer lifestyles to increase the effectiveness of the proposed solutions. Despite increasing public awareness, surveys showed that households in Australia believe that lighting accounts for only around 3.8 % of energy costs (Australian Bureau of Statistics, 2012), in reality, lighting accounts for 8 % to 15 % of total household electricity costs (Milne & Riedy, 2013). A simpler solution, switching off unnecessary light sources, is recommended to lower energy consumption in buildings (Masoso & Grobler, 2010) but this method can be problematic as it depends solely on occupant behaviour, which is difficult to influence.

The global energy crisis and the need for increased sustainability have had a significant impact on the lighting industry in the last few decades. The increasing luminous efficacy of lighting products, public awareness, and government interventions can be considered as natural reactions to the changing political, social and economic climate. However, the advancement of SSL products, plummeting energy prices and increasing energy efficiency of lighting technologies may not be enough to secure a sustainable future. There are still 1.2 billion people in the world who do not have access to electric lighting (WEC, 2016). Additionally, recent developments in the lighting industry have several limitations. For example, lighting technologies have theoretical efficacy limits, such as the theoretical boundary of the LER (683 lm/W) that can only be achieved by a monochromatic green light, and the maximum luminous efficacy of white light sources, which can only achieve efficacies between 250 lm/W and 370 lm/W (Murphy Jr, 2012), depending on the radiant efficiency and definition of *whiteness* of the light source. Furthermore, occupants' interactions with lighting systems through controls and their attitudes toward lighting products are crucial for reducing lighting consumption. These factors limit the full potential of current technological capabilities. Intelligent lighting approaches may address the issues of energy efficiency and consumer acceptance by creating adaptive systems, instead of solely producing lighting products with higher efficacies.

3.4 Sensors and projection systems

A tuneable lighting system that minimises light absorption by objects would require a number of technological features, such as the ability to scan the built environment, estimate the reflectance properties of the objects and emit customised light onto objects with high precision. Although implementing such a system seems challenging in terms of current technological capabilities, there are several important developments worth mentioning. This section presents the relevant literature on sensing and projection technologies with potential applications in the proposed lighting system.

3.4.1 Reflectance estimation

Humans have a great ability to distinguish the identity of an object (e.g. food) and its physical state (e.g. fresh, rotten) under various illumination conditions. Research shows that humans rely on pre-stored assumptions about the illumination conditions of the real world when estimating the reflectance of objects (Dror, 2002). Following the human vision model, computer vision studies have established a similar set of assumptions about light sources and reflective surfaces that form the basis of surface estimation algorithms (Wandell, 1995). These assumptions are centred on the

lack of variety in the surface reflectance factors of real objects and the spectral properties of physical illumination sources. Although computer vision systems are not as accurate as the human visual system at recognising objects in real-world environments, there is a growing body of research investigating the recognition of objects' surface properties (i.e. reflectance, texture) by computer systems.

In the field of digital colour imaging and computer vision, several different techniques have been proposed to estimate the surface reflectance of objects (Chou & Lin, 2012; Hardeberg, 2001; Imai, Berns, & Tzeng, 2000; Yu, Debevec, Malik, & Hawkins, 1999; Yu & Malik, 1998), light source position (Hara & Nishino, 2005), and the spectrum of the light sources (Tominaga & Wandell, 1989). Recent research showed that some of these estimation algorithms and models (i.e. principle component analysis, pseudoinverse matrix, dichromatic reflection model, Wiener model, Shi-Healey model, and Imai-Berns model) can also be used to estimate the reflectance functions of real objects (Agahian, Amirshahi, & Amirshahi, 2008; Shimano, 2006; Shimano, Terai, & Hironaga, 2007; Tominaga, 1991). Studies estimating the reflectance factor of real objects deployed different scanning techniques and technologies, such as multispectral cameras (Shimano et al., 2007; Shrestha, Mansouri, & Hardeberg, 2011), colour encoded light projection (SY Chen, Li, Guan, & Xiao, 2006), and hyperspectral imaging (Klein, Alderink, Padoan, De Bruin, & Steemers, 2008). Most of these studies estimated the reflectance factors of surfaces in environments where objects and light sources were immobile. Other studies aimed to investigate real-time motion and surface recognition (Newcombe, Izadi, et al., 2011), real-time object tracking and mapping (Newcombe, Lovegrove, & Davison, 2011), and surface estimation under changing illumination conditions and viewpoints (Birkbeck, Cobzas, Sturm, & Jagersand, 2006). The increasing precision and accuracy of surface reflectance estimation of 3-D real objects in real time by computer systems has the potential to enable the implementation of spectrally optimised smart lighting systems as proposed in this thesis.

3.4.2 Projection systems

Adaptive and tuneable lighting systems have been previously proposed and developed for research purposes (Dong, Hombal, & Sanderson, 2012; Miller, Ohno, Davis, Zong, & Dowling, 2009). However, the materialisation of the spectrally tuneable lighting system that is proposed in this thesis requires higher precision of the projected light to illuminate each object in the built environment. The *spatial resolution* of the projection system, the size of the smallest detectable object, is a key parameter, and it is primarily determined by the field of view, the surface of the projection area, and the distance between the source and projection area (Canada Centre for Remote Sensing, 2015). Low resolution of an optical system implies a reduction in the sharpness and contrast of the illuminated surface. Although the implementation of the proposed system is fundamentally an engineering problem, some significant progress in the field of optics and engineering will be discussed here.

Research investigating high-resolution projection systems covers various fields, such as film projection (Zheng et al., 2008), augmented reality (Torres, Jassel, & Tang, 2012), biomedical engineering (C.-C. Hung, 2016), and stage lighting (Chakrabarti et al., 2016; Dorsey, Sillion, & Greenberg, 1991). Recent studies utilised several optical design techniques to enhance the focus, speed, luminance and optical efficiency of projection systems using micro-optics (Mönch, 2015), freeform optics (surfaces fabricated beyond standard shapes that have rotational symmetry) (Bruneton, Bäuerle, Wester, Stollenwerk, & Loosen, 2013), planar waveguides (optical structures that guide electromagnetic waves) (Melletto, Schuster, & Ford, 2014) and tuneable lenses (Blum, Büeler, Grätzel, & Aschwanden, 2011). For example, multifocal projectors can alter the focal depth of a projection system independent of the ambient luminance, surface colour and texture, projector orientation, luminance and *chrominance* (chroma signal in video systems approximating hue and saturation) (Bimber & Emmerling, 2006). Another study described an optical simulation and mechanical design of a three-colour (RGB) projection system which aimed to maintain a constant CCT at a *surface area* (the area where the maximum illuminance is 50 % of the illuminance of the centre point) of 1 cm² and 2.5 cm², at distances of 80 cm and 120 cm from the light source, respectively (C.-C. Hung, 2016). Hung maintained constant CCT, instead of using a colour rendering metric, to reduce the errors in colour judgments during medical procedures. The results were considered feasible for biomedical purposes, although architectural applications may require

better control over illumination levels and size of the light patch at varying distances from the light source. It appears that, with the help of advanced materials, techniques and technological systems, the capabilities of projection systems may advance to a point where detecting the colour of an object and projecting spectrally optimised light with precision will be possible.

Although research investigating advanced projection and sensing systems show promising results, real-time tracking, projection, and reflectance estimation systems are likely to be the main future challenge in the implementation of the proposed lighting system. Current projection and sensing technology is not quite mature enough to currently support this opportunity. High-precision indoor positioning and sensing systems are required to successfully detect an object's position, movement, and surface reflectance. Consequently, a real-time projection system that can cover a wide visual field is required to illuminate moving objects. The proposed lighting system is likely to include several projectors that work together to illuminate the space and objects in it.

4 OPTIMISING LIGHT SOURCE SPECTRUM FOR OBJECT REFLECTANCE

Optimising light source spectrum for object reflectance

Dorukalp Durmus,^{1,*} Wendy Davis^{1,2}

¹Wilkinson Building (G04), 148 City Road, The University of Sydney, NSW 2006, Australia

²wendy.davis@sydney.edu.au

*ddur2395@uni.sydney.edu.au

Abstract: Much light in architectural spaces is absorbed by objects and never perceived by occupants. The colour appearance of objects illuminated by light spectra that minimized this absorption was determined. Colour differences were calculated for 15 reflective samples when illuminated by various coloured test light sources and reference white illuminants. Coloured test spectral power distributionos (SPDs) can reduce energy consumption by up to 44% while maintaining identical colour appearance of illuminated objects. Energy consumption can be reduced further, but with noticeable colour shifts. Results quantify the trade-off between colour fidelity and energy consumption with this approach.

© 2015 Optical Society of America

OCIS codes: (330.1710) Color, measurement; (330.1715) Color, rendering and metamerism; (120.5700) Reflection.

References and links

1. P. Waide and S. Tanishima, *Light's Labour's Lost: Policies for Energy-efficient Lighting* (OECD Publishing, 2006).
 2. W. R. McCluney, *Introduction to Radiometry and Photometry* (Artech House Publ., 1994).
 3. R. A. Newcombe, S. Izadi, O. Hilliges, D. Molyneaux, D. Kim, A. Davison, P. Kohi, J. Shotton, S. Hodges, and A. Fitzgibbon, "KinectFusion: Real-time dense surface mapping and tracking," in *10th IEEE International Symposium on Mixed and Augmented Reality (ISMAR)*, (IEEE, 2011), pp. 127–136.
 4. C. C. Miller, Y. Ohno, W. Davis, Y. Zong, and K. Dowling, "NIST spectrally tunable lighting facility for color rendering and lighting experiments" in *Proceedings of CIE 2009: Light and Lighting Conference*, (Light & Engineering, 2009).
 5. W. Davis and Y. Ohno, "Color quality scale," *Opt. Eng.* **49**(3), 033602 (2010).
 6. R. W. G. Hunt and R. M. Pointer, *Measuring Colour* (John Wiley & Sons, 2011), Chap. 3.
-

1. Introduction

Electric lighting is one of the major contributors to energy usage worldwide. It is estimated that electric lighting consumed 2650 TWh per annum in 2005, around 19% of the world's total electricity consumption [1]. Solid-state lighting (SSL), which generates light from a semiconductor, has the potential to deliver better control over spectral output while consuming less power than incumbent lighting technologies. However, energy efficient lighting must deliver quality illumination to be accepted by users.

Most light sources emit light of many different wavelengths, but objects' optical properties, such as reflectance, transmittance and absorbance, are dependent on the incident wavelength [2]. The perceived colour of an object, an important dimension of light quality and user acceptance, depends on the spectral power distribution (SPD) of the source illumination and the light reflected from the surface of the object. Humans perceive only the light reflected by the object; and absorbed light is transformed into internal energy, most notably heat, and is considered a loss. For example, a saturated red object reflects most of the power from longer visible wavelengths, but very little light from the shorter wavelengths. Since the short wavelength light is absorbed by the object, it is never seen by the observer; for illumination purposes, it is wasted.

It is plausible that wavelength-adjustable lighting systems can realise the true energy saving potential of SSL by not emitting unnecessary (absorbed) wavelengths from the light source's spectrum and minimizing the energy wasted by absorption from objects and other surfaces. Figure 1 shows a simplified possible implementation of a lighting system that detects the colour of the objects with sensors and emits light of optimized SPDs onto the objects. In this example, the network of sensors detects the position and colour of the red sofa and a controller (not shown) signals the luminaires to direct red light to its location. Though the technical implementation of these types of lighting systems is beyond the scope of this research, it is simply an engineering problem that could be solved with the use of modern sensor and lighting technologies [3,4].

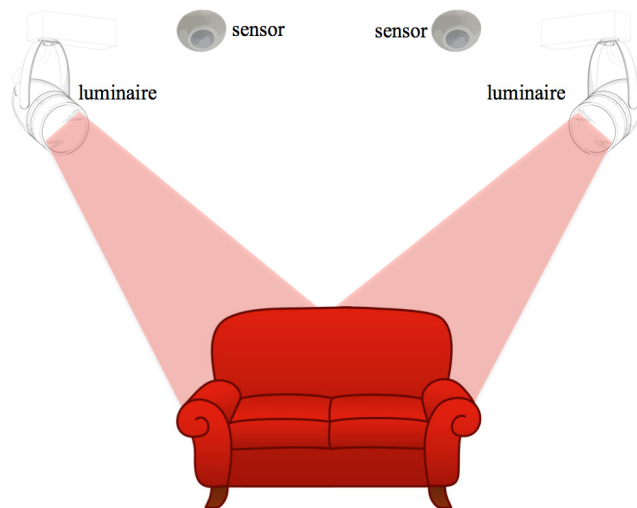


Fig. 1. Simplified layout of lighting system that detects the position and colour of objects and tunes the SPD of the lighting to minimize absorption.

For a saturated red object, like the sofa, the spectral composition of light that minimizes absorption is expected to contain little or no power in the shortest wavelengths of the visible spectrum. This research investigates the feasibility of using light sources with SPDs that are tuned to the reflectance of the illuminated objects.

2. Methods

Computational simulations of the impact of light source spectral power distribution (SPD) on the perceived colour of objects were achieved by calculating the colour differences in the CIE 1976 $L^*a^*b^*$ colour space of reflective samples when illuminated by a reference illuminant and numerous narrowband SPD test light sources. In this analysis, the 15 reflective samples used in the colour quality scale (CQS) [5] were used. CIE 1976 $L^* a^* b^*$ coordinates were calculated for each sample under two SPDs (the reference illuminant and the narrowband test light source) and colour differences were calculated with ΔE^*_{ab} , where $\Delta E^*_{ab} = 1.0$ is considered to be a barely recognizable difference [6].

Simulations were carried out with the assumption that the observer has an adapted white point. For example, if an observer viewed a complex illuminated scene in which all of the coloured objects were lit with spectrally narrow light, optimized to the reflectance of each object, they would not be adapted to those narrow spectra. Instead, all of the achromatic objects in the scene would be illuminated by white light, which would be the observer's adapted white point. For these calculations, the adapted white point corresponds to the chromaticity of the reference illuminant.

All calculations were performed for two different reference illuminants: a standard incandescent SPD and an equal-energy radiator. For each reflective sample and reference illuminant condition, iterative simulations were performed with many narrow SPDs. The first test SPD consisted of a single wavelength, referred to as the “starting point.” The peak of this monochromatic SPD was determined such that the luminance of the sample would be the same with the test and reference SPD. For each subsequent SPD, a single wavelength was added to each side of this starting point, thus creating a “bandwidth” for the test light source. Throughout the iterative simulations, the bandwidth was increased to the edges of the visible spectrum (i.e. shorter wavelengths until ultraviolet, longer wavelengths until infrared), ranging from 1.0 nm to 401 nm. For example, for the starting point of 600 nm, bandwidth of 11 nm means that the SPD ranges from 595 nm to 605 nm.

A second method of incrementally constructing spectra, adding relative power to all wavelengths of the visible spectrum of the test source in 0.05 increments, is referred to as the SPD “baseline.” The equal energy reference illuminant has a relative power of 1.0 for all wavelengths in the visible spectrum (i.e. straight horizontal line). Therefore, when the reference illuminant is the equal energy radiator, the test SPDs have rectangular shapes. When the reference illuminant is an incandescent SPD, the test SPD takes on the same shape for the wavelengths included. An example of bandwidth and baseline power is shown in Fig. 2.

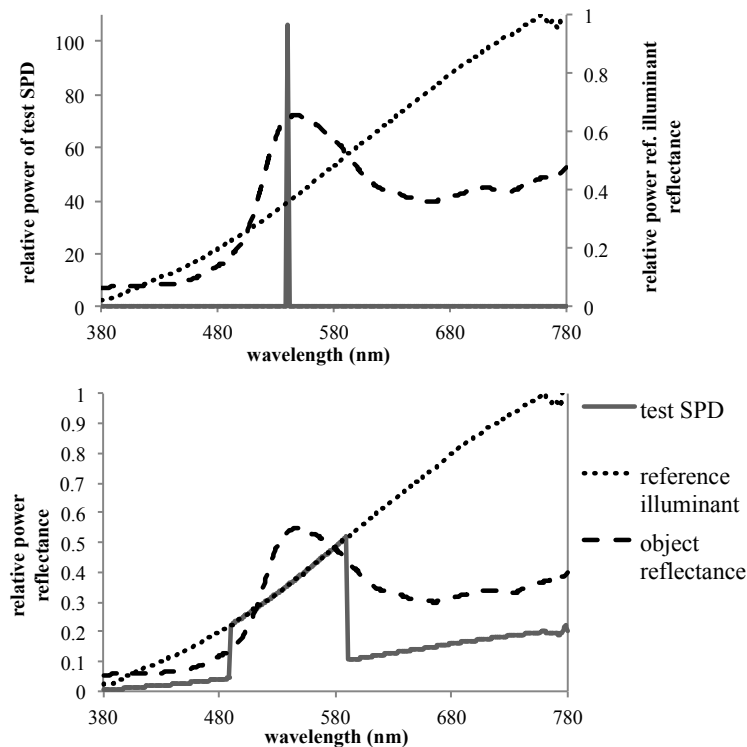


Fig. 2. Relative power as a function of wavelength for test SPDs (solid lines) and incandescent reference illuminant (dotted lines). Reflectance as a function of wavelength (dashed lines) for a saturated yellow object (sample 5).

Colour differences (ΔE^*_{ab}) were calculated for every possible starting point, bandwidth, and baseline condition. Each colorimetric calculation was accompanied by a calculation of the energy consumption of each narrowband SPD relative to the reference illuminant. For example, the energy consumption of the test SPD in Fig. 2 is calculated by integrating the

total area under the solid line. Then, the relative energy consumption of this particular SPD is determined as the ratio of this to the integrated area under reference illuminant SPD (short dashed line). This ratio of test SPD's energy consumption to the reference illuminant's energy consumption is expressed as a percentage that indicates the relative energy consumption of the test SPD.

3. Results & discussion

Results show that differences in object colour appearance are generally inversely related to energy consumption. Under both incandescent and equal-energy reference illuminants, the 15 reflective samples had lower colour differences with SPDs that saved relatively little energy. However, several variables impact both colour differences and energy consumption, such as starting point, bandwidth, baseline power, reference light source and object reflectance type.

5.1 Bandwidth and baseline

Baseline, in tandem with bandwidth, has a noteworthy influence on the colour appearance of the samples. As an example, Fig. 3 and Fig. 4 show the magnitude of colour shifts and energy consumption relative to an incandescent reference illuminant when an orange sample (sample 2) is illuminated by narrow SPDs. Figure 3 shows the effect of bandwidth on both colour differences and energy consumption, while Fig. 4 shows the effect of baseline power changes on the same two variables.

For this particular sample, when the baseline is held at 0.0 relative power, shown in the top plot of Fig. 3, colour appearance is indistinguishable from incandescent illumination when bandwidth is higher than 250 nm. Increasing bandwidth greater than 250 nm does not substantially improve colour appearance, but does result in increased energy consumption. When the baseline is higher than 0.0 relative power, shown in the bottom plot of Fig. 3, a bandwidth of approximately 20 nm is sufficient to reach a colour difference of $\Delta E^*_{ab} < 1.0$. However, energy consumption, in this case, is dramatically higher than the first situation.

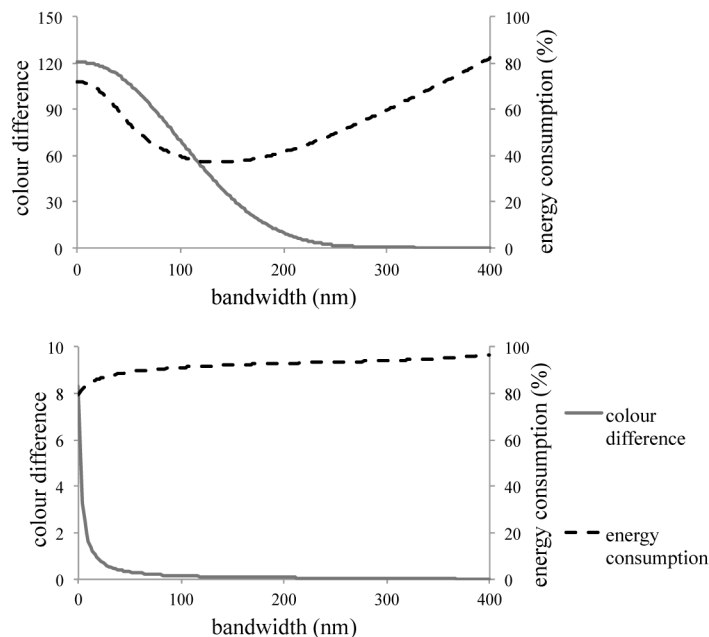


Fig. 3. Effect of bandwidth on energy consumption (dashed line, right y-axis) and colour differences (solid line, left y-axis) for sample 2, while baseline is held constant at 0.00 (relative power) for the top plot and 0.50 (relative power) for the bottom plot, for a starting point of 544 nm, relative to illumination by an incandescent light source.

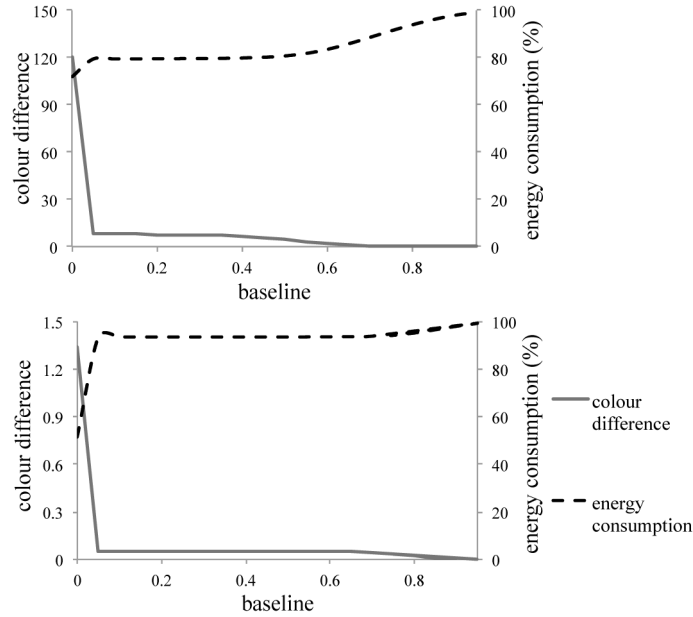


Fig. 4. Effect of baseline power on energy consumption (dashed line, right y-axis) and colour differences (solid line, left y-axis) for sample 2, while bandwidth is held constant at 3 nm for the top plot and 261 nm for the bottom plot, for a starting point of 544 nm, relative to illumination by incandescent light source.

Baseline has a more straightforward influence on both energy consumption and colour appearance. The addition of even a small amount of baseline power greatly decreases the perceived colour shift from illumination by the test SPD compared to illumination by the reference source. However, even a minimal use of baseline power reduced the energy savings from the test light source. The initial addition of baseline power, from 0.0 relative power to 0.05 relative power, has the biggest impact on the colour difference of the sample, regardless of the bandwidth. The top plot of Fig. 4 shows a sustained increase in energy consumption when baseline is further increased, for a fixed bandwidth of 3 nm. For the broader bandwidths, the impact of the initial addition of baseline power on energy consumption is not as great, as shown in the bottom plot of Fig. 4. In both cases, after the first step (baseline > 0.05), additional baseline has a minor effect on both energy consumption and colour differences.

5.2 Reference illuminant

This analysis shows that the difference between the two reference light illuminants is only limited to energy consumption. The average optimal starting point for all reflective samples to reach a $\Delta E^*_{ab} < 10$ (a difference that is likely noticeable, but also potentially acceptable to viewers) is 535 nm when the reference illuminant is an equal energy radiator and an incandescent illuminant, as shown in Table 1. An average of 202 – 203 nm of bandwidth is needed in the constructed test SPD when compared to both the incandescent and the equal energy radiator. However, using an incandescent lamp as a reference in the computation has an increased positive effect on the energy saving potential of test SPDs. A maximum of 61% of energy, on average, can be saved when the reference is incandescent, in comparison with 47% when the equal energy radiator is the reference.

Table 1. Energy saving potential of the test SPDs relative to reference illuminants when target colour difference $\Delta E^*_{ab} < 10$.

Reference light source	Avg. starting point (nm)	Avg. bandwidth (nm)	Avg. baseline	Energy saving* (%)
Equal energy	535	203	0	47
Incandescent	535	202	0	61

*Values are the average of all the reflective samples' highest energy saving condition

When the analysis is restricted to consider $\Delta E^*_{ab} < 1$ (a just noticeable difference in a laboratory setting), similarly there is minimal difference in starting point, bandwidth and baseline between the two reference illuminants, as shown in Table 2. When tolerance for colour shifts decreases to $\Delta E^*_{ab} < 1$, energy saving drops from 47 – 61% to 35 – 48%, due to the trade-off between colour fidelity and energy consumption. The gap between the energy saving potentials of these two reference illuminants is still apparent. The optimal starting points are shifted from 535 nm to the 558 – 561 nm range, and average bandwidth increased to 263 – 266 nm from 202 – 203 nm.

Table 2. Energy saving potential of the test SPDs relative to reference illuminants when target colour difference $\Delta E^*_{ab} < 1$.

Reference light source	Avg. starting point (nm)	Avg. bandwidth (nm)	Avg. baseline	Energy saving* (%)
Equal energy	558	263	0	35
Incandescent	561	266	0	48

*Values are the average of all the reflective samples' highest energy saving condition

A further step was taken in the analysis where SPDs with two starting points (peaks) and no additional bandwidth or baseline were investigated. Since the SPDs consisted of only two single wavelengths, their peak values were much higher (denoted RL_{cons}). With no baseline and bandwidth, these SPDs can save much more energy: 45.7% when the reference is equal energy and 61.6% when it is incandescent. However, colour differences only go as low as $\Delta E^*_{ab} = 3.0$ for equal energy reference and $\Delta E^*_{ab} = 3.9$ for incandescent references, as shown in Table 3.

Table 3. Energy saving potential of the test SPDs relative to reference light sources when SPD consists of only two single wavelengths as starting points, and no baseline or additional bandwidth.

Reference light source	Avg. 1. starting point (nm)	Avg. 2. starting point (nm)	RL_{cons}	ΔE^*_{ab}	Energy saving* (%)
Equal energy	459	577	109	3.0	46
Incandescent	472	591	102	3.9	62

*Values are the average of all the reflective samples' highest energy saving condition

In short, test SPD parameters (i.e. bandwidth, baseline and starting point) that give the optimal results vary with the chosen reference illuminant. Test SPDs can be created that reduce energy consumption and render object colours the same as the reference illuminants. Energy consumption can be reduced even further, but the test SPDs would induce perceptible shifts in object colour.

5.3 Object reflectance types

An analysis was carried out to identify the relevance of different reflectance characteristics of coloured samples. Based on their pattern of reflectance across the visible spectrum, five types of samples were categorized: peak, peak + incline, plateau, peak + plateau, and plateau +

peak. The impact of sample characteristics, as well as the interactions between starting point, bandwidth, and baseline power was examined.

The 15 reflective samples were grouped according to the presence of three major components in their spectral reflectance factors: peak, plateau and inclination. All of the five groups consist of these three major elements. While peak and plateau are the main two shapes in the graphical representation of the surface reflectance values of the CQS samples, incline is a small slanted deviation from horizontal. Additionally, 'plateau + peak' and 'peak + plateau' embody two different graphical representations, where the former consists of a larger plateau and a smaller peak. The latter is primarily a peak type reflectance with a smaller plateau extension. A hypothesized relationship between optimal starting point in SPD construction and peak reflectance of the sample was not supported by the calculation results. For colour differences $\Delta E^*_{ab} < 10$, each sample, regardless of its spectral reflectance characteristics, has an optimal starting point in the 520 – 551 nm range, which doesn't necessarily match with the peak of the sample reflectance. When these individual starting points are averaged, they range between 525 nm and 549 nm, as shown in Fig. 5. As expected, peak type samples have the highest energy saving potential, while more complicated reflectance characteristics (i.e. plateau, plateau + peak) require more relative power when lit under narrow spectra to limit perceived colour differences.

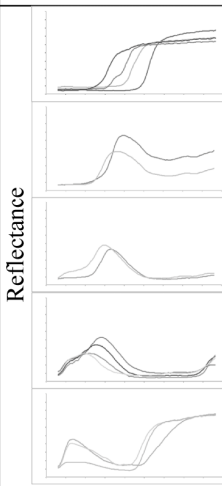
	Object Reflectance Type	CQS Sample	Starting Point (nm)	Bandwidth (nm)	Baseline	Max. Energy Saving (%)
	Plateau	S1, S2, S3, S4	546	203	0.0	52
	Peak + Plateau	S5, S6	539	198	0.0	56
	Peak	S7, S8	529	196	0.0	58
	Peak + Incline	S9, S10, S11, S12	525	199	0.0	56
	Plateau + Peak	S13, S14, S15	540	218	0.0	49
Wavelength (nm)						

Fig. 5. Effect of object reflectance types on energy saving and starting point values when $\Delta E^*_{ab} < 10$.

This analysis can be restricted to $\Delta E^*_{ab} < 1$, which is considered a just noticeable difference, as shown in Fig. 6. As previously discussed, bandwidth broadens and baseline goes to zero in order to achieve an efficient SPD that induces minimal shift in object colour appearance. Consequently, the energy savings potential of the test light sources decreases to approximately 40%, due to the smaller tolerance for colour shifts. Similar to the previous analysis, reflective samples that primarily consist of a peak have higher energy savings potential than plateau types.

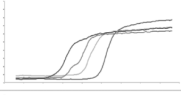
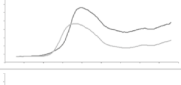
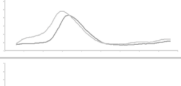


		Object Reflectance Type	CQS Sample	Starting Point (nm)	Bandwidth (nm)	Baseline	Max. Energy Saving (%)
Reflectance		Plateau	S1, S2, S3, S4	548	265	0.0	40
		Peak + Plateau	S5, S6	544	262	0.0	42
		Peak	S7, S8	538	261	0.0	44
		Peak + Incline	S9, S10, S11, S12	537	260	0.0	44
		Plateau + Peak	S13, S14, S15	547	275	0.0	38
	Wavelength (nm)						

Fig. 6. Effect of object reflectance types on energy saving and starting point values when $\Delta E^*_{ab} < 1$.

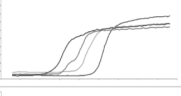
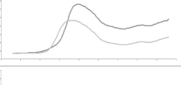
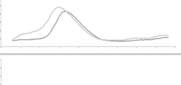
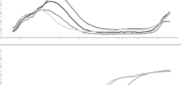
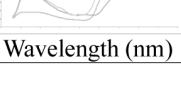
		Object Reflectance Type	CQS Sample	1. Starting Point (nm)	2. Starting Point (nm)	ΔE	Max. Energy Saving (%)
Reflectance		Plateau	S1, S2, S3, S4	461	589	6.9	60
		Peak + Plateau	S5, S6	484	573	1.7	61
		Peak	S7, S8	476	564	1.0	62
		Peak + Incline	S9, S10, S11, S12	471	588	1.5	43
		Plateau + Peak	S13, S14, S15	443	592	4.3	50
	Wavelength (nm)						

Fig. 7. Effect of object reflectance types on energy saving and starting point values when there are two starting points and no additional bandwidth or baseline.

These iterations were repeated using two starting points instead of just one. This time SPDs were created using two single wavelengths without any additional bandwidth or baseline. Results show that the smallest colour shifts and highest energy savings are achieved with peak type samples, as shown in Fig. 7. Unlike the previous analysis, plateau type samples can save as much energy as the peak type, but with larger colour differences.

Interestingly, peak + incline sample types were worst in terms of energy savings, although they maintain relatively good colour appearance. Overall, peak types are ideal object reflectance types in terms of colour appearance and energy saving potential for customized lighting that minimizes light absorption.

To summarize, object reflectance characteristics have a slight impact on the energy saving potential and starting point of the constructed SPD. The starting point of a test SPD does not necessarily match the peak (highest value) of the surface reflectance factor of a given sample. Peak type objects can lead to greater energy savings than other object types.

The analyses presented here demonstrate that coloured objects could be illuminated by spectrally narrow light sources to minimize absorbed light, and save energy, in ways that do not negatively impact colour appearance. However, if such a lighting system were to be designed and implemented, the spatial resolution of the light projecting system and observers' preferences for object chromaticity would need to be considered.

Acknowledgments

The authors are grateful to Dean Scott for the initial concept for this research.

5 COLOUR DIFFERENCE AND ENERGY CONSUMPTION OF ABSORPTION-MINIMIZING SPECTRAL POWER DISTRIBUTIONS

Colour difference and energy consumption of absorption-minimizing spectral power distributions

D. Durmus, W. Davis

*Faculty of Architecture, Design and Planning, University of Sydney, NSW
2006, Australia*

Contact: ddur2395@uni.sydney.edu.au
wendy.davis@sydney.edu.au

ABSTRACT

Electric lighting contributes substantially to worldwide energy use. New lighting technologies, such as solid-state lighting (SSL), consume less energy than incumbent light technologies, but the colour appearance of illuminated objects, an important aspect of light quality and user acceptance, must be considered. Since objects don't reflect all the radiation emitted from a light source, energy that is absorbed by objects becomes heat, which is considered loss for illumination purposes. The spectral power distributions (SPDs) of SSL devices can be optimized for objects' reflectances to minimize the absorbed energy. To investigate the energy saving potential of iteratively optimized SPDs, colour differences for 15 reflective samples under reference illuminants and test SPDs are calculated, using the CIE 1976 (L^* , a^* , b^*) colour space [1]. SPDs that reduce energy consumption and do not negatively impact colour appearance are recorded for each sample. Previous results indicate that a single block of spectral power can save, on average, between 38% and 44% of energy for all sample types, compared to incandescent or equal-energy illumination [2]. In this research, SPDs consisting of two separated blocks of spectral power are investigated. These results show that energy consumption can be reduced up to 71%, without inducing perceptible shifts in object colour. Results also indicate that object reflectance characteristics influence the amount of energy that can be saved and optimal illuminant properties.

INTRODUCTION

Light sources emit light of many different wavelengths and the light incident on an object or other surface is reflected, absorbed and/or transmitted. The optical properties of objects (i.e. reflectance, transmittance and absorption) and spectral power distribution (SPD) of the illumination determine the perceived colour of an object [3]. Since humans perceive only the light reflected from the surface of the object, light that is absorbed and transformed into heat in an object does not aid visibility and is wasted for illumination purposes. For example, a green object reflects light predominantly in medium wavelengths while light in shorter and longer wavelengths is mostly absorbed and not seen by the observer.

This study aims to evaluate the potential to save energy by adjusting the spectral power illuminating individual objects to minimize the wasted energy. By not emitting light of wavelengths that are primarily absorbed by objects, significant energy can be saved.

LITERATURE REVIEW

Earlier research discusses the feasibility of using light sources with SPDs customised to minimise light absorption by objects, while maintaining high colour fidelity [2]. Colorimetric simulations have shown that single-peak coloured SPDs illuminating individual objects can reduce energy consumption by up to an average of 44% without inducing any detectable differences in object colour appearance.

Energy savings could be increased even more, up to 58%, if noticeable, but not greatly disturbing, colour differences were induced. Additionally, SPDs consisting of only two single wavelengths were investigated. They yielded the highest energy savings (62%) among all analysed scenarios, but noticeable colour differences were induced for almost all of the reflective samples tested. Therefore, it is hypothesized that SPDs with two peaks, instead of one, can be optimized to maximize energy efficiency, without inducing detectable differences in colour appearance. This possibility is analysed here.

METHODS

The colour appearance of the 15 reflective samples used in the colour quality scale (CQS) [4] when illuminated by test SPDs and reference illuminants was determined in the CIE 1976 $L^*a^*b^*$ colour space [1]. The 15 reflective samples were grouped into categories according to their spectral reflectance characteristics. These groups had either one of the three major shapes (i.e. peak, plateau and incline) in their spectral reflectance factors, or a combination of two.

While a standard incandescent lamp and an equal-energy radiator were chosen as reference illuminants, test SPDs were based around two single wavelengths. These two single wavelengths, building blocks of the test SPDs, are called ‘starting points’.

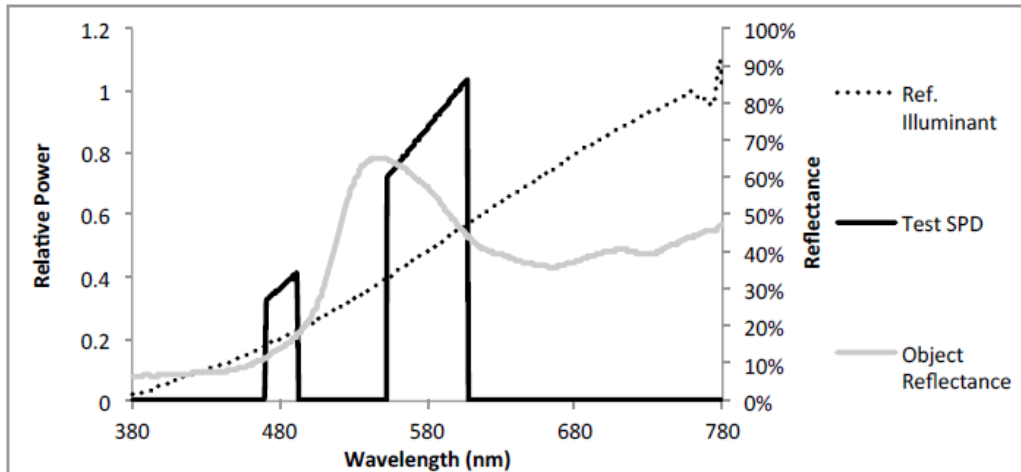


Figure 1 - Relative power as a function of wavelength for test SPDs (black solid lines) and incandescent reference illuminant (dotted lines). Reflectance as a function of wavelength (grey solid lines) for a saturated yellow object (sample 5).

These two starting points were not the only elements that constructed the test SPD. Single wavelengths of optical power were iteratively added to each side of these starting points to create a ‘bandwidth’. The two starting points could have different bandwidths. Bandwidths extended to the edges of the visible spectrum in odd numeric intervals, ranging from 1.0 nm to 401 nm. Test SPDs were created such that the two starting points and their bandwidths would not overlap. Therefore, instead of a continuous spectrum, test SPDs consisted of two separated components, or peaks as shown in Fig. 1. For instance, if 480 nm were to be taken as the first starting point and 21 nm as the first bandwidth, one part of the test SPD would range from 470 nm to 490 nm. Further, if 580 nm was the second starting point with a bandwidth of 51 nm, the second part of the test SPD would range from 555 nm to 605 nm. Thus, the test SPD would consist of two separate fragments: 470 nm – 490 nm and 555 – 605 nm.

Combinations of different starting points and bandwidths were iteratively simulated, and colour differences (ΔE^*_{ab}) were recorded for each condition, where $\Delta E^*_{ab} = 1.0$ is considered to be a barely recognizable difference [5]. Colour difference calculations were accompanied by calculations of energy consumption of the test SPD relative to the reference illuminant. Simulations assumed that the observer had an adapted white point, which corresponds to the chromaticity of the reference illuminant.

Furthermore, the spectral power of the test SPD was adjusted, so that illuminated objects had the same luminance as when lit by the reference illuminant. A scaling variable, RL_{cons} , was calculated for each test SPD to ensure that the amount of light reflected by each object was the same for the test SPD and reference illuminant. When the reference illuminant was an equal energy radiator, RL_{cons} corresponded to the peak value of the test SPD. When the reference was incandescent, this variable was used to scale the SPD, but the overall shape of the SPD was dictated by the spectrum of an incandescent lamp.

RESULTS AND DISCUSSION

Simulation results show that object reflectance characteristics have a marked influence on the energy

saving potential of the customised-SPD lighting systems. Additionally, the reference illuminant, serving as the point of comparison for energy consumption, influences the relative energy saving potential of test SPDs.

Table 1 shows the impact of the different reference illuminants on the calculation results. When comparing colour appearance and energy consumption to an incandescent, a considerably high energy saving of 61.5% is possible. When comparing test SPD performance to an equal-energy radiator, 51.7% of energy can be saved. The impact of these two reference illuminants is consistent with previous results [2]. For both reference conditions, optimised test SPDs have similar starting points and bandwidths. However, to match the reflected light given under an equal-energy radiator, test SPDs require higher peak values ($RL_{cons} = 10.2$) compared to the incandescent reference ($RL_{cons} = 3.3$).

*Table 1. Summary of test SPD characteristics when optimised for energy savings, as a function of the two reference illuminance, when target colour difference $E^*_{ab} < 1.0$. Values are the average of all reflective samples' highest energy saving condition*

Reference Illuminant	Starting Point 1 (nm)	Bandwidth 1 (nm)	Starting Point 2 (nm)	Bandwidth 2 (nm)	Max. Energy Saving (%)	RL_{cons}
Equal-energy	468	42	575	52	51.7	10.2
Incandescent	477	60	588	69	61.5	3.3

The results were also examined to determine the impact of the object reflectance characteristics for both reference illuminant conditions. The analysis shows that different sample types required different patterns of spectral power to minimize perceived colour difference. Therefore, optimal test SPDs for each sample differ in terms of their starting points, bandwidths and RL_{cons} values. As a result, notable variation is noted in energy saving potential among samples.

When the reference illuminant is an equal-energy radiator, energy savings values are lower than when the reference illuminant is an incandescent. As shown in Figure 2, peak sample types have the highest energy savings potential among all the sample types. Conversely, plateaus in spectral reflectance (e.g. plateau and plateau + peak) leads to reduced energy savings. For all sample types, one starting points ranged from 450 nm to 482 nm, and the other starting point ranged from 558 nm to 590 nm. The optimal SPDs have bandwidths between 21 nm and 73 nm. In the previous study, a minimum of 196 nm bandwidth was required for colour differences $\Delta E^*_{ab} < 1.0$ [2].

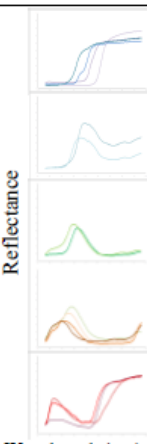
	Object Reflectance Type	CQS Sample	1. Starting Point (nm)	1. Bandwidth (nm)	2. Starting Point (nm)	2. Bandwidth (nm)	RL_{cons}	Max. Energy Saving (%)
	Plateau	S1, S2, S3, S4	476	69	590	63	2.0	47
	Peak + Plateau	S5, S6	482	24	571	21	47.4	52
	Peak	S7, S8	475	24	558	27	3.9	57
	Peak + Incline	S9, S10, S11, S12	463	38	565	51	8.9	56
	Plateau + Peak	S13, S14, S15	450	34	584	73	2.5	50

Figure 2 – Effect of object reflectance types on energy saving, starting point wavelengths and bandwidth, when the reference illuminant is an equal-energy radiator

When incandescent is used as a reference illuminant, optimal test SPDs differ from when the reference illuminant is an equal energy radiator, except for plateau type samples. Under both reference illuminants, plateau type samples have the same peak value, $RL_{cons} = 2.0$, and bandwidth and starting points don't differ by more than 8 nm. However, other sample types have notable bandwidth differences, as large as 59 nm.

Figure 3 shows optimal SPD characteristics for each sample type when the reference illuminant is incandescent. The first starting point range from 458 nm to 491 nm, and the second starting point ranges from 566 nm to 597 nm. Bandwidths range from 17 nm and 110 nm. RL_{cons} values are also much smaller than they are in Figure 2, meaning that the test SPDs are broader and shorter when the reference illuminant is incandescent. Parallel to findings from the previous research, illumination of peak + incline type samples results in the smallest energy savings, while illumination of peak type samples results in the highest energy savings, among all samples tested.

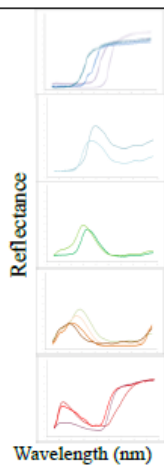
	Object Reflectance Type	CQS Sample	1. Starting Point (nm)	1. Bandwidth (nm)	2. Starting Point (nm)	2. Bandwidth (nm)	RL_{cons}	Max. Energy Saving (%)
	Plateau	S1, S2, S3, S4	484	67	595	61	2.0	61
	Peak + Plateau	S5, S6	491	33	579	33	4.3	67
	Peak	S7, S8	476	17	566	19	11.7	71
	Peak + Incline	S9, S10, S11, S12	478	96	597	110	1.2	55
	Plateau + Peak	S13, S14, S15	458	50	591	79	1.6	62

Figure 3 – Effect of object reflectance types on energy saving, starting point wavelengths and bandwidth, when the reference illuminant is incandescent

Test SPDs with two starting points and added bandwidth can save 55% - 71% of energy relative to the reference illumination. In contrast, SPDs that consist of only two starting points, with no additional bandwidth, can save 43% - 62% energy relative to the reference illuminants [2], but with induced shifts in object colour appearance. Optimised, additional bandwidth decreases energy consumption and eliminates perceived object colour differences. At the very least, energy consumption of a lighting system can be reduced by half if object colours were detected, and tailored spectra were projected onto illuminated objects. The spatial resolution of the projected light and observer preferences for object chromaticity need further examination before realizing such a lighting system.

REFERENCES

- [1] CIE, Colorimetry, Publication no. 15. Vienna: Central Bureau of the CIE, (2004).
- [2] D. Durmus, W. Davis, Optimising Light Source Spectrum for Object Reflectance. Optics Express, 23, A456-A464 (2015) 11.
- [3] W. R. McCluney, Introduction to Radiometry and Photometry. Artech House Publ., (1994). [4] W. Davis, Y. Ohno, Color quality scale. Opt. Eng. 49, 033602-033602-033616 (2010) 3. [5] R. W. G. Hunt, R. M. Pointer, Measuring Colour. John Wiley & Sons, (2011) Chap. 3.

6 OBJECT COLOUR NATURALNESS AND ATTRACTIVENESS WITH SPECTRALLY OPTIMIZED ILLUMINATION



Object color naturalness and attractiveness with spectrally optimized illumination

DORUKALP DURMUS* AND WENDY DAVIS

Wilkinson Building (G04), 148 City Road, The University of Sydney, NSW 2006, Australia

*alp.durmus@sydney.edu.au

Abstract: Previous analyses have shown that optimizing illuminants' spectral power distributions for object reflectance can yield energy savings in excess of 40% by reducing the light lost to absorption. Here, commercially available LEDs and real objects, instead of theoretical spectra and test sample colors, are investigated. Simulations show that energy savings of up to 15% are possible when illuminating common objects with mixtures of narrowband LEDs, compared to illumination by reference phosphor-coated white LEDs, without inducing changes in color appearance. Experiments show that higher energy savings are achievable without degrading object appearance. Object optical properties impact the success of this approach.

© 2017 Optical Society of America

OCIS codes: (330.1710) Color, measurement; (330.1715) Color, rendering and metamerism; (120.5700) Reflection; (230.3670) Light-emitting diodes; (330.1730) Colorimetry.

References and links

1. W. R. McCluney, *Introduction to Radiometry and Photometry* (Artech House Publ., 1994).
2. D. Durmus and W. Davis, "Optimising Light Source Spectrum For Object Reflectance," *Opt. Express* **23**(11), A456–A464 (2015).
3. J. Zhang, R. Hu, B. Xie, X. Yu, X. Luo, Z. Yu, L. Zhang, H. Wang, and X. Jin, "Energy-Saving Light Source Spectrum Optimization by Considering Object's Reflectance," *IEEE Photonics J.* **9**(2), 1–11 (2017).
4. D. Durmus and W. Davis, "Absorption-Minimizing Spectral Power Distributions," *Light, Energy and the Environment* (Optical Society of America, OSA Technical Digest (online), 2015), paper JTU5A.2.
5. W. Davis and Y. Ohno, "Color quality scale," *Opt. Eng.* **49**(3), 033602 (2010).
6. CIE, *Colorimetry* (CIE 15, 2004).
7. R. W. G. Hunt and R. M. Pointer, *Measuring Colour* (John Wiley & Sons, 2011).
8. G. Smets, "A tool for measuring relative effects of hue, brightness and saturation on color pleasantness," *Percept. Mot. Skills* **55** (3f), 1159–1164 (1982).
9. N. Camgöz, C. Yener, and D. Guvenc, "Effects of hue, saturation, and brightness on preference," *Color Res. Appl.* **27**(3), 199–207 (2002).
10. Y. Ohno, M. Fein, and C. Miller, "Vision experiment on chroma saturation for colour quality preference," *Light Eng.* **23**(4), 6–14 (2015).
11. K. McLaren, "CIELAB hue-angle anomalies at low tristimulus ratios," *Color Res.* **5**(3), 139–143 (1980).
12. S. Jost-Boissard, P. Avouac, and M. Fontoynt, "Assessing the colour quality of LED sources: Naturalness, attractiveness, colourfulness and colour difference," *Light. Res. Technol.* **47**(7), 769–794 (2015).

Introduction

Electric lighting systems are widely used in the built environment, and the quality of light they provide has a significant impact on occupant satisfaction. In the past few decades, more efficient lighting technologies, such as solid-state lighting (SSL) devices, emerged. These technologies behave quite differently from their predecessors in a number of respects and present a range of opportunities for changing the way that lighting is provided within architectural spaces.

The spectral power distribution (SPD) of a light source, the power emitted as a function of wavelength, and the reflectance characteristics of materials determine objects' color appearance [1]. Objects reflect, absorb and/or transmit the light incident on their surfaces. Reflected light reaches observers. However, absorbed light transforms into heat and remains within the object, having no impact on human vision. For example, a yellow rubber duck predominantly reflects light from middle and longer wavelengths, while much light of shorter

wavelengths are absorbed by the duck and do not reach the observer. Energy absorbed in the objects is useless for illumination and can be considered a source of loss. Therefore, an SPD-adjustable lighting system could leverage the spectral properties of SSL devices by minimizing the unnecessary spectral power emitted by the light source to reduce absorption by illuminated objects.

Though a previous publication has speculated on one way in which lighting systems intended to reduce the light lost to absorption might be designed [2], the engineering of such a system cannot be undertaken until the spectral design considerations are better understood, which is the aim of this research. It is reasonable to envision, however, that sensors could detect the surface colors of all objects within a space and luminaires could distribute light in spatially precise ways, much like video projectors (but without filters). By doing this, individual objects within the space could be illuminated by light spectrally tailored to minimize absorbed light, while still facilitating the appropriate object color appearance. A related approach, that is more spatially simple, involves optimizing the light spectrum for more than one object color [3], which sacrifices some of the possible reduction in absorbed light for likely increased ease of implementation.

Recent research has shown that computationally generated SPDs can minimize the absorption of light by optimizing light source spectrum for object reflectance, without inducing perceptible color differences [2,4]. In these previous studies, color differences were calculated for the 15 reflective samples used in the color quality scale (CQS) [5], when illuminated by a reference illuminant and test light source, in CIE 1976 $L^*a^*b^*$ color space using the CIE 2° standard colorimetric observer [6]. Results showed that spectrally optimized single-peak SPDs could reduce the energy used to light the objects between 38% and 44%, without reducing luminance or inducing visible color shifts [2]. Although an imperceptible difference of $\Delta E^*_{ab} < 1.0$ [7] was the focus of the research, the analysis also showed that increased energy savings are possible, between 43% and 62%, with higher tolerances for color shifts ($\Delta E^*_{ab} < 10$). Using a similar research approach, theoretical two-peak test SPDs have been shown to result in energy savings of up to 71%, without inducing perceptible color shifts [4]. In both studies, incandescent and equal-energy radiators were used as reference illuminants, and theoretical test SPDs were simulated across a broad range of spectral possibilities. Therefore, the test SPDs that resulted in the greatest energy savings had spectral shapes that cannot be easily manufactured with current commercialized technologies. These earlier studies established the theoretical feasibility of reducing the energy consumed by lighting, by minimizing absorption, without consideration of current technological limitations. Building on the previous research, this project focuses on the possibility of nearer-term implementation of this approach, by quantifying the potential energy savings when commercially available light sources are optimized for the reflective characteristics of commonly found objects, to minimize the loss of light to absorption. Absorption-reducing, spectrally optimized SPDs were used in experiments to investigate observers' judgments of the naturalness and attractiveness of object color appearance.

Methods

Computational analyses

The color appearance of ten objects was determined when illuminated by reference white light sources and various combinations of nine different real narrowband light emitting diodes (LEDs) in CIE 1976 $L^*a^*b^*$ color space [6]. Ten objects that have generally recognizable color appearances were selected across five different hues (red, orange, yellow, green and blue). The spectral reflectance of a Coca-Cola can and a tomato for the red hue, a mandarin and a carrot for the orange hue, a 3M Post-it Note and a lemon for the yellow hue, a Granny Smith apple and a lime for the green hue, and a container of Nivea Creme moisturizer and a blueberry for the blue hue were measured with a Konica Minolta CM-2600d spectrophotometer. Figure 1 shows the spectral reflectance factors of these objects.

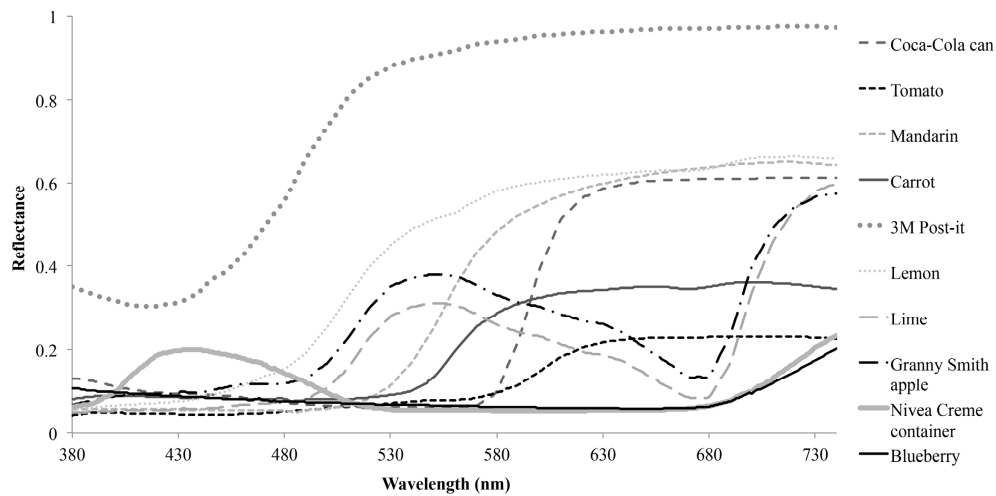


Fig. 1. Spectral reflectance as a function of wavelength for the 10 reflective objects.

In previous studies [2,4], object color appearance was compared when illuminated by computationally generated test SPDs and reference illuminants (incandescent and a theoretical equal-energy radiator). In this research, commercially available light sources, in both the test and reference conditions, are investigated to analyze the real-world implementation of the concept. Two white light sources that are readily available in the lighting market were chosen as reference illuminants; their SPDs are shown in Fig. 2. The color appearance of objects was compared when illuminated by either a phosphor-coated LED (pcLED) (CCT = 4101 K, CRI $R_a = 81$, $R_9 = 15$, CQS $Q_a = 80$) or a phosphor-coated LED with an additional red peak (pcLED + red) (CCT = 3061 K, CRI $R_a = 90$, $R_9 = 64$, CQS $Q_a = 89$) and when illuminated by test SPDs that were created by mixing the SPDs of commercially available narrow peak LEDs.

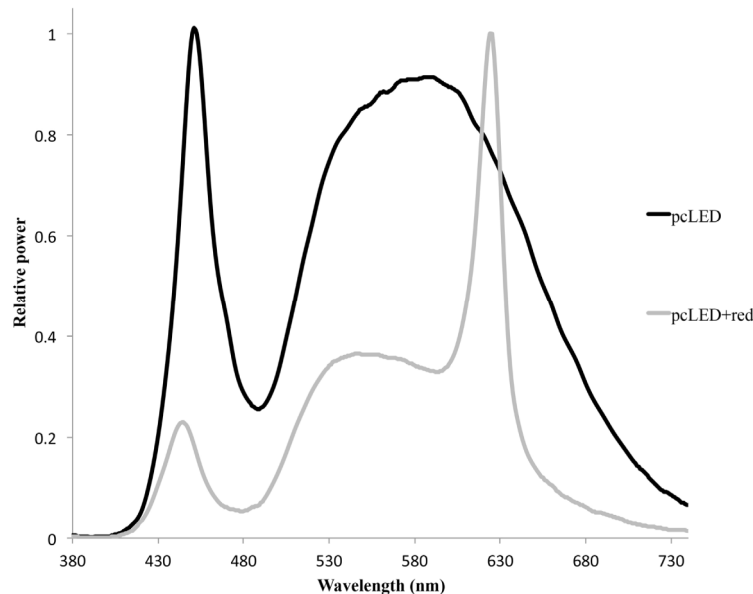


Fig. 2. Power as a function of wavelength for the two reference illuminants.

For the test light sources, the SPDs of nine different LEDs were measured with a Photo Research Spectrascan PR-730 Spectroradiometer. These SPDs were arranged according to peak wavelength and assigned a channel number. Channels 1, 2, 3, 4, 5, 7 and 8 belong to Source Four LED Profile x7 Color System theatrical lights, and channels 6 and 9 are from Innovations in Optics Lumibright LED engines. The spectral properties of the narrowband LEDs that were combined to generate test SPDs are shown in Fig. 3.

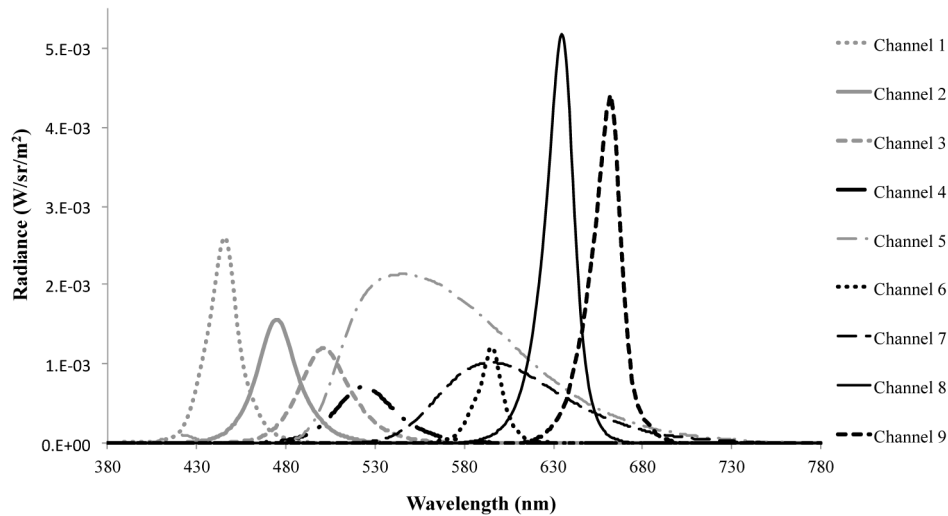


Fig. 3. The spectral power distributions of the nine narrowband LEDs that were mixed to simulate test SPDs.

Test SPDs were iteratively simulated by mixing these nine components, after their peak intensities were normalized, in different proportions. For example, a test SPD could be generated by combining 100% of channel 1, 0% of channel 2, 20% of channel 3, 10% of channel 4, 60% of channel 5, 70% of channel 6, 0% of channel 7, 100% of channel 8, and 50% of channel 9. In the iterative process, each step added 10% relative power to a channel until it reaches 100%, and then the next channel would be increased iteratively. As a result, numerous variations were tested for each object to identify the optimal SPD—the SPD that results in the smallest shift in object color and the largest decrease in absorbed light, relative to the reference source. Once the channels were combined, the overall magnitude of the test SPD was rescaled so that the amount of light reflected from the object was the same for both the reference and test light source. This means that the object would have the same luminance in both conditions, making the calculation of the amount of energy saved with the test SPD meaningful. Finally, the test SPD was used to calculate energy consumption, object color coordinates, object chroma difference and total color difference between illumination by the test and reference SPDs. The calculations assumed that the observer's white adaptation point ($X_n Y_n Z_n$) was the chromaticity of the reference light source.

In the first analysis, only test SPDs that yielded a color appearance of the illuminated object that was imperceptibly different from its color under the reference light, with a $\Delta E^*_{ab} < 1.0$, were considered. A higher, but likely not greatly disturbing color difference of $\Delta E^*_{ab} < 5$, was also analyzed. Since several studies suggest that users prefer increased saturation of the colors of illuminated objects [8–10], chroma differences were restricted to $dC^*_{ab} > 0$ (a signed measure of chroma difference in which positive values indicate increased chroma when illuminated by the test SPD). Hue and lightness changes were limited to be imperceptible, such that $\Delta E^*_{ab} - dC^*_{ab} < 1.0$. Test SPDs were selected in which energy consumption and the differences in hue and lightness were minimal, and chroma differences were positive.

Psychophysical experiments

Following the computational analyses, two experiments were conducted in the University of Sydney Lighting Lab to investigate the perceived naturalness and attractiveness of objects under selected test SPDs. Five of the ten objects that were computationally investigated were chosen as stimuli (i.e., tomato for red, mandarin for orange, lemon for yellow, Granny Smith apple for green, blueberry for blue).

Twenty-one naive participants, aged between 18 and 40 years, took part in each of the two visual experiments, which used a two-alternative forced choice method. All participants had normal color vision as tested by Ishihara plates. Participants were asked to judge the naturalness of object color appearance in the first experiment, and attractiveness in the second experiment. These two experiments were conducted several weeks apart, to mitigate possible association and confusion between perceived attractiveness and naturalness of object appearance. Participants were asked to make judgments related to the color appearance of the presented stimuli in two adjacent black booths within four seconds. Booths were placed 1.5 m from the observers. The interiors of the booths were covered with Protostar[®] flocked light trap material with 0.4% average reflectivity at 0° incidence angle.

Table 1. The narrowband LED channels that were mixed to generate the test SPDs, and the resulting color differences ΔE^*_{ab} , energy consumption relative to the reference source, and chroma difference dC^*_{ab} values, when the reference light source was the pcLED.

	Ch. 1 (%)	Ch. 2 (%)	Ch. 3 (%)	Ch. 4 (%)	Ch. 5 (%)	Ch. 6 (%)	Ch. 7 (%)	ΔE^*_{ab}	Energy consumption (%)	dC^*_{ab}
Apple	0	20	80	60	20	0	100	0.7	96.4	0.4
	0	40	60	20	20	60	40	1.9	95.0	1.3
	0	40	40	20	0	0	80	3.9	88.8	3.8
	0	40	20	0	0	20	40	5.9	86.4	5.7
	0	40	60	40	10	0	80	8.3	88.4	8.3
Blueberry	0	40	60	60	0	0	80	12.3	86.1	11.6
	0	20	50	40	0	10	70	0.7	93.7	0.5
	0	40	20	0	0	0	70	2.8	90.4	2.7
	0	40	30	20	0	0	90	4.0	91.5	3.9
	0	40	30	30	0	0	100	6.2	91.9	5.8
Lemon	0	40	20	10	0	0	90	8.0	93.3	7.9
	0	40	0	10	0	0	80	13.8	90.9	13.2
	0	40	40	0	20	40	40	0.7	93.7	-0.3
	0	40	40	0	20	0	80	1.8	93.0	1.1
	0	60	40	0	0	60	40	3.8	88.7	3.3
Mandarin	0	60	60	0	20	20	80	6.4	89.3	6.1
	0	60	40	0	0	80	0	8.4	85.7	7.9
	0	60	60	0	0	80	0	12.7	84.8	12.3
	0	40	40	0	20	0	80	0.8	91.3	0.3
	0	40	40	10	0	0	80	2.6	87.7	1.9
Tomato	0	40	40	0	0	0	80	4.0	85.8	3.5
	0	40	50	0	0	10	80	6.2	85.6	5.3
	0	40	70	20	0	0	90	8.7	84.6	8.5
	0	40	70	10	0	0	80	12.5	81.6	12.1
	0	20	40	20	10	0	60	0.7	93.6	0.4
	0	20	50	30	0	0	70	2.3	91.7	2.3
	0	20	60	30	0	0	80	4.3	91.6	3.8
	0	40	50	0	0	0	80	5.8	88.0	5.6
	0	20	60	30	0	0	60	8.0	87.6	7.7
	0	40	60	0	0	0	60	12.7	82.9	12.4

One of the booths was illuminated by the reference light source (either pcLED or pcLED + red), and the other by one of the test SPDs selected from the computational analysis. Six different test SPDs, yielding gradually increasing color differences, $\Delta E^*_{ab} < 1.0$, $\Delta E^*_{ab} = 1-3$, $\Delta E^*_{ab} = 3-5$, $\Delta E^*_{ab} = 5-7$, $\Delta E^*_{ab} = 7-9$ and $\Delta E^*_{ab} = 9-15$, were used to illuminate each object. The characteristics of the test SPDs when the reference light source was the pcLED and the

pcLED + red are shown in Table 1 and Table 2, respectively. As stated previously, hue and lightness changes were imperceptible and limited to $\Delta E^*_{ab} - dC^*_{ab} < 1.0$ for these SPDs. For each object and each reference light source, each participant reported their judgments for six test SPDs, which were presented ten times each in a random sequence, resulting in 60 experimental trials. Since there were five objects and two reference light sources, each participant completed a total of 600 trials for each experiment.

Table 2. The narrowband LED channels that were mixed to generate the test SPDs, and the resulting color differences ΔE^*_{ab} , energy consumption relative to the reference source, and chroma difference dC^*_{ab} values, when the reference light source was the pcLED + red.

	Ch. 1 (%)	Ch. 2 (%)	Ch. 3 (%)	Ch. 4 (%)	Ch. 5 (%)	Ch. 6 (%)	Ch. 7 (%)	ΔE^*_{ab}	Energy consumption (%)	dC^*_{ab}
Apple	0	50	60	0	0	20	40	1.0	92.1	0.7
	0	50	60	0	0	60	0	2.7	92.6	2.5
	0	40	40	0	0	0	40	4.1	89.5	3.4
	0	60	80	0	0	0	60	5.9	90.3	5.3
	0	60	80	20	0	20	40	7.9	89.7	7.5
Blueberry	0	60	60	0	0	40	0	14.6	86.8	14.6
	0	50	60	0	0	20	40	0.6	93.7	0.3
	0	50	60	10	0	0	60	2.4	92.8	2.0
	0	70	60	0	0	20	60	4.1	92.5	3.6
	0	60	100	60	0	0	100	6.3	93.5	5.5
Lemon	0	70	40	0	0	20	60	8.2	91.6	7.7
	0	70	20	10	0	0	80	14.7	89.9	14.0
	0	20	60	0	40	0	20	0.8	98.5	0.0
	0	20	60	20	0	0	40	2.0	94.7	1.6
	0	60	100	0	0	0	80	4.0	92.4	3.9
Mandarin	0	60	100	0	20	0	60	6.2	92.1	5.7
	0	60	100	0	0	60	0	8.0	90.5	7.9
	0	40	80	0	0	0	40	13.8	89.6	13.7
	50	10	90	60	0	20	40	0.7	99.7	0.0
	60	20	90	50	0	0	60	2.0	96.7	1.4
Tomato	60	40	70	10	0	0	60	4.0	91.9	2.7
	60	40	80	10	0	0	60	6.0	90.5	5.0
	60	40	90	10	0	0	60	7.9	89.3	7.0
	60	40	70	0	0	0	40	13.1	86.9	11.9
	0	30	80	0	0	60	0	0.6	98.6	0.1
	0	30	80	0	0	10	40	2.1	95.9	1.9
	0	30	90	0	0	10	40	4.2	95.0	3.9
	0	30	100	0	0	10	40	6.0	94.3	5.7
	0	30	90	0	0	0	40	7.8	93.0	6.9
	0	20	90	0	0	10	20	13.1	91.7	12.3

Both of the reference light source SPDs, pcLED and pcLED + red, and all of the test SPDs were generated by mixing the seven channels of the Source Four LED Profile x7 Color System theatrical lights. These luminaires were mounted above the booths, with their light projecting through a hole in the top panel of the booth, as shown in Fig. 4. Using seven channels from one light source, instead of nine channels from two separate light sources (as were used in the computational analyses), allowed the lighting in the adjacent booths to be easily alternated between the reference and test SPDs, reducing bias. The intensity of each light source was adjusted for each object, so that the intensity of reflected light (luminance) was the same for both stimuli.



Fig. 4. The test and reference SPDs were generated by the Source Four LED Profile x7 Color System theatrical lights, which were positioned on top of the two adjacent black booths.

Results and discussion

Computational results

The data from the computational study demonstrated that it is possible to optimize the spectrum, using a combination of existing narrowband LEDs, to reduce the energy lost to absorption, without inducing shifts in the color appearance of illuminated objects. Among all combinations of test SPDs that yielded the specified object color appearance, those that resulted in the lowest energy consumption were identified for each object. Figure 5 shows an example: the test SPD that was optimized for the green Granny Smith apple's spectral reflectance factor when compared to a reference pcLED source. When the green Granny Smith apple is illuminated by a combination of 40% of channel 2, 20% of channel 3, 20% of channel 4, 100% of channel 6 and 80% of channel 9, energy consumption is reduced by 8% without inducing any visible changes in color or luminance.

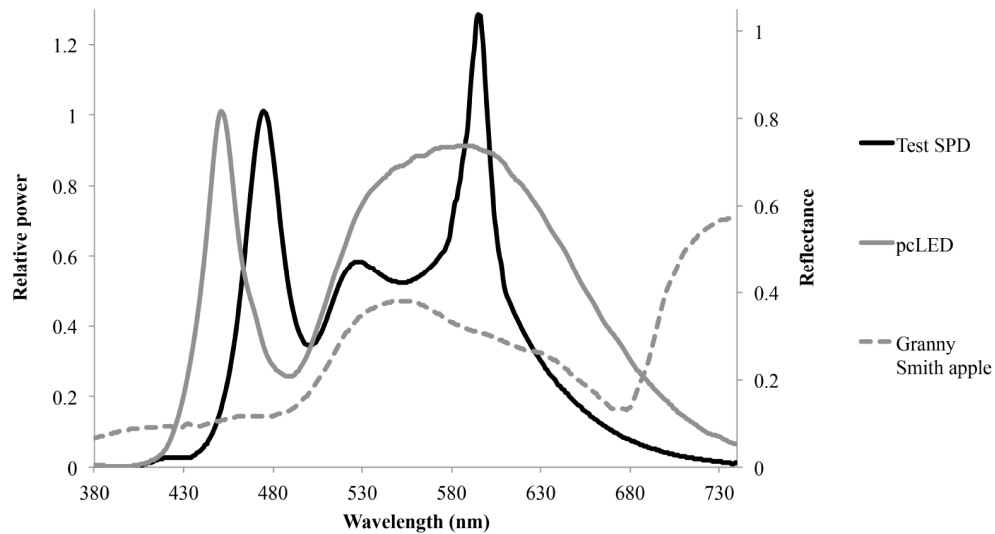


Fig. 5. When the green Granny Smith apple (dashed gray line; right y-axis) is illuminated by the test SPD (continuous black line; left y-axis), which consists of five different LEDs, 8% of energy is saved, compared to illumination by the reference pcLED (continuous gray line; left y-axis), without inducing any noticeable color shifts ($\Delta E^*_{ab} < 1.0$).

Similarly, energy consumption decreases by 17%, compared to the pcLED reference, when the green Granny Smith apple is lit by a combination of 40% of channel 2, 60% of channel 7 and 70% of channel 9, as shown in Fig. 6. However, in this case, the appearance of the green apple shifted slightly ($\Delta E^*_{ab} = 3.6$).

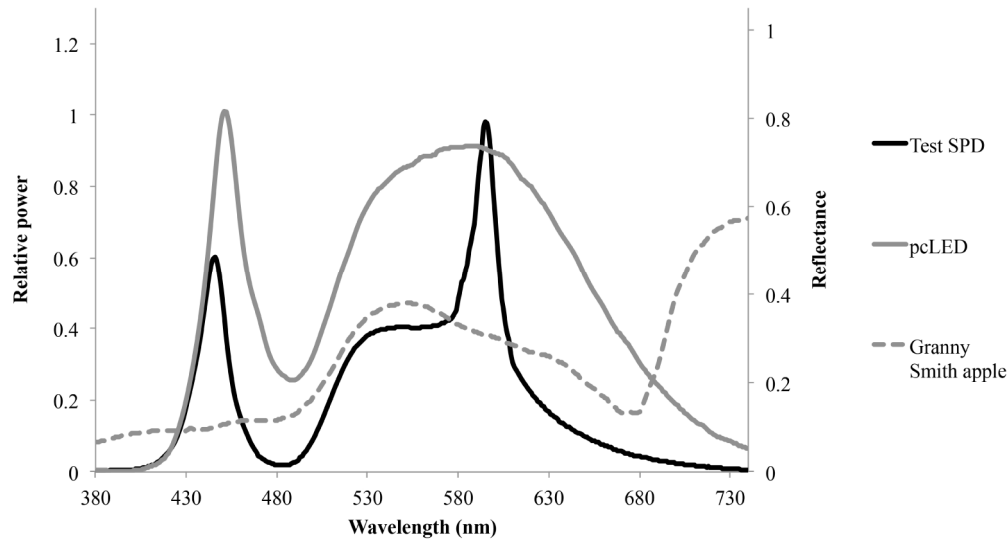


Fig. 6. When the green Granny Smith apple (dashed gray line; right y-axis) is illuminated by the test SPD (continuous black line; left y-axis), which consists of three different LEDs, 17% less energy is required than when it is illuminated by the reference pcLED (continuous gray line; left y-axis) if a slight color shift ($\Delta E^*_{ab} = 3.6$) is allowed.

The results indicate that spectrally optimized SPDs can result in energy savings between 11% and 15% when the reference illuminant is a pcLED with a $\Delta E^*_{ab} < 1.0$, as shown in Table 3. There is a greater variability between the results for different objects, 2% - 15%, when test SPDs were compared to the pcLED + red reference. When a slight difference in color

appearance was tolerated ($\Delta E^*_{ab} < 5$), higher energy savings were achieved, as expected: 14% - 19% when compared to the pcLED and 9% - 16% when compared to the pcLED + red.

Table 3. Percentage of energy savings for illumination of individual objects, compared to reference light sources, when color difference is imperceptible ($\Delta E^*_{ab} < 1.0$) and detectable, but not large ($\Delta E^*_{ab} < 5$).

	Energy Savings (%) $\Delta E^*_{ab} < 1.0$		Energy Savings (%) $\Delta E^*_{ab} < 5$	
	pcLED	pcLED + red	pcLED	pcLED + red
Coca-Cola can	11	2	17	9
Tomato	13	6	16	9
Mandarin	13	4	19	10
Carrot	14	4	19	9
3M Post-it	13	8	15	9
Lemon	14	10	17	16
Lime	13	15	18	15
Granny Smith apple	15	10	17	13
Nivea Creme container	14	10	14	13
Blueberry	15	14	16	15

Although the difference between the magnitudes of energy savings for illumination of individual items is not noteworthy for the pcLED reference, there is a clear pattern when the pcLED + red reference is considered. Understandably, objects with red-orange hues absorb relatively little light when illuminated by the pcLED + red reference, due to its sizable spectral peak in the long wavelengths. Therefore, the absorption decreases less when illuminated by the optimized test SPD. This pattern is more clear when objects are grouped into their associated hues, as presented in Table 4. When test SPDs were compared to the pcLED reference, optimized energy savings for different object colors were quite similar. When the reference was the pcLED + red, optimization of SPDs for red-orange object reflectance yielded the smallest energy savings, due to the high reflectance of longer wavelength light by these objects.

Table 4. Average percentage of optimized energy savings for illumination of each hue group of objects, compared to the reference light sources, when color difference is imperceptible ($\Delta E^*_{ab} < 1.0$) and detectable ($\Delta E^*_{ab} < 5$).

	Energy Savings (%) $\Delta E^*_{ab} < 1.0$		Energy Savings (%) $\Delta E^*_{ab} < 5$	
	pcLED	pcLED + red	pcLED	pcLED + red
Red	12	4	16	9
Orange	13	4	19	10
Yellow	14	9	16	13
Green	14	13	17	14
Blue	14	12	15	14

Experimental results

Both experiments used a two-alternative forced choice task and the percentage of the trials in which observers selected the test SPD as rendering the object more naturally or attractively (k) was calculated. For these experiments, a k of 50% corresponds to chance and suggests that participants judge neither the test nor reference light source to render the object color more naturally/attractively than the other. A k of 25% or 75% corresponds to threshold and suggests that participants judge the test (75%) or reference (25%) light source to render the object color more naturally/attractively. This percentage is shown, as a function of dC^*_{ab} of the test SPD for each object when compared to the pcLED reference in Fig. 7. Analogous results, when judgments were made against the pcLED + red reference source, are shown in Fig. 8.

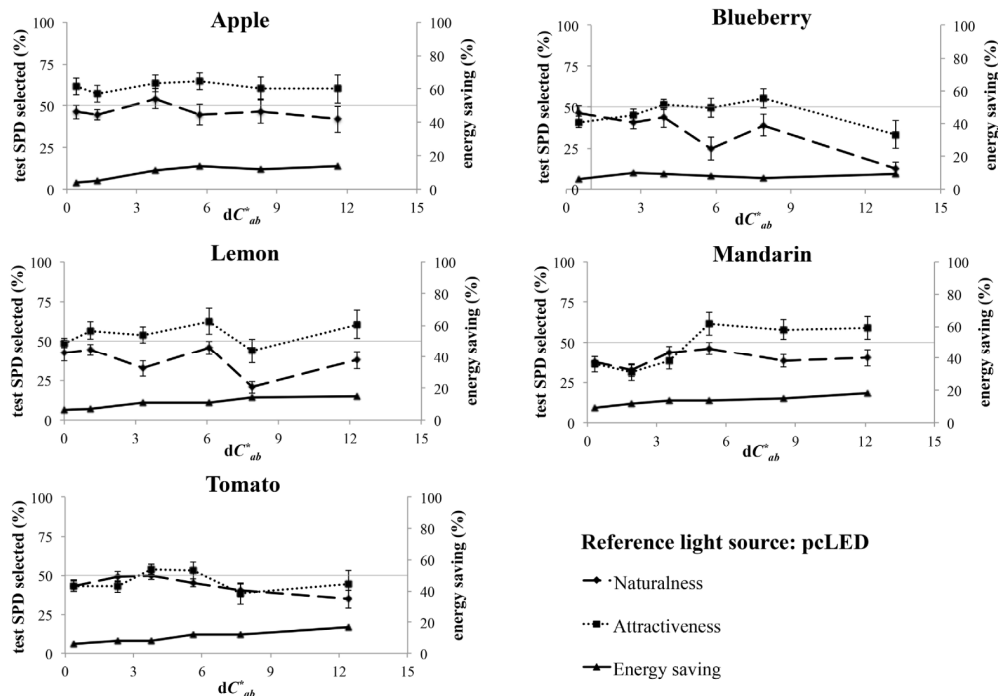


Fig. 7. Percentage of trials in which participants judged object color to appear more natural (long dashed line; left y-axes) and attractive (dotted line; left y-axes) as a function of the difference in chroma (dC^*_{ab}), when the object was illuminated by the test SPDs, than when illuminated by the pcLED reference light source. Error bars show the standard error of the mean (SEM). Generally, increases in object chroma were associated with increased energy savings (continuous black line; right y-axes).

The results for the green Granny Smith apple suggest that, for both reference light sources, the range of test SPD dC^*_{ab} values tested in these experiments did not impact perceived naturalness or attractiveness. Aside from a reduction in judgments of naturalness for one of the apple's test SPDs ($dC^*_{ab} = 5.3$) compared to the pcLED + red reference, the k value was quite close to 50% for all test SPDs.

When the chroma of blueberries was very large, participants judged them to appear unnatural and unattractive, particularly compared to the pcLED reference, as shown in Fig. 7. This was likely because the pcLED has significant power in the shorter wavelengths, rendering blue colors vividly. When test SPDs further increased the blueberries' chroma, the appearance was unnatural and unattractive. A similar, but less pronounced, pattern of results is seen for judgments of naturalness when compared to the pcLED + red. For this reference light source, no marked differences in attractiveness were reported across the range of dC^*_{ab} values tested.

The lemon appeared equally attractive across the chroma values under the optimized spectra and the reference pcLED + red. With the possible exception of the highest chroma condition, observers did not report differences between naturalness and attractiveness when comparing with this reference light source. When compared to the pcLED, participants judged the lemon to appear more attractive than natural for test SPDs of all chroma values.

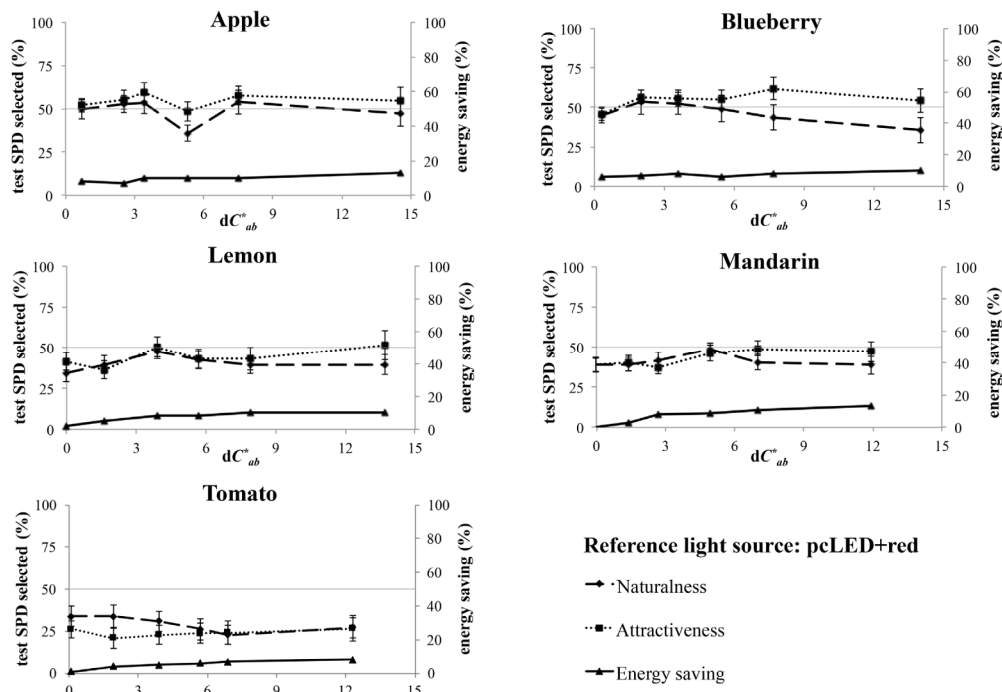


Fig. 8. Percentage of trials in which participants judged object color to appear more natural (long dashed line; left y-axes) and attractive (dotted line; left y-axes) as a function of the difference in chroma (dC^*_{ab}), when the object was illuminated by the test SPDs, than when illuminated by the pcLED + red reference light source. Error bars show the standard error of the mean (SEM). Generally, increases in object chroma were associated with increased energy savings (continuous black line; right y-axes).

The color appearance of mandarin appeared equally natural and attractive under all optimized test spectra when compared with the pcLED + red reference, as shown in Fig. 8. When compared to the pcLED reference, test SPDs yielding lower chroma differences ($dC^*_{ab} < 4$) resulted in judgments of reduced naturalness and attractiveness. Objects with higher chroma ($dC^*_{ab} > 4$) were judged to be slightly more attractive, but slightly less natural, than when illuminated by the pcLED reference.

When compared to the pcLED, the naturalness and attractiveness of the tomato was indistinguishable when illuminated by the rest and reference light sources at lower chroma differences ($dC^*_{ab} < 6$). At higher chroma differences, participants judged the pcLED to render the tomato slightly more naturally and attractively than the test SPDs. Observers consistently judged all test light sources to render the tomato less naturally and less attractively than the pcLED + red reference. Based on comments from the participants and observations of the experimenters, the translucent properties of the tomato appeared to interact with the test SPDs in ways that were not predicted by colorimetric calculations. Participants verbally reported perceiving hue shifts in the appearance of the tomato, despite the fact that test SPDs were chosen to render imperceptible hue and lightness changes ($\Delta E^*_{ab} - dC^*_{ab} < 1.0$). Problems with the perceptual uniformity (i.e., distances within color spaces corresponding to magnitudes of perceptual color differences) of the CIE 1976 $L^*a^*b^*$ color space for transparent objects might explain these observations [11]. This, combined with the strongly directional nature of the light sources used in this experiment, appeared to result in a visual artifact in which the top half of the tomato appeared significantly different from its bottom half, making the task very difficult for observers.

Naturalness vs. attractiveness

Participants were more likely to select the object illuminated by the test SPD as appearing more attractive than natural, especially when dC^*_{ab} values were higher. This result parallels other studies [8–10], reinforcing suggestions that observers prefer saturated colors. Many researchers believe that naturalness and attractiveness are two distinct characteristics of the color rendering ability of a light source [12]. Judgments of these two aspects also depend on the reference light source used for comparison. There was a notable difference in k values for judgments of naturalness and attractiveness when the reference light source was the pcLED. When the reference light source was the pcLED + red, k values were very similar, especially for the lower chroma test SPDs ($dC^*_{ab} < 5$), except for the tomato.

Reference light source

Computational analysis showed that the two reference light sources, pcLED and pcLED + red, had a slightly different impact on the ability to reduce energy consumption with optimized spectra, especially for the red-orange hue objects. Resulting energy savings for these objects were lower, due to the additional red peak in the pcLED + red reference light source's spectrum.

Experimental data showed that observers' judgments of the naturalness and the attractiveness of object color appearances were very similar and consistent among dC^*_{ab} values when the reference light source was the pcLED + red. When the reference was the pcLED, there was a more pronounced difference in the observers' evaluations of the naturalness and attractiveness of the stimuli, except for the tomato. Observers judged the color appearance of the tomato to be equally natural and attractive when compared to this reference light source.

Discussion

In this study, computational analyses and psychophysical experiments were conducted to investigate the potential use of real narrowband light sources to minimize the light energy absorbed by common objects to create more efficient lighting systems. Following previous research, which showed that energy could be reduced by up to 71% with theoretical SPDs [4], the computational simulations performed here demonstrate that currently commercially available LEDs can also be optimized for object reflectance, to save between 2% and 15% energy, depending on the object reflectance characteristics and reference light source being considered. Simulations showed that higher savings, between 9% and 19%, were achievable if slightly greater color differences, $\Delta E^*_{ab} < 5$, were deemed acceptable. The amount of energy that could be saved with this approach is expected to increase as lighting technology evolves and spectral design flexibility is increased.

Subsequently, test SPDs optimized in the computational analysis were physically realized and used in a laboratory setting to investigate the perceived color appearance of real objects with these energy-saving light sources. The experimental data further supports the proposition that, by optimizing the light spectrum for object reflectance, the energy consumed by lighting can be reduced without negatively impacting the visual appearance of illuminated objects. Although the object color appearance under most of the test SPDs resulted in naturalness and attractiveness comparable to illumination by the reference light sources, especially when the chroma increase was low, the translucency of the tomato negatively impacted the results. Data from the experiments showed that higher energy savings can be achieved, even when the color difference was as high as $\Delta E^*_{ab} = 15$, as long as the hue change was minimized ($\Delta E^*_{ab} - dC^*_{ab} < 1.0$) and an increase in chroma was maintained ($dC^*_{ab} > 0$), with a natural and attractive object color appearance.

7 CONCLUSIONS

The series of three studies that comprise this thesis investigated absorption-minimising spectra and their impact on the colour appearance of objects and energy consumption. In the first investigation, the spectral properties of absorption-minimising theoretical test SPDs were identified. The optimised single-peak test spectra demonstrated that energy savings up to between 38 % and 62 % could be achieved if they were used to light objects in architectural spaces (Durmus & Davis, 2015b). The results were expanded in the subsequent study, where double-peak theoretical spectra were shown capable of reducing energy consumption by up to 71 % (Durmus & Davis, 2015a). Consequently, the data from the psychophysical experiments presented in Chapter 6 supported the proposition that optimisation of the light source spectrum can lower the energy consumed by lighting without diminishing the colour appearance of illuminated objects. Participants in two separate experiments found real objects to appear equally natural and attractive under the optimised test light sources and reference white light sources, with a small caveat (Durmus & Davis, 2017). The data showed that further investigation of the optical surface properties of objects (i.e. translucency) is required. Future work is recommended to consider how bidirectional reflectance distribution function (BRDF) of objects can be considered to account for translucent objects. The details of the implementation of the system and challenges associated with adjusting the lighting for moving objects are topics for future research.

The optimisation studies were also expanded to address a museum lighting application. In this supplementary study, the theoretical test spectra were optimised for five single-colour paintings to reduce energy consumption and light absorption, while maintaining the colour appearance of the paintings (Abdalla, Duis, Durmus, & Davis, 2016). The theoretical study presented in Chapter 4 has already inspired other researchers to explore light source spectrum optimisation to reduce energy consumption by minimising absorption (J. Zhang et al., 2017). In that study, researchers optimised the test spectra for a set of coloured samples rather than single coloured samples.

It is regrettable that the CIELAB is not perfectly uniform, particularly in the blue region (Luo, Cui, & Li, 2006), despite the fact that it is a widely used colour space and an ISO standard (ISO, 2008). Despite its shortcomings, CIELAB is relevant and commonly used in non-imaging applications, since it does not depend on assumptions about the viewing conditions. Viewing condition parameters (e.g. relative background luminance, adapting field luminance, observer's level of adaptation) used in more uniform colour spaces might increase the accuracy of the colour difference calculations, and these warrant further investigation. However, if a lighting system to minimise absorbed light involved real-time calculations, the additional equations used in the advanced colour spaces may drastically increase the time and computational power needed to produce results.

The computing power needed for the proposed lighting system and the unsuitability of projection technologies available today may appear to pose implementation difficulties. However, technologies in the fields of sensing, projection and electronics are advancing rapidly. It is plausible to hypothesise that higher precision, accuracy and speed can be achieved in the near future to realise the proposed absorption-minimising lighting system.

Future studies will investigate to provide more dynamic optimisation parameters, such as object hue groupings, CCT preferences, and spatial resolution of the projection system. This thesis forms a basis to facilitate the additional research necessary to realise intelligent lighting systems designed to improve the visual environment and increase the sustainability of architectural lighting.

REFERENCES

- Abdalla, D., Duis, A., Durmus, D., & Davis, W. (2016). *Customization of light source spectrum to minimize light absorbed by artwork*. Paper presented at the CIE Lighting Quality and Energy Efficiency Conference 2016. Commission Internationale de L'Eclairage, Melbourne, Australia.
- Agahian, F., Amirshahi, S. A., & Amirshahi, S. H. (2008). Reconstruction of reflectance spectra using weighted principal component analysis. *Color Research & Application*, 33(5), 360-371.
- Agoston, G. A. (1979). *Color theory and its application in art and design* (Vol. 19). New York, Berlin: Springer-Verlag.
- ASTM. (1989). 1729-89. *Standard practice for visual evaluation of color differences of opaque materials*. Philadelphia, PA: ASTM.
- Aston, S. M., & Bellchamber, H. (1969). Illumination, colour rendering and visual clarity. *Lighting Research & Technology*, 1(4), 259-261.
- Aubé, M., Roby, J., & Kocifaj, M. (2013). Evaluating potential spectral impacts of various artificial lights on melatonin suppression, photosynthesis, and star visibility. *PLoS one*, 8(7), e67798.
- Australian Bureau of Statistics. (2012). *Household Energy Consumption Survey*. Retrieved from <http://www.abs.gov.au/ausstats%5Cabs@.nsf/0/66AC0659BF300142CA257BEF0013D900?OpenDocument>.
- Bartleson, C. (1979). Changes in color appearance with variations in chromatic adaptation. *Color Research & Application*, 4(3), 119-138.
- Beek, H. v., & Heertjes, P. (1966). Fading by light of organic dyes on textiles and other materials. *Studies in Conservation*, 11(3), 123-132.
- Bellia, L., Bisegna, F., & Spada, G. (2011). Lighting in indoor environments: Visual and non-visual effects of light sources with different spectral power distributions. *Building and Environment*, 46(10), 1984-1992.
- Berns, R. S. (2011). Designing white - light LED lighting for the display of art: A feasibility study. *Color Research & Application*, 36(5), 324-334.
- Berson, D. M., Dunn, F. A., & Takao, M. (2002). Phototransduction by retinal ganglion cells that set the circadian clock. *Science*, 295(5557), 1070-1073.
- Bimber, O., & Emmerling, A. (2006). Multifocal projection: A multiprojector technique for increasing focal depth. *IEEE Transactions on Visualization and Computer Graphics*, 12(4), 658-667.
- BIPM. (1979). The 16th Conférence Générale des Poids et Mesures (CGPM). *Bureau International des Poids et Mesures*, 100, 55-61. Sevres, France.
- Birkbeck, N., Cobzas, D., Sturm, P., & Jagersand, M. (2006). Variational shape and reflectance estimation under changing light and viewpoints. *Computer Vision—ECCV 2006*, 536-549.
- Blum, M., Büeler, M., Grätzel, C., & Aschwanden, M. (2011). *Compact optical design solutions using focus tunable lenses*. Paper presented at the Proc. SPIE. 8167, Optical Design and Engineering IV, Marseille, France.
- Bodrogi, P., Brückner, S., & Khanh, T. Q. (2011). Ordinal scale based description of colour rendering. *Color Research & Application*, 36(4), 272-285.
- Bodrogi, P., Brückner, S., Khanh, T. Q., & Winkler, H. (2013). Visual assessment of light source color quality. *Color Research & Application*, 38(1), 4-13.
- Boissard, S., & Fontoynt, M. (2009). Optimization of LED - based light blendings for object presentation. *Color Research & Application*, 34(4), 310-320.
- Bowmaker, J. K., & Dartnall, H. (1980). Visual pigments of rods and cones in a human retina. *The Journal of Physiology*, 298(1), 501-511.
- Boynton, R. M. (1979). *Human color vision*. New York, NY: Holt, Rinehart and Winston.
- Brainard, G. C., Hanifin, J. P., Greeson, J. M., Byrne, B., Glickman, G., Gerner, E., & Rollag, M. D. (2001). Action spectrum for melatonin regulation in humans: evidence for a novel circadian photoreceptor. *Journal of Neuroscience*, 21(16), 6405-6412.
- Brown, C. S., Schuerger, A. C., & Sager, J. C. (1995). Growth and photomorphogenesis of pepper plants under red light-emitting diodes with supplemental blue or far-red lighting. *Journal of the American Society for Horticultural Science*, 120(5), 808-813.
- Bruneton, A., Bäuerle, A., Wester, R., Stollenwerk, J., & Loosen, P. (2013). High resolution irradiance tailoring using multiple freeform surfaces. *Optics Express*, 21(9), 10563-10571.

- Burns, S. A. (2015). Subtractive color mixture computation. Retrieved from <http://scottburns.us/subtractive-color-mixture/>
- Cajochen, C. (2007). Alerting effects of light. *Sleep Medicine Reviews*, 11(6), 453-464.
- Camgöz, N., Yener, C., & Güvenç, D. (2002). Effects of hue, saturation, and brightness on preference. *Color Research & Application*, 27(3), 199-207.
- Canada Centre for Remote Sensing. (2015). *Fundamentals of remote sensing*. Retrieved from http://sesremo.eu/downloads/teaching-material/gis-course_itc/ebooks/Fundamentals of Remote Sensing.pdf
- Casey, A. (2014). Cree first to break 300 lumens-per-watt barrier. *Business Wire U6*. Retrieved from <http://www.businesswire.com/news/home/20140326005242/en/Cree-Break-300-Lumens-Per-Watt-Barrier>
- Chakrabarti, M., Pedersen, H. C., Petersen, P. M., Poulsen, C., Poulsen, P. B., & Dam-Hansen, C. (2016). High-flux focusable color-tunable and efficient white-light-emitting diode light engine for stage lighting. *Optical Engineering*, 55(8), 085101.
- Chellappa, S. L., Steiner, R., Blattner, P., Oelhafen, P., Götz, T., & Cajochen, C. (2011). Non-visual effects of light on melatonin, alertness and cognitive performance: can blue-enriched light keep us alert? *PloS one*, 6(1), e16429.
- Chen, S., Li, Y., Guan, Q., & Xiao, G. (2006). Real-time three-dimensional surface measurement by color encoded light projection. *Applied Physics Letters*, 89(11), 111108.
- Chen, S., Tan, G., Wong, W. Y., & Kwok, H. S. (2011). White organic light emitting diodes with evenly separated red, green, and blue colors for efficiency/color rendition trade-off optimization. *Advanced Functional Materials*, 21(19), 3785-3793.
- Chhajer, S., Xi, Y., Li, Y.-L., Gessmann, T., & Schubert, E. (2005). Influence of junction temperature on chromaticity and color-rendering properties of trichromatic white-light sources based on light-emitting diodes. *Journal of Applied Physics*, 97(5), 054506.
- Chien, M. C., & Tien, C. H. (2011). Cluster LEDs mixing optimization by lens design techniques. *Optics Express*, 19(104), A804-A817.
- Chien, M. C., & Tien, C. H. (2012). Multispectral mixing scheme for LED clusters with extended operational temperature window. *Optics Express*, 20(102), A245-A254.
- Chou, T.-R., & Lin, W.-J. (2012). *Optimal estimation of spectral reflectance based on metamerism*. Paper presented at the Color Imaging XVII: Displaying, Processing, Hardcopy, and Applications, Burlingame, CA.
- CIE. (1951). *CIE Proceedings*, Bureau Central de la CIE, Paris. Vienna, Austria: Commission Internationale de l'Eclairage.
- CIE. (1965). Method of measuring and specifying colour rendering properties of light sources. *Publication No. 13-1965*. Vienna, Austria: Commission Internationale de l'Eclairage.
- CIE. (1989). Mesopic photometry: History, special problems and practical solutions. *Publication No. 81*. Vienna, Austria: Commission Internationale de l'Eclairage.
- CIE. (1994). Light as a true visual quantity: Principles of measurement. *Publication No. 41*. Vienna, Austria: Commission Internationale de l'Eclairage.
- CIE. (1995). Method of measuring and specifying colour rendering properties of light sources. *Publication No. 13.3*. Vienna, Austria: Commission Internationale de l'Eclairage.
- CIE. (2004a). Colorimetry. *Publication No. 15*. Vienna, Austria: Commission Internationale de l'Eclairage.
- CIE. (2004b). Control of damage to museum objects by optical radiation. *Publication No. 157*. Vienna, Austria: Commission Internationale de l'Eclairage.
- CIE. (2004c). Standard method of assessing the spectral quality of daylight simulators for visual appraisal and measurement of colour. *Publication No. 012*. Vienna, Austria: Commission Internationale de l'Eclairage.
- CIE. (2006). Colorimetry – Part 2: CIE standard illuminants. *Publication No. 014*. Vienna, Austria: Commission Internationale de l'Eclairage.
- CIE. (2007). Colour rendering of white LED light sources. *Publication No. 177*. Vienna, Austria: Commission Internationale de l'Eclairage.
- CIE. (2010). Practical daylight sources for colorimetry. *Publication No. 192*. Vienna, Austria: Commission Internationale de l'Eclairage.

- CIE. (2011). ILV: International Lighting Vocabulary 017. *Publication No. 017*. Vienna, Austria: Commission Internationale de l'Eclairage.
- CIE. (2017). Colour Fidelity Index for accurate scientific use. *Publication No. 224:2017*. Vienna, Austria: Commission Internationale de l'Eclairage.
- Council of Australian Governments. (2012). *Baseline energy consumption and greenhouse gas emissions in commercial buildings in Australia*. Retrieved from <https://industry.gov.au/Energy/EnergyEfficiency/Non-residentialBuildings/Documents/CBBS-Part-1.pdf>.
- Curcio, C. A., Sloan, K. R., Kalina, R. E., & Hendrickson, A. E. (1990). Human photoreceptor topography. *Journal of Comparative Neurology*, 292(4), 497-523.
- Cuttle, C. (1996). Damage to museum objects due to light exposure. *International Journal of Lighting Research and Technology*, 28(1), 1-9.
- Cuttle, C. (2000). A proposal to reduce the exposure to light of museum objects without reducing illuminance or the level of visual satisfaction of museum visitors. *Journal of the American Institute for Conservation*, 39(2), 229-244.
- Dacey, D. M., Liao, H.-W., Peterson, B. B., Robinson, F. R., Smith, V. C., Pokorny, J., . . . Gamlin, P. D. (2005). Melanopsin-expressing ganglion cells in primate retina signal colour and irradiance and project to the LGN. *Nature*, 433(7027), 749-755.
- Dangol, R., Islam, M., LiSc, M. H., Bhusal, P., Puolakka, M., & Halonen, L. (2013). Subjective preferences and colour quality metrics of LED light sources. *Lighting Research & Technology*, 45(6), 666-688.
- Dartnall, H. J., Bowmaker, J. K., & Mollon, J. D. (1983). Human visual pigments: Microspectrophotometric results from the eyes of seven persons. *Proceedings of the Royal Society of London B: Biological Sciences*, 220(1218), 115-130.
- Dash, M. C., & Dash, S. P. (2011). *Fundamentals of ecology 3E*. New Delhi: Tata McGraw-Hill Education.
- David, A., Fini, P. T., Houser, K. W., Ohno, Y., Royer, M. P., Smet, K. A., . . . Whitehead, L. (2015). Development of the IES method for evaluating the color rendition of light sources. *Optics Express*, 23(12), 15888-15906.
- Davis, W., & Ohno, Y. (2005). *Toward an improved color rendering metric*. Paper presented at the Proceedings of SPIE Volume 5941, Fifth International Conference on Solid State Lighting, San Diego, CA.
- Davis, W., & Ohno, Y. (2009). Approaches to color rendering measurement. *Journal of Modern Optics*, 56(13), 1412-1419.
- Davis, W., & Ohno, Y. (2010). Color quality scale. *Optical Engineering*, 49(3), 033602-033602-033616.
- De Fabo, E. C., Harding, R. W., & Shropshire, W. (1976). Action spectrum between 260 and 800 nanometers for the photoinduction of carotenoid biosynthesis in *Neurospora crassa*. *Plant Physiology*, 57(3), 440-445.
- De Valois, R. L., & De Valois, K. K. (1993). A multi-stage color model. *Vision Research*, 33(8), 1053-1065.
- De Valois, R. L., Smith, C., Kitai, S., & Karoly, A. (1958). Response of single cells in monkey lateral geniculate nucleus to monochromatic light. *Science*, 127(3292), 238-9.
- DeCusatis, C. (1997). *Handbook of applied photometry*. New York, NY: Springer-Verlag.
- Delgado, M. F., Dirk, C. W., Druzik, J., & WestFall, N. (2011). Lighting the world's treasures: Approaches to safer museum lighting. *Color Research & Application*, 36(4), 238-254.
- Derrington, A. M., Krauskopf, J., & Lennie, P. (1984). Chromatic mechanisms in lateral geniculate nucleus of macaque. *The Journal of Physiology*, 357(1), 241-265.
- Dixon, E. (1978). Spectral distribution of Australian daylight. *JOSA*, 68(4), 437-450.
- Dong, F., Hombal, V., & Sanderson, A. C. (2012). Adaptive light field sampling and sensor fusion for smart lighting control. *IEEE 15th International Conference on Information Fusion (FUSION)*, Singapore, Singapore.
- Dorsey, J. O. B., Sillion, F. X., & Greenberg, D. P. (1991). Design and simulation of opera lighting and projection effects. *Paper presented at the ACM SIGGRAPH Proceedings of the 18th annual conference on Computer graphics and interactive techniques*, New York, NY.

- Draper, J. W. (1847). On the production of light by heat. *Journal of the Franklin Institute*, 44(3), 197-203.
- Dror, R. O. (2002). Surface reflectance recognition and real-world illumination statistics. (Doctoral dissertation). Retrieved from https://people.cs.umass.edu/~elm/Teaching/Docs/dror_phd_thesis.pdf
- Durmus, D., & Davis, W. (2015a). *Colour difference and energy consumption of absorption-minimizing spectral power distributions*. Paper presented at Asia-Pacific Lighting Systems Workshop, Sydney, Australia.
- Durmus, D., & Davis, W. (2015b). Optimising light source spectrum for object reflectance. *Optics Express*, 23(11), A456-A464.
- Durmus, D., & Davis, W. (2017). Object color naturalness and attractiveness with spectrally optimized illumination. *Optics Express*, 25(11), 12839-12850.
- EIA. (2017). *Annual energy outlook 2017*. Retrieved from <https://www.eia.gov/tools/faqs/faq.php?id=86&t=1>.
- Eisner, A., & MacLeod, D. I. (1980). Blue-sensitive cones do not contribute to luminance. *JOSA*, 70(1), 121-123.
- EMSD. (2016). Energy-efficient fluorescent tubes. Retrieved from <http://www.energyland.emsd.gov.hk/en/appAndEquip/equipment/lighting/tubes.html>
- Encke, J. (Producer). (2014). A representation of the most important cells in the retina. Retrieved from https://commons.wikimedia.org/wiki/File:Rods_Conos_Synapse.svg
- Enezi, J. A., Revell, V., Brown, T., Wynne, J., Schlangen, L., & Lucas, R. (2011). A “melanopic” spectral efficiency function predicts the sensitivity of melanopsin photoreceptors to polychromatic lights. *Journal of Biological Rhythms*, 26(4), 314-323.
- Fairchild, M. D. (2013). *Color appearance models* (3rd ed.). Chichester, England: John Wiley & Sons.
- Feller, R. L. (1964). Control of deteriorating effects of light upon museum objects. *Museum International*, 17(2), 57-98.
- Feng, X., Xu, W., Han, Q., & Zhang, S. (2016). LED light with enhanced color saturation and improved white light perception. *Optics Express*, 24(1), 573-585.
- Feng, X., Xu, W., Han, Q., & Zhang, S. (2017). Colour-enhanced light emitting diode light with high gamut area for retail lighting. *Lighting Research & Technology*, 49(3), 329-342.
- Fotios, S., & Levermore, G. J. (1997). Perception of electric light sources of different colour properties. *International Journal of Lighting Research and Technology*, 29(3), 161-171. doi:doi:10.1177/14771535970290030701
- Fouquet, R., & Pearson, P. J. (2006). Seven centuries of energy services: The price and use of light in the United Kingdom (1300-2000). *The Energy Journal*, 139-177.
- Fumagalli, S., Bonanomi, C., & Rizzi, A. (2015). Experimental assessment of color-rendering indices and color appearance under varying setups. *Journal of Modern Optics*, 62(1), 56-66.
- Gall, D., & Lapuente, V. (2002). Beleuchtungsrelevante Aspekte bei der Auswahl eines förderlichen Lampenspektrums. *Licht*, 54(7), 8.
- Geffroy, B., Le Roy, P., & Prat, C. (2006). Organic light-emitting diode (OLED) technology: materials, devices and display technologies. *Polymer International*, 55(6), 572-582.
- Goins, G. D., Yorio, N., Sanwo, M., & Brown, C. (1997). Photomorphogenesis, photosynthesis, and seed yield of wheat plants grown under red light-emitting diodes (LEDs) with and without supplemental blue lighting. *Journal of Experimental Botany*, 48(7), 1407-1413.
- Goldstein, E. B., & Brockmole, J. (2016). *Sensation and perception*. Belmont, CA: Wadsworth Cengage Learning.
- Grassmann, H. (1854). On the theory of compound colors. *Phil. Mag*, 7, 254-264.
- Grondzik, W. T., Kwok, A. G., Stein, B., & Reynolds, J. S. (2009). *Mechanical and electrical equipment for buildings*. Hoboken, NJ: John Wiley & Sons.
- Guild, J. (1931). The colorimetric properties of the spectrum. *Philosophical Transactions of the Royal Society of London. Series A, Containing Papers of a Mathematical or Physical Character*, 230, 149-187.
- Guo, Z., Shih, T., Gao, Y., Lu, Y., Zhu, L., Chen, G., . . . Chen, Z. (2013). Optimization studies of two-phosphor-coated white light-emitting diodes. *IEEE Photonics Journal*, 5(2), 8200112-8200112.

- Hara, K., & Nishino, K. (2005). Light source position and reflectance estimation from a single view without the distant illumination assumption. *IEEE Transactions on Pattern Analysis and Machine Intelligence*, 27(4), 493-505.
- Hardeberg, J. Y. (2001). *Acquisition and reproduction of color images: Colorimetric and multispectral approaches*. Retrieved from <https://pdfs.semanticscholar.org/210d/01465ffa350fdb19daf04c84d5f5793fec08.pdf>
- Harrington, L., & Foster, R. (2008). *Energy use in the Australian residential sector 1986-2020*. Canberra, Australia: Department of the Environment, Water, Heritage and the Arts.
- Hashimoto, K., & Nayatani, Y. (1994). Visual clarity and feeling of contrast. *Color Research & Application*, 19(3), 171-185.
- Hashimoto, K., Yano, T., Shimizu, M., & Nayatani, Y. (2007). New method for specifying color rendering properties of light sources based on feeling of contrast. *Color Research & Application*, 32(5), 361-371.
- Hattar, S., Liao, H.-W., Takao, M., Berson, D. M., & Yau, K.-W. (2002). Melanopsin-containing retinal ganglion cells: architecture, projections, and intrinsic photosensitivity. *Science*, 295(5557), 1065-1070.
- He, G., & Yan, H. (2011). Optimal spectra of the phosphor-coated white LEDs with excellent color rendering property and high luminous efficacy of radiation. *Optics Express*, 19(3), 2519-2529.
- Hering, E. (1868). *Die lehre vom binocularen sehen*. Leipzig, Germany: Wilhelm Engelmann.
- Hernández-Andrés, J., Nieves, J. L., Valero, E. M., & Romero, J. (2004). Spectral-daylight recovery by use of only a few sensors. *JOSA A*, 21(1), 13-23.
- Hernández-Andrés, J., Romero, J., García-Beltrán, A., & Nieves, J. L. (1998). Testing linear models on spectral daylight measurements. *Applied Optics*, 37(6), 971-977.
- Hernández-Andrés, J., Romero, J., Nieves, J. L., & Lee, R. L. (2001). Color and spectral analysis of daylight in southern Europe. *JOSA A*, 18(6), 1325-1335.
- Herring, H., & Roy, R. (2007). Technological innovation, energy efficient design and the rebound effect. *Technovation*, 27(4), 194-203.
- Hertog, W., Llenas, A., Quintero, J. M., Hunt, C. E., & Carreras, J. (2014). Energy efficiency and color quality limits in artificial light sources emulating natural illumination. *Optics Express*, 22(107), A1659-A1668.
- Houser, K. W., Wei, M., David, A., Krames, M. R., & Shen, X. S. (2013). Review of measures for light-source color rendition and considerations for a two-measure system for characterizing color rendition. *Optics Express*, 21(8), 10393-10411.
- Hung, C.-C. (2016). Development of the RGB LEDs color mixing mechanism for stability the color temperature at different projection distances. *Technology and Health Care*, 24(s1), S271-S280.
- Hung, P. C., & Papamichael, K. (2015). *Application-specific spectral power distributions of white light*. Paper presented at the SID Symposium Digest of Technical Papers Advanced Light Sources, Components, and Systems II, San Jose, CA.
- Hung, P. C., & Tsao, J. Y. (2013). Maximum white luminous efficacy of radiation versus color rendering index and color temperature: Exact results and a useful analytic expression. *Journal of Display Technology*, 9(6), 405-412.
- Hunt, R. W. G. (1952). Light and dark adaptation and the perception of color. *JOSA*, 42(3), 190-199.
- Hunt, R. W. G. (1989). Hue shifts in unrelated and related colours. *Color Research & Application*, 14(5), 235-239.
- Hunt, R. W. G., & Pointer, M. R. (2011). *Measuring colour*. Chichester, England: John Wiley & Sons.
- Hurvich, L. M. (1981). *Color vision*. Sunderland, MA: Sinauer Associates.
- Hurvich, L. M., & Jameson, D. (1957). An opponent-process theory of color vision. *Psychological Review*, 64(6p1), 384.
- IEA. (2013a). *Redrawing the energy-climate map: World energy outlook special report*. Paris, France: International Energy Agency.
- IEA. (2013b). *Transition to sustainable buildings: Strategies and opportunities to 2050*. Paris, France: International Energy Agency.

- IEA. (2014). *World energy outlook 2014*. Paris, France: International Energy Agency.
- IEA. (2016). *World energy outlook 2016*. Paris, France: International Energy Agency.
- IES. (2015). *TM-30-15 IES method for evaluating light source color rendition*. New York, NY: Illuminating Engineering Society.
- Imai, F. H., Berns, R. S., & Tzeng, D.-Y. (2000). A comparative analysis of spectral reflectance estimated in various spaces using a trichromatic camera system. *Journal of Imaging Science and Technology*, 44(4), 280-287.
- International Color Consortium. (2004). *Specification ICC. 1: 2004-10: Image technology colour management—Architecture, profile format, and data structure*.
- Iqbal, M. (1983). *An introduction to solar radiation*. Toronto, Canada: Academic Press.
- ISO. (1998). 3668.1998 *Paints and varnishes -- Visual comparison of the colour of paints*.
- ISO. (2008). 11664-4:2008 *Colorimetry -- Part 4: CIE 1976 L*a*b* Colour space*.
- Ito, K., Higashi, H., Ota, Y., & Nakauchi, S. (2015). Spectral-difference enhancing illuminant for improving visual detection of blood vessels. *Paper presented at Advanced Informatics: Concepts, Theory and Applications (ICAICTA)*, 2nd International Conference on IEEE, Chonburi, Thailand.
- Jameson, D., & Hurvich, L. M. (1955). Some quantitative aspects of an opponent-colors theory. I. Chromatic responses and spectral saturation. *JOSA*, 45(7), 546-552.
- Jost-Boissard, S., Avouac, P., & Fontoynont, M. (2015). Assessing the colour quality of LED sources: Naturalness, attractiveness, colourfulness and colour difference. *Lighting Research & Technology*, 47(7), 769-794.
- Jost-Boissard, S., Fontoynont, M., & Blanc-Gonnet, J. (2009). Perceived lighting quality of LED sources for the presentation of fruit and vegetables. *Journal of Modern Optics*, 56(13), 1420-1432.
- Judd, D. B. (1967). A flattery index for artificial illuminants. *Illuminating Engineering*, 62(10), 593.
- Judd, D. B., MacAdam, D. L., & Wyszecki, G. (1964). Spectral distribution of typical daylight as a function of correlated color temperature. *JOSA*, 54(8), 1031-1040.
- Kalloniatis, M., & Luu, C. (2007). *The perception of color*. Salt Lake City, UT: University of Utah Health Sciences Center.
- Khanh, T., & Bodrogi, P. (2016). Colour preference, naturalness, vividness and colour quality metrics, Part 3: Experiments with makeup products and analysis of the complete warm white dataset. *Lighting Research & Technology*, 0, 1-19.
- Klein, M. E., Aalderink, B. J., Padoan, R., De Bruin, G., & Steemers, T. A. (2008). Quantitative hyperspectral reflectance imaging. *Sensors*, 8(9), 5576-5618.
- Klipstein, D. L. (1996). *The great internet light bulb book* (Part 1). DL Klipstein, 19. Retrieved from <http://www.iar.unicamp.br/lab/luz/ld/L%E2mpadas/The%20Great%20Internet%20Light%20Bulb%20Book.pdf>
- Koedam, M., & Opstelten, J. (1971). Measurement and computer-aided optimization of spectral power distributions. *Lighting Research & Technology*, 3(3), 205-210.
- Kozakov, R., Franke, S., & Schöpp, H. (2008). Approach to an effective biological spectrum of a light source. *Leukos*, 4(4), 255-263.
- Lamb, T. D., & Pugh, E. N. (2006). Phototransduction, dark adaptation, and rhodopsin regeneration the proctor lecture. *Investigative Ophthalmology & Visual Science*, 47(12), 5138-5152.
- Li, C., Luo, M. R., Cui, G., & Li, C. (2011). Evaluation of the CIE colour rendering index. *Coloration Technology*, 127(2), 129-135.
- Li, C., Luo, M. R., Li, C., & Cui, G. (2012). The CRI-CAM02UCS colour rendering index. *Color Research & Application*, 37(3), 160-167.
- Li, H., Mao, X., Han, Y., & Luo, Y. (2013). Wavelength dependence of colorimetric properties of lighting sources based on multi-color LEDs. *Optics Express*, 21(3), 3775-3783.
- Lin, Y., Deng, Z., Guo, Z., Liu, Z., Lan, H., Lu, Y., & Cao, Y. (2014). Study on the correlations between color rendering indices and the spectral power distribution. *Optics Express*, 22(104), A1029-A1039.
- Liu, Q., Huang, Z., Xiao, K., Pointer, M. R., Westland, S., & Luo, M. R. (2017). Gamut Volume Index: A color preference metric based on meta-analysis and optimized colour samples. *Optics Express*, 25(14), 16378-16391.

- Lodish, H., Baltimore, D., Berk, A., Zipursky, S. L., Matsudaira, P., & Darnell, J. (1995). *Molecular cell biology* (Vol. 3). New York, NY: Scientific American Books.
- Lu, Y., Gao, Y., Chen, H., & Chen, Z. (2007). Intelligent spectral design and colorimetric parameter analysis for light-emitting diodes. Paper presented at *14th International Conference on IEEE Mechatronics and Machine Vision in Practice, M2VIP 2007*, Xiamen, China.
- Luo, M. R., Cui, G., & Li, C. (2006). Uniform colour spaces based on CIECAM02 colour appearance model. *Color Research & Application*, 31(4), 320-330.
- Lynch, D. K., & Livingston, W. C. (2001). *Color and light in nature*. Cambridge University Press.
- MacEvoy, B. (2015). Additive & subtractive color mixing. Retrieved from <https://www.handprint.com/HP/WCL/color5.html>
- MacLeod, D. I., & Hayhoe, M. (1974). Three pigments in normal and anomalous color vision. *JOSA*, 64(1), 92-96.
- MacNichol, E. F. (1964). Three-pigment color vision. *Scientific American*, 211, 48-57.
- Malacara, D. (2011). *Color vision and colorimetry: Theory and applications* (Vol. 2). Bellingham, WA: SPIE.
- Masoso, O., & Grobler, L. J. (2010). The dark side of occupants' behaviour on building energy use. *Energy and Buildings*, 42(2), 173-177.
- Massa, G. D., Kim, H.-H., Wheeler, R. M., & Mitchell, C. A. (2008). Plant productivity in response to LED lighting. *HortScience*, 43(7), 1951-1956.
- McLaren, K. (1985). Newton's indigo. *Color Research & Application*, 10(4), 225-229.
- Mellette, W. M., Schuster, G. M., & Ford, J. E. (2014). Planar waveguide LED illuminator with controlled directionality and divergence. *Optics Express*, 22(103), A742-A758.
- Miller, C., Ohno, Y., Davis, W., Zong, Y., & Dowling, K. (2009). NIST spectrally tunable lighting facility for color rendering and lighting experiments. *Proceedings of Light and Lighting Conference with Special Emphasis on LEDs and Solid State Lighting*, Budapest, Hungary.
- Milne, G., & Riedy, C. (2013). *Your home*. Retrieved from <http://www.yourhome.gov.au/sites/prod.yourhome.gov.au/files/pdf/YOURHOME-Energy-Lighting.pdf>.
- Mohr, H. (1972). *Lectures on photomorphogenesis*. Berlin, Germany: Springer-Verlag.
- Mohr, P. J., Taylor, B. N., & Newell, D. B. (2012). CODATA recommended values of the fundamental physical constants: 2010 a. *Journal of Physical and Chemical Reference Data*, 41(4), 1527.
- Mönch, W. (2015). Micro-optics in lighting applications. *Advanced Optical Technologies*, 4(1), 79-85.
- Morrow, R. C. (2008). LED lighting in horticulture. *HortScience*, 43(7), 1947-1950.
- Moss, R., & Loomis, W. (1952). Absorption spectra of leaves. I. The visible spectrum. *Plant Physiology*, 27(2), 370.
- Munsell, A. H. (1915). *Atlas of the Munsell color system*. Boston, MA: Wadsworth, Howland & Company, Incorporated, Printers.
- Murphy Jr, T. W. (2012). Maximum spectral luminous efficacy of white light. *Journal of Applied Physics*, 111(10), 104909.
- Narendran, N., & Deng, L. (2002). Color rendering properties of LED light sources. Paper presented at the *Proc. SPIE. Volume 4776*, p. 61-67, Seattle, WA.
- NASA. (2016). Sun: By the numbers. Retrieved from <https://solarsystem.nasa.gov/planets/sun/facts>
- National Research Council. (2013). *Assessment of Advanced Solid-State Lighting*. Washington, DC: The National Academies Press.
- Neumann, A., Wierer, J., Davis, W., Ohno, Y., Brueck, S., & Tsao, J. (2011). Four-color laser white illuminant demonstrating high color-rendering quality. *Optics Express*, 19(104), A982-A990.
- Newcombe, R. A., Izadi, S., Hilliges, O., Molyneaux, D., Kim, D., Davison, A. J., . . . Fitzgibbon, A. (2011). *KinectFusion: Real-time dense surface mapping and tracking*. Paper presented at *10th IEEE International Symposium on Mixed and Augmented Reality (ISMAR)*, Basel, Switzerland.
- Newcombe, R. A., Lovegrove, S. J., & Davison, A. J. (2011). DTAM: Dense tracking and mapping in real-time. Paper presented at *IEEE 2011 International Conference on Computer Vision (ICCV)*, Barcelona, Spain.

- Newhall, S., Burnham, R., & Clark, J. R. (1957). Comparison of successive with simultaneous color matching. *JOSA*, 47(1), 43-56.
- Newton, I. (1704). *Opticks: or a treatise of the reflexions, refractions, inflexions and colours of light*. London, England: Sam. Smith, and Benj. Walford, Printers to the Royal Society, at the Prince's Arms in St. Paul's Church-Yard.
- Ochoa, C. E., Aries, M. B., van Loenen, E. J., & Hensen, J. L. (2012). Considerations on design optimization criteria for windows providing low energy consumption and high visual comfort. *Applied Energy*, 95, 238-245.
- Oh, J. H., Kang, H., Park, H. K., & Do, Y. R. (2015). Optimization of the theoretical photosynthesis performance and vision-friendly quality of multi-package purplish white LED lighting. *Rsc Advances*, 5(28), 21745-21754.
- Oh, J. H., Oh, J. R., Park, H. K., Sung, Y.-G., & Do, Y. R. (2011). New paradigm of multi-chip white LEDs: combination of an InGaN blue LED and full down-converted phosphor-converted LEDs. *Optics Express*, 19(103), A270-A279.
- Oh, J. H., Yang, S. J., & Do, Y. R. (2014). Healthy, natural, efficient and tunable lighting: four-package white LEDs for optimizing the circadian effect, color quality and vision performance. *Light: Science and Applications*, 3(2), e141.
- Ohno, Y. (1999). *OSA handbook of optics Visual optics and vision chapter for photometry and radiometry*. (Vol. 3). *Optical Technology Division*, 1-17, New York, NY: McGraw-Hill Professional.
- Ohno, Y. (2004). *Color rendering and luminous efficacy of white LED spectra*. Paper presented at the SPIE International Symposium on Optical Science and Technology, the SPIEs 49th Annual Meeting, Denver, CO.
- Ohno, Y. (2005). Spectral design considerations for white LED color rendering. *Optical Engineering*, 44(11), 111302-111302-111309.
- Ohno, Y., Fein, M., & Miller, C. (2015). Vision experiment on chroma saturation for color quality preference. Paper presented at the 28th CIE Session, Manchester, England.
- Okawa, H., & Sampath, A. P. (2007). Optimization of single-photon response transmission at the rod-to-rod bipolar synapse. *Physiology*, 22(4), 279-286.
- Paltsev, S. (2017). Energy scenarios: The value and limits of scenario analysis. *Wiley Interdisciplinary Reviews: Energy and Environment*, 6(4).
- Perrin, T., Druzik, J., & Miller, N. (2014). *SSL adoption by museums: Survey results, analysis, and recommendations*. Retrieved from https://energy.gov/sites/prod/files/2015/02/f19/gateway_museums-report_0.pdf
- Perry, F. N., Henry, S., Perry, M. E., & MacArthur, L. (2015). *California Green Innovation Index: International edition*. Retrieved from <http://next10.org/sites/next10.org/files/2015-Green-Innovation-Index.pdf>
- Pointer, M. R. (1986). Measuring colour rendering—a new approach. *Lighting Research & Technology*, 18(4), 175-184.
- Porra, R., Thompson, W., & Kriedemann, P. (1989). Determination of accurate extinction coefficients and simultaneous equations for assaying chlorophylls a and b extracted with four different solvents: Verification of the concentration of chlorophyll standards by atomic absorption spectroscopy. *Biochimica et Biophysica Acta (BBA)-Bioenergetics*, 975(3), 384-394.
- Poulet, L., Massa, G., Morrow, R., Bourget, C., Wheeler, R., & Mitchell, C. (2014). Significant reduction in energy for plant-growth lighting in space using targeted LED lighting and spectral manipulation. *Life Sciences in Space Research*, 2, 43-53.
- Pridmore, R. W. (1999). Bezold–Brücke hue-shift as functions of luminance level, luminance ratio, interstimulus interval and adapting white for aperture and object colors. *Vision research*, 39(23), 3873-3891.
- Pridmore, R. W. (2004). Bezold–Brücke effect exists in related and unrelated colors and resembles the Abney effect. *Color Research & Application*, 29(3), 241-246.
- Provencio, I., Rodriguez, I. R., Jiang, G., Hayes, W. P., Moreira, E. F., & Rollag, M. D. (2000). A novel human opsin in the inner retina. *Journal of Neuroscience*, 20(2), 600-605.
- Purdy, D. M. (1937). The Bezold–Brücke phenomenon and contours for constant hue. *The American Journal of Psychology*, 313-315.

- Ramachandran, V. S., & Gregory, R. L. (1991). Perceptual filling in of artificially induced scotomas in human vision. *Nature*, 350(6320), 699.
- Rea, M. S., Deng, L., & Wolsey, R. (2003). *Lighting answers: Full-spectrum light sources*. Troy, NY: National Lighting Product Information Program Rensselaer Polytechnic Institute.
- Rea, M. S., Figueiro, M. G., Bierman, A., & Hamner, R. (2012). Modelling the spectral sensitivity of the human circadian system. *Lighting Research & Technology*, 44(4), 386-396.
- Rea, M. S., Figueiro, M. G., & Bullough, J. D. (2002). Circadian photobiology: an emerging framework for lighting practice and research. *Lighting Research & Technology*, 34(3), 177-187.
- Rea, M. S., & Freyssinier-Nova, J. P. (2008). Color rendering: A tale of two metrics. *Color Research & Application*, 33(3), 192-202.
- Reitz, J. R., Milford, F. J., & Christy, R. W. (2008). *Foundations of electromagnetic theory*. San Francisco, CA: Addison-Wesley Publishing Company.
- Ries, H., Leike, I., & Muschaweck, J. (2004). Optimized additive mixing of colored light-emitting diode sources. *Optical Engineering*, 43(7), 1531-1536.
- Romero, J., García-Beltrán, A., & Hernández-Andrés, J. (1997). Linear bases for representation of natural and artificial illuminants. *JOSA A*, 14(5), 1007-1014.
- Roy, A. E., & Clarke, D. (2003). *Astronomy: Principles and practice* (Vol. 4). Philadelphia, PA: Institute of Physics Pub.
- Royer, M., Houser, K., & Wilkerson, A. (2012). Color discrimination capability under highly structured spectra. *Color Research & Application*, 37(6), 441-449.
- Rushton, W. A. H. (1962). Visual pigments in man. *Scientific American*, 207, 120.
- Rushton, W. A. H. (1972). Review lecture. Pigments and signals in colour vision. *The Journal of Physiology*, 220(3), 1P.
- Rushton, W. A. H. (1975). Visual pigments and color blindness. *Scientific American*, 232(3), 64.
- Sager, J., Smith, W., Edwards, J., & Cyr, K. (1988). Photosynthetic efficiency and phytochrome photoequilibria determination using spectral data. *Transactions of the ASAE*, 31(6), 1882-1889.
- Sandahl, L. J., Gilbride, T. L., Ledbetter, M. R., Steward, H. E., & Calwell, C. (2006). *Compact fluorescent lighting in America: Lessons learned on the way to market*. Retrieved from https://www1.eere.energy.gov/buildings/publications/pdfs/ssl/cfl_lessons_learned_web.pdf
- Sanders, C. (1959). Color preferences for natural objects. *Illuminating Engineering*, 54, 452-456.
- Sándor, N., & Schanda, J. (2006). Visual colour rendering based on colour difference evaluations. *Lighting Research and Technology*, 38(3), 225-239.
- Sansonetti, C. J., Salit, M. L., & Reader, J. (1996). Wavelengths of spectral lines in mercury pencil lamps. *Applied Optics*, 35(1), 74-77.
- Sastri, V., & Das, S. (1968). Typical spectral distributions and color for tropical daylight. *JOSA*, 58(3), 391-398.
- Schanda, J. (1985). A combined colour preference-colour rendering index. *Lighting Research & Technology*, 17(1), 31-34.
- Schanda, J. (2007). *Colorimetry: Understanding the CIE system*. Hoboken, NJ: John Wiley & Sons.
- Schanda, J., Csuti, P., & Szabo, F. (2016). A new concept of color fidelity for museum lighting: based on an experiment in the Sistine Chapel. *Leukos*, 12(1-2), 71-77.
- Schiler, M. (1997). *Simplified design of building lighting* (Vol. 28). New York, NY: John Wiley & Sons.
- Schipper, L., & Grubb, M. (2000). On the rebound? Feedback between energy intensities and energy uses in IEA countries. *Energy Policy*, 28(6), 367-388.
- SharkD (Producer). (2009). Munsell 1929 color solid cylinder (modified). Retrieved from https://commons.wikimedia.org/wiki/File:Munsell_1929_color_solid_cylindrical_coordinates.png
- Sharpe, L. T., Stockman, A., Jägle, H., & Nathans, J. (1999). Opsin genes, cone photopigments, color vision, and color blindness. In K.R. Gegenfurtner & L.T. Sharpe (eds.), *Color vision: From genes to perception* (3-51). Cambridge, England: Cambridge University Press.
- Shimano, N. (2006). Recovery of spectral reflectances of objects being imaged without prior knowledge. *IEEE Transactions on Image Processing*, 15(7), 1848-1856.

- Shimano, N., Terai, K., & Hironaga, M. (2007). Recovery of spectral reflectances of objects being imaged by multispectral cameras. *JOSA A*, 24(10), 3211-3219.
- Shrestha, R., Mansouri, A., & Hardeberg, J. Y. (2011). Multispectral imaging using a stereo camera: Concept, design and assessment. *EURASIP Journal on Advances in Signal Processing*, 2011(1), 57.
- Siple, P., & Springer, R. M. (1983). Memory and preference for the colors of objects. *Attention, Perception, & Psychophysics*, 34(4), 363-370.
- Sliney, D. H. (2016). What is light? The visible spectrum and beyond. *Eye*. London, England: Macmillan Publishers Limited.
- Sliney, D. H., Wangemann, R. T., Franks, J. K., & Wolbarsht, M. L. (1976). Visual sensitivity of the eye to infrared laser radiation. *JOSA*, 66(4), 339-341.
- Smet, K. A., Ryckaert, W. R., Pointer, M. R., Deconinck, G., & Hanselaer, P. (2010). Memory colours and colour quality evaluation of conventional and solid-state lamps. *Optics Express*, 18(25), 26229-26244.
- Smet, K. A., Ryckaert, W. R., Pointer, M. R., Deconinck, G., & Hanselaer, P. (2011). Correlation between color quality metric predictions and visual appreciation of light sources. *Optics Express*, 19(9), 8151-8166.
- Smet, K. A., Ryckaert, W. R., Pointer, M. R., Deconinck, G., & Hanselaer, P. (2012). Optimization of colour quality of LED lighting with reference to memory colours. *Lighting Research & Technology*, 44(1), 7-15.
- Smet, K. A., Schanda, J., Whitehead, L., & Luo, M. R. (2013). CRI2012: A proposal for updating the CIE colour rendering index. *Lighting Research & Technology*, 45(6), 689-709.
- Smets, G. (1982). A tool for measuring relative effects of hue, brightness and saturation on color pleasantness. *Perceptual and Motor Skills*, 55(3 suppl), 1159-1164.
- Speier, I., & Salsbury, M. (2006). *Color temperature tunable white light LED system*. Paper presented at the Proc. SPIE. 6337, Sixth International Conference on Solid State Lighting, San Diego, CA.
- Sprengers, L., Campbell, R., & Kostlin, H. (1985). Low pressure sodium lamps with a luminous efficacy of 200 lm/W. *Journal of the Illuminating Engineering Society*, 14(2), 607-615.
- Stockman, A., MacLeod, D. I., & Johnson, N. E. (1993). Spectral sensitivities of the human cones. *JOSA A*, 10(12), 2491-2521.
- Strathern, M. (1997). 'Improving ratings': Audit in the British University system. *European Review*, 5(3), 305-321.
- Stutte, G. W. (2009). Light-emitting diodes for manipulating the phytochrome apparatus. *HortScience*, 44(2), 231-234.
- Svaetichin, G. (1956). Spectral response curves from single cones. *Acta physiologica Scandinavica. Supplementum*, 39(134), 17-46.
- Szabo, F., Zilizi, I., Bodrogi, P., & Schanda, J. (2007). Visual experiments on colour harmony: A formula and a rendering index. *CIE 26th Session, CIE*, 178, D1-2, Beijing, China.
- Tamulaitis, G., Duchovskis, P., Bliznikas, Z., Breive, K., Ulinskaite, R., Brazaityte, A., . . . Žukauskas, A. (2005). High-power light-emitting diode based facility for plant cultivation. *Journal of Physics D: Applied Physics*, 38(17), 3182.
- Tan, K. E. W. P. (1971). *Vision in the ultraviolet*. (Doctoral dissertation). University of Utrecht, Utrecht, Netherlands.
- Tan, S. T., Sun, X., Demir, H. V., & DenBaars, S. (2012). Advances in the LED materials and architectures for energy-saving solid-state lighting toward "lighting revolution". *IEEE Photonics Journal*, 4(2), 613-619.
- Tarrant, A. (1968). The spectral power distribution of daylight. *Transactions of the Illuminating Engineering Society*, 33(3_IEStrans), 75-82.
- Teunissen, C., van der Heijden, F., Poort, S., & de Beer, E. (2017). Characterising user preference for white LED light sources with CIE colour rendering index combined with a relative gamut area index. *Lighting Research & Technology*, 49(4), 461-480.
- Thapan, K., Arendt, J., & Skene, D. J. (2001). An action spectrum for melatonin suppression: evidence for a novel non-rod, non-cone photoreceptor system in humans. *The Journal of physiology*, 535(1), 261-267.

- Thornton, W. A. (1971). Luminosity and color-rendering capability of white light. *JOSA*, 61(9), 1155-1163.
- Thornton, W. A. (1972). Color-discrimination index. *JOSA*, 62(2), 191-194.
- Thornton, W. A. (1974). A validation of the color-preference index. *Journal of the Illuminating Engineering Society*, 4(1), 48-52.
- Thorseth, A. (2012). *Optimization of light quality from color mixing light-emitting diode systems for general lighting*. Paper presented at the Proc. of SPIE 8278, Light-Emitting Diodes: Materials, Devices, and Applications for Solid State Lighting XVI, San Francisco, CA.
- Tilbury, D., Douglas, B., & Rowland, J. (2006). Australia's first retail lighting experiment dramatically reduces lighting energy costs and greenhouse emissions [Press release], Canberra, Australia.
- Tominaga, S. (1991). Surface identification using the dichromatic reflection model. *IEEE transactions on pattern analysis and machine intelligence*, 13(7), 658-670.
- Tominaga, S., & Wandell, B. A. (1989). Standard surface-reflectance model and illuminant estimation. *JOSA A*, 6(4), 576-584.
- Tong, F., & Engel, S. A. (2001). Interocular rivalry revealed in the human cortical blind-spot representation. *Nature*, 411(6834), 195.
- Torres, M., Jassel, R., & Tang, Y. (2012). *Augmented reality using spatially multiplexed structured light*. Paper presented at Mechatronics and Machine Vision in Practice (M2VIP), 19th International Conference IEEE, Auckland, New Zealand.
- Tuzikas, A., Žukauskas, A., Vaicekauskas, R., Petrulis, A., Vitta, P., & Shur, M. (2014). Artwork visualization using a solid-state lighting engine with controlled photochemical safety. *Optics Express*, 22(14), 16802-16818.
- van der Burgt, P., & van Kemenade, J. (2006). *The challenge in communicating color rendition of light sources, The balance between simplicity and accuracy*. Paper presented at the Proc. 6th Int. Symp. Light Color, Orlando, FL.
- Vandewalle, G., Maquet, P., & Dijk, D.-J. (2009). Light as a modulator of cognitive brain function. *Trends in cognitive sciences*, 13(10), 429-438.
- Viénot, F., Coron, G., & Lavédrine, B. (2011). LEDs as a tool to enhance faded colours of museums artefacts. *Journal of Cultural Heritage*, 12(4), 431-440.
- von Helmholtz, H., & Southall, J. P. C. (1962). *Helmholtz's treatise on physiological optics*. New York, NY: Dover Publications.
- von Kries, J. (1902). Chromatic adaptation. *Festschrift der Albrecht-Ludwigs-Universität*, 135, 145-158.
- Vrabel, P. L., Bernecker, C., & Mistrick, R. (1998). Visual performance and visual clarity under electric light sources: Part II—visual clarity. *Journal of the Illuminating Engineering Society*, 27(1), 29-41.
- Waide, P. (2010). *Phase out of incandescent lamps: Implications for international supply and demand for regulatory compliant lamps*. Paris, France: International Energy Agency.
- Waide, P., & Tanishima, S. (2006). *Light's labour's lost*. Paris, France: International Energy Agency.
- Wandell, B. A. (1995). *Foundations of vision*. Sunderland, MA: Sinauer Associates.
- Wang, H., Cuijpers, R. H., Luo, M. R., Heynderickx, I., & Zheng, Z. (2015). Optimal illumination for local contrast enhancement based on the human visual system. *Journal of Biomedical Optics*, 20(1), 015005-015005.
- Webb, A. R. (2006). Considerations for lighting in the built environment: Non-visual effects of light. *Energy and Buildings*, 38(7), 721-727.
- WEC. (2016). *World energy resources 2016*. Retrieved from <https://www.worldenergy.org/wp-content/uploads/2016/10/World-Energy-Resources-Full-report-2016.10.03.pdf>
- Wellburn, A. R. (1994). The spectral determination of chlorophylls a and b, as well as total carotenoids, using various solvents with spectrophotometers of different resolution. *Journal of Plant Physiology*, 144(3), 307-313.
- Whitehead, L. A., & Mossman, M. A. (2012). A Monte Carlo method for assessing color rendering quality with possible application to color rendering standards. *Color Research & Application*, 37(1), 13-22.
- Wiesel, T. N., & Hubel, D. H. (1966). Spatial and chromatic interactions in the lateral geniculate body of the rhesus monkey. *Journal of Neurophysiology*, 29(6), 1115-1156.

- Winch, G., Boshoff, M., Kok, C., & Du Toit, A. (1966). Spectroradiometric and colorimetric characteristics of daylight in the southern hemisphere: Pretoria, South Africa. *JOSA*, 56(4), 456-464.
- Wright, W. D. (1929). A re-determination of the trichromatic coefficients of the spectral colours. *Transactions of the Optical Society*, 30(4), 141.
- Wyszecki, G., & Stiles, W. S. (1982). *Color science: concepts and methods, quantitative data and formulae* (2nd ed.). New York, NY: Wiley.
- Xu, H. (1993). Colour rendering capacity and luminous efficiency of a spectrum. *International Journal of Lighting Research and Technology*, 25(3), 131-132.
- Yaguchi, H., Takahashi, Y., & Shioiri, S. (2001). *A proposal of color rendering index based on categorical color names*. Paper presented at the Internat Lighting Congress, Istanbul, Turkey.
- Yano, T., & Hashimoto, K. (1997). Preference for Japanese complexion color under illumination. *Color Research & Application*, 22(4), 269-274.
- Yao, Q. (2016). Application-dependent spectrum optimization of four-package LEDs. *Lighting Research & Technology*, 48(7), 844-856.
- Yao, Q., Yuan, L., & Bian, Y. (2016). Establishment of vision effect diagram for optimization of smart LED lighting. *IEEE Photonics Journal*, 8(4), 1-8.
- Young, T. (1802). The Bakerian lecture: On the theory of light and colours. *Philosophical Transactions of the Royal Society of London*, 92, 12-48.
- Yu, Y., Debevec, P., Malik, J., & Hawkins, T. (1999). *Inverse global illumination: Recovering reflectance models of real scenes from photographs*. Proceedings from 26th Annual Conference on Computer Graphics and Interactive Techniques. New York, NY: ACM Press/Addison-Wesley Publishing Co.
- Yu, Y., & Malik, J. (1998). *Recovering photometric properties of architectural scenes from photographs*. Proceedings from 25th Annual Conference on Computer Graphics and Interactive Techniques. New York, NY: ACM.
- Yun, G. Y., Jung, H., & Kim, J. T. (2013). Energy-saving potential of LED lighting systems. *Indoor and Built Environment*, 22(1), 235-241.
- Zaidi, F. H., Hull, J. T., Peirson, S. N., Wulff, K., Aeschbach, D., Gooley, J. J., . . . Czeisler, C. A. (2007). Short-wavelength light sensitivity of circadian, pupillary, and visual awareness in humans lacking an outer retina. *Current Biology*, 17(24), 2122-2128.
- Zhang, J., Hu, R., Xie, B., Yu, X., Luo, X., Yu, Z., . . . Jin, X. (2017). Energy-saving light source spectrum optimization by considering object's reflectance. *IEEE Photonics Journal*, 9(2), 1-11.
- Zhang, M., Chen, Y., & He, G. (2014). Color temperature tunable white-light LED cluster with extrahigh color rendering index. *The Scientific World Journal*, 2014.
- Zheng, G., Wang, B., Fang, T., Cheng, H., Qi, Y., Wang, Y., . . . Chu, S. (2008). Laser digital cinema projector. *Journal of Display Technology*, 4(3), 314-318.
- Zhong, P., He, G., & Zhang, M. (2012a). Optimal spectra of white light-emitting diodes using quantum dot nanophosphors. *Optics Express*, 20(8), 9122-9134.
- Zhong, P., He, G., & Zhang, M. (2012b). Spectral optimization of the color temperature tunable white light-emitting diode (LED) cluster consisting of direct-emission blue and red LEDs and a diphosphor conversion LED. *Optics Express*, 20(105), A684-A693.
- Žukauskas, A., & Vaicekauskas, R. (2015). Tunability of the circadian action of tetrachromatic solid-state light sources. *Applied Physics Letters*, 106(4), 041107.
- Žukauskas, A., Vaicekauskas, R., Ivanauskas, F., Gaska, R., & Shur, M. S. (2002). Optimization of white polychromatic semiconductor lamps. *Applied Physics Letters*, 80(2), 234-236.
- Zukauskas, A., Vaicekauskas, R., Ivanauskas, F., Vaitkevicius, H., Vitta, P., & Shur, M. S. (2009). Statistical approach to color quality of solid-state lamps. *IEEE Journal of Selected Topics in Quantum Electronics*, 15(6), 1753-1762.
- Žukauskas, A., Vaicekauskas, R., & Shur, M. S. (2010). Colour-rendition properties of solid-state lamps. *Journal of Physics D: Applied Physics*, 43(35), 354006.
- Žukauskas, A., Vaicekauskas, R., & Vitta, P. (2012). Optimization of solid-state lamps for photobiologically friendly mesopic lighting. *Applied Optics*, 51(35), 8423-8432.

APPENDICES

Appendix A: Ethics approval

Research Integrity

Human Research Ethics Committee

Tuesday, 24 May 2016

Dr Wendy Davis

Architectural & Design Science; Faculty of Architecture, Design & Planning

Email: wendy.davis@sydney.edu.au

Dear Wendy

I am pleased to inform you that the University of Sydney Human Research Ethics Committee (HREC) has approved your project entitled "**Optimising light source spectrum for object reflectance**".

Details of the approval are as follows:

Project No.: 2016/383**Approval Date:** 24 May 2016**First Annual Report Due:** 24 May 2017**Authorised Personnel:** Davis Wendy; Durmus Dorukalp;**Documents Approved:**

Date Uploaded	Type	Document Name
17/05/2016	Advertisements/Flyer	Experiment 1 Flyer - version 2
17/05/2016	Advertisements/Flyer	Experiment 2 Flyer - version 2
17/05/2016	Advertisements/Flyer	Experiment 3 Flyer - version 2
17/05/2016	Participant Consent Form	PCF Experiment 1 - Final/clean version
17/05/2016	Participant Consent Form	PCF Experiment 2 - Final/clean version
17/05/2016	Participant Consent Form	PCF Experiment 3 - Final/clean version
17/05/2016	Participant Info Statement	PIS Experiment 1 - Final/clean version
17/05/2016	Participant Info Statement	PIS Experiment 2 - Final/clean version
17/05/2016	Participant Info Statement	PIS Experiment 3 - Final/clean version



HREC approval is valid for four (4) years from the approval date stated in this letter and is granted pending the following conditions being met:

Condition/s of Approval

- Continuing compliance with the National Statement on Ethical Conduct in Research Involving Humans.
- Provision of an annual report on this research to the Human Research Ethics Committee from the approval date and at the completion of the study. Failure to submit reports will result in withdrawal of ethics approval for the project.
- All serious and unexpected adverse events should be reported to the HREC within 72 hours.
- All unforeseen events that might affect continued ethical acceptability of the project should be reported to the HREC as soon as possible.
- Any changes to the project including changes to research personnel must be approved by the HREC before the research project can proceed.
- Note that for student research projects, a copy of this letter must be included in the candidate's thesis.

Chief Investigator / Supervisor's responsibilities:

1. You must retain copies of all signed Consent Forms (if applicable) and provide these to the HREC on request.
2. It is your responsibility to provide a copy of this letter to any internal/external granting agencies if requested.

Please do not hesitate to contact Research Integrity (Human Ethics) should you require further information or clarification.

Yours sincerely

Professor Glen Davis
Chair
Human Research Ethics Committee

This HREC is constituted and operates in accordance with the National Health and Medical Research Council's (NHMRC) National Statement on Ethical Conduct in Human Research (2007), NHMRC and Universities Australia Australian Code for the Responsible Conduct of Research (2007) and the CPMP/ICH Note for Guidance on Good Clinical Practice.

Appendix B: Conference paper

Abdalla, D., Duis, A., Durmus, D., & Davis, W. (2016). *Customization of light source spectrum to minimize light absorbed by artwork*. Paper presented at the CIE Lighting Quality and Energy Efficiency Conference 2016. Commission Internationale de L'Eclairage, Melbourne, Australia.

Authorship attribution statement

As the corresponding author, I grant permission to include this published material in this thesis.

.....
Dianna Abdalla

CUSTOMISATION OF LIGHT SOURCE SPECTRUM TO MINIMISE LIGHT ABSORBED BY ARTWORK

Abdalla D.¹, Duis, A.¹, Durmus, D.¹, Davis, W.¹

¹Faculty of Architecture, Design and Planning, The University of Sydney, AUSTRALIA

abdalla.dianna@gmail.com

Abstract

Museum lighting is provided to allow visitors to visually perceive displayed works of art, but it also harms illuminated items. Many types of museum exhibits are susceptible to damage caused by exposure to light, and current recommendations for artwork displays include the avoidance of non-visible radiant power, limitations on illuminance levels and restrictions on the duration of exposure. While artists' usually create their works under daylight, the lighting in most museum displays is of lower correlated colour temperature (CCT) and illuminance, which greatly impacts the colour appearance of the artwork. Custom spectral power distribution (SPD) light sources could be developed that decrease the amount of light absorbed by a pigment, thereby minimising damage, and also increase the chroma of a pigment, resulting in increased chromatic saturation and thus apparent brightness. Computational simulations were performed to compare custom SPD test illuminants with a reference illuminant for five oil paint colours.

Keywords: customised SPD, artwork, chroma, damage

1 Introduction

The lighting of displays in museums is a major contributor to the degradation of displayed artefacts. However, since the lighting is provided primarily for the purpose of enhancing the visual experience of visitors and allowing them to visually perceive the displayed works of art, it is a necessity in museums. Thus, in the display of art, there are two main competing criteria: appearance and damage (Berns 2010). In terms of preservation, the optimal lighting, which minimises irreversible damage, is complete darkness – in such a situation, appearance is non-existent. Current conservation standards are based on the damage curve by Harrison (CIE157 2004), which stipulates that spectral power in the longer wavelength region causes less damage than shorter wavelengths. As such, artwork in museum settings has traditionally been illuminated by incandescent lamps.

One issue that arises is the integrity of the appearance of the artwork, when compared to the artists' intent during the time that the artwork was created. As many artists utilised daylight when creating their artwork, it is a practical assumption that the artwork was also intended to be viewed under such conditions.

Existing guidelines stipulate that artwork with high sensitivity is to be illuminated to approximately 50 lx (CIE157 2004) and this is usually combined with a low correlated colour temperature (CCT), as seen in incandescent sources. This combination usually results in the appearance of the artwork being altered. The Hunt effect characterises the impact of light intensity on perceived colour saturation.

2 Damage

When viewing illuminated environments, people perceive the light reflected by the illuminated objects. Absorbed light is transferred into internal energy – most notably heat, and is considered a loss and is damaging to artwork (Durmus & Davis 2015). Photochemical action is the process by which a molecule undergoes a chemical change – with the activation for that change being derived by the absorption of a photon (CIE157 2004). The probability of a photon chemical reaction increases with photon energy. The absorption of light energy can start many possible sequences of chemical reactions, all of which damage objects. Each molecule in an object requires a minimum amount of energy to begin a chemical reaction with other molecules – known as activation energy. Different types of materials have different

activation energies (CIE157 2004). If the light energy from natural or electric light equals or exceeds the activation energy of a particular molecule, the molecule is then excited, or made available for chemical reactions, resulting in deterioration. Photochemical action can be induced by several factors, with those most likely to initiate the damaging process being irradiance, duration of exposure, spectral power distribution (SPD) of incident radiation and action spectrum of receiving material (CIE157 2004).

The principle of reciprocity states that the net photochemical effect is the result of the total exposure that an object receives – a product of intensity and time (Feller 2009). Therefore, it is often assumed that the extent of photochemical action will be reduced in direct proportion to the reduction in the incident radiant power or exposure time. However, it is to be noted that illuminance is not a reliable measure of damage alone, as it takes into account the radiant flux evaluated by a typical human visual response, defined by the photopic spectral luminous efficiency function, $V(\lambda)$ (CIE157 2004).

Different light sources, and thus different SPDs, affect the rate of fading and damage in artists' pigments. Harrison described the relationship between wavelength and damage to materials, resulting in what is known as the damage factor curve.

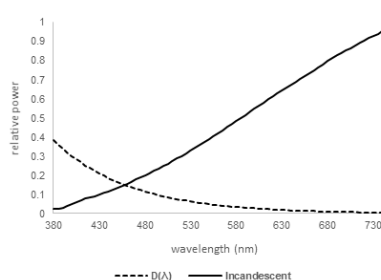


Figure 1 – Solid line is damage index, $D(\lambda)$, as a function of wavelength. Dashed line is relative power as a function of wavelength (SPD) of an incandescent light source.

As can be seen from figure 1, the damage index, $D(\lambda)$, indicates that damage factor is reduced as wavelength is increased. The overlaid incandescent SPD illustrates that relatively little light is emitted in the region of the spectrum considered to be most damaging, surely contributing to museum directors' belief that incandescent light sources are safest. In addition, the Kruithof curve claims that lower CCTs are considered more 'pleasant' at lower illuminances (Vienot 2009). Lighting of sensitive objects is limited to 50 lx, thus a low CCT source is considered ideal in this scenario.

However, it is recognised that it is impractical and impossible to assign a damage factor that would be appropriate for all museum objects, as damage is largely dependent on the absorbed radiation, which is dependent on the spectral reflectance of the material exposed. Studies of artists' pigments exposed to light have shown that the wavelength susceptibility of a pigment is largely determined by its spectral absorption (Saunders & Kirby). An artists' palette that includes a wide range of colours invariably includes pigments that absorb different portions of the visible spectrum. The spectral reflectance factor of a pigment largely determines the damage caused, as it is absorbed light that causes damage to occur. If a photon of light is not absorbed, it will not trigger photochemical action.

Radiant heating refers to an increase of the surface temperature above the ambient temperature due to absorption of incident radiant flux. A small portion of the absorbed radiation may induce a photochemical action. When taking into account the damaging impact of heat and the principle of reciprocity used to predict damage, 10 W/m² at 10 hours may not emit the same heat as 20 W/m² for five hours, particularly since incandescent sources have a majority of their radiant power near the infrared (IR) region of the electromagnetic spectrum. Of particular concern are settings in which lamps are mounted close to museum objects, such as in display cabinets. However, the effects of radiant heating are considered less of a concern than photochemical action and it is not uncommon for it to be disregarded completely. As museums become more rigorous in the control of photochemical action, radiant heating effects are more likely to become a concern.

3 Current Guidelines

Early work on conserving artworks led to the establishment of the recommended illuminance of 50 lx for materials with high to medium responsivity (very sensitive to light) and 200 lx for those with low responsivity (Thompson 1967). The CIE has also published recommendations to control damage by optical radiation. UV radiation is to be severely restricted or eliminated, visible light below 400 nm is to be eliminated and exposure to light is to be limited in both intensity and duration (Cuttle 2000). In addition to this, exposure limits in lux-hours per year are also recommended, as shown in Table 1.

Table 1 – CIE recommended exposure limits for different materials.

Material Classification	Illuminance Limitation (lx)	Exposure (lx-hr / yr)
Irresponsive	No Limit	No Limit
Low	200	600,000
Medium	50	150,000
High	50	15,000

Such restrictions, in particular regarding illuminance limits, arose from knowledge that colour discriminability drops dramatically below 50 lx. As such, it is important in museum lighting to maintain a certain level of illumination to enable viewing of artwork in a reasonable manner. However, it is not only the ability to see colours that needs to be taken into account, but also colour appearance. As the level of light increases, the illuminated object colour appears to be more saturated – it has a greater sense of colourfulness. This is important in the display of artwork and is referred to as the Hunt effect.

4 The Hunt Effect

The Hunt effect describes a phenomenon that occurs when a displayed object is illuminated by higher light levels. As illumination increases, the apparent colourfulness of an object also increases. When the light intensity is very low (<0.001 cd/m² reflected from the object), human vision is essentially homochromatic and is presumably mediated by rods alone. As the level of illumination increases, the colourfulness of colours increases continually all the way up to very high luminances (1000s cd/m²), as encountered in bright sunlight (Hunt 1977).

Hunt (1977) investigated the change in colourfulness that occurs as illumination level increases. His experiment involved an observer whose right eye was adapted to a reference field of 8.1 cd/m² of standard illuminant B. The left eye was adapted to various luminances of the same illuminant. Changes in colourfulness of stimuli presented to the left eye were then measured by determining the change in stimulus required to produce the same sensation in the right eye. This was done by presenting swatches of more saturated colours to the right eye (at a constant illuminance), until they matched that of the left eye (varied illuminance).

Point D in figure 2 represents an approximate illumination level of 42 lx. This is quite similar to the levels used to illuminate sensitive objects in museums. When compared to point A, representative of cloudy daylight at approximately 16,900 lux, it is evident that there is a considerable difference in the appearance of art in museum exhibitions when compared to that of the artists' intent. Whilst brightness will increase the appearance of saturation in a colour, the spectral composition of the light source also plays an important role.

A customised SPD could assist in increasing the chroma of the artwork, whilst allowing it to be rendered in a manner otherwise consistent with current illumination sources used. This could offer additional benefits, such as a reduction in the consumption of energy and a reduction in the absorption of light by the artwork. Advancements in lighting technology, in particular that of solid-state lighting (SSL), allows greater flexibility in a custom SPD solution.

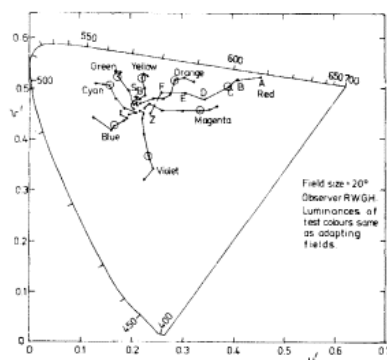


Figure 2 – The Hunt effect, showing increases in chroma with luminance, shown in CIE 1976 (u' , v') (Hunt, 1977).

The principle of univariance and metamerism allow for different SPDs to elicit a similar perception of colour appearance by the human visual system. Due to this, the customisation of SPDs becomes feasible, whereby they can lead to a similar colour appearance whilst having characteristics that aid in the conservation of illuminated art. This approach, however, is not new. Various investigations and attempts have been made to modify the illuminants' SPD to reduce the effects of light exposure.

5 Previous Research

Thornton (1975) proposed an approach to spectral design that sought to maintain or enhance the colour rendering properties of lighting, while reducing irradiance. Cuttle (2000) further attempted to improve the proposal put forward by Thornton by using a light source with three spectral peaks. The light source demonstrated a reduction in irradiance – thus a strategy was discovered which could reduce the damage exposure without reducing illuminance. Delgado, Dirk, Druzik and WestFall (2010) undertook further research based on Cuttle's strategy, which was centred on optimising the lumens per optical watt of a light source, whilst maintaining colour rendering. This followed the principle that reducing the radiant energy projected onto the artwork will lead to decreased photochemical reactions in the object.

Others took a different approach. Chalmers, Cuttle and Van Ryn (2006) used an optical fibre system, whilst Vienot, Coron and Lavedrine (2011) investigated the use of customised SPDs to enhance already faded colours of museum artefacts. More recently, however, explorations into customised SPDs for specific pigments have been investigated. Durmus and Davis (2015) demonstrated that wavelength adjustable lighting systems can reduce the energy consumed by lighting by not emitting unnecessary (absorbed) wavelengths from a light source and, thereby, minimise the energy wasted by absorption of objects and other surfaces.

6 Customised SPDs

When developing ways that SSL could be leveraged to customise illumination on museum objects to minimise damage and increase colourfulness, the aspects of light that are considered damaging to objects of art were considered:

- Irradiance and duration of exposure,
- SPD of incident radiation,
- Action spectrum of receiving material, and
- Radiant heating.

The guidelines currently available to combat such effects were also considered. The CIE (CIE157 2004) recommends the following:

- Illuminance level limits of 50 lx for high to moderately sensitive objects and 200 lx for objects with low sensitivity,
- Radiation below 400 nm is to be omitted, and
- A restriction in the total lux-hours per year depending on the artefact (per table 1).

These principles have been satisfactory in illuminating artwork, considering the traditional sources of light and the flexibility they afforded. However, there are some aspects the current

guidelines do not take into account, the first being the action spectrum of the receiving material. The damage curve by Harrison (CIE157 2004) assumed that all pigments would react in a similar manner when exposed to photons of light and did not take into account the differing reflectance and absorption characteristics of different pigment colours. Recent investigations by Saunders and Kirby (1994) demonstrated that the damage factor curve does not adequately represent the behaviour of all pigments. Samples of different paint colours were exposed to a limited part of the spectrum via the application of filters on the light source, allowing only light in certain areas of the electromagnetic spectrum to pass. It was found that, for all colours, damage (a change in colour due to fading) was greatest at 400 nm. The yellow and red pigments were shown to have a reduced rate of colour change as wavelength increased, reflecting Harrison's damage curve. However, the results for the various blue pigments assessed were very interesting. Damage was shown to be greatest at 400 nm. However, damage was lowest between 440 nm and 480 nm, increasing again between 500 nm and 600 nm. This behaviour is explained by the way in which the pigments reflect and absorb light.

The second aspect that needs to be taken into account is the original intent of the artist. As has been discussed thus far and demonstrated by the Hunt effect, low CCTs and low illuminance levels currently used in museum displays do not render artworks as they would appear under daylight conditions. However, with conservation, compromises must be made. Therefore, what can be provided is a light source that increases the chroma of the colours in an artwork, allowing for a shift towards how they would appear under daylight and allowing the art to look more natural to observers.

This research seeks to further the investigations by Durmus and Davis, whereby light sources with custom SPDs would be generated to illuminate specific pigment colours. However, additional criteria are considered. Three main questions were posed:

1. Can a light source be designed to achieve specific colour appearance attributes, such as an increase in chroma in paint colours?
2. Is it possible for such a source to reduce the absorption of light by coloured paints, whilst achieving the desired colour appearance?
3. Is it possible for such a source to also provide a reduction in energy?

6.1 Experiment

The experiment was conducted in the Lighting Lab of the University of Sydney. Computational simulations of the impact of the light source spectral power distributions on the perceived colours of objects, the absorption of light and energy consumption were conducted.

6.2 Methods

Oil paint of five colours – blue (r-b), green (r-g), yellow (r-y), orange (r-o) and red (r-r) – were each applied to an art canvas measuring 61 cm by 76 cm. The spectral reflectance factor for each of the dry paint colours was measured with a Konica Minolta CM-2600d spectrophotometer. The reflectance of each of the paint colours is shown in figure 3.

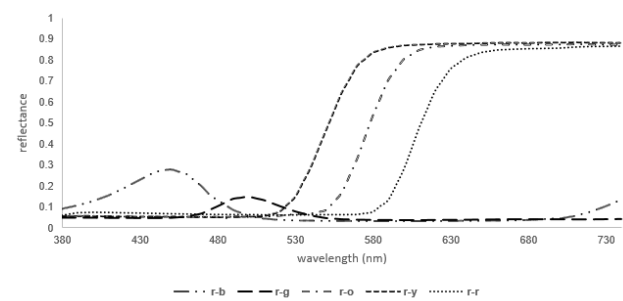


Figure 3 – Reflectance as a function of wavelength for the five paint colours.

Iterative calculations were then set up using MATLAB R2015b software. The following quantities were calculated for each paint colour and each test SPD:

ΔE^*_{ab} : a measure of the difference in appearance of a paint colour when illuminated by the incandescent reference illuminant and the test SPD, calculated in CIE 1976 $L^*a^*b^*$.

dC^*_{ab} : the difference in chroma for the paint colour when illuminated by the reference illuminant and the test SPD. Unlike ΔC^*_{ab} , which is unsigned, this quantity had a positive value when the paint colour had a higher chroma under the test SPD than under the reference illuminance and a negative value when it had a lower chroma under the test SPD. The research aimed to achieve a dC^*_{ab} of $\geq +5.0$, but < 6.0 , as this was considered to be a reasonable increase in chroma, whilst achieving a reduction in absorption and energy. The increase in chroma was independent of illuminance.

Energy Consumption: the energy consumption of the test SPD was compared to that of the reference illuminant when illuminating a specific paint colour. The peak of the test SPD was scaled so that each paint sample would maintain the same luminance (total amount of reflected light) when illuminated by the test SPD and reference illuminant.

Light Absorption: the absorption of light for each paint colour illuminated with the reference illuminant and test SPD was assessed and compared. This quantity was scaled such that reference illuminant illuminating a given paint colour had an absorption level of 1. To achieve the goals of this study, the test SPD was required provide a reduction in absorption.

Three sets of computational simulations were performed for each of the paint colours.

SIMULATION (S1)

The first simulation involved the use of a two-peak test SPD with power emitted at only two wavelengths, with no additional bandwidth. The calculations considered all combinations of wavelengths in the 380 nm to 740 nm range. For example, the colorimetric and energy quantities were calculated for a test SPD comprised of two 'starting points', 380 nm and 381 nm. Then, the same quantities were calculated when the test SPD was comprised of power at 380 nm and 382 nm, then 380 nm and 383 nm, and so on. This sequence continued until all combinations were exhausted. Whilst providing promising results, the results from S1 could be further improved by including additional characteristics to the test SPDs.

SIMULATION (S2)

The second set of computational simulations elaborated on the first in that a single wavelength was added to each of the 'starting points' (SP), creating larger bandwidths for the test SPD. Throughout the simulations, the bandwidth was increased towards the edges of the visible spectrum (with limitations set between 380 nm and 740 nm).

The results from S1 were analysed and promising start point wavelengths were identified for use in S2. If the starting points of 435 nm and 566 nm are taken as an example, each with an initial bandwidth (BW) of 1 nm, the following set of calculations simulate test SPD with 435 nm SP1, 3 nm BW, 566 nm SP2, 1 nm BW. The bandwidth would continue increasing for the first starting point, while the second remained constant, until all options were exhausted. Then, the first starting point and bandwidth would remain constant while the second bandwidth would iteratively increase. Once the bandwidth of the second starting point had reached its limitations, the both starting points would begin with a BW of 3 nm and the sequence would repeat. After analysing the results, it was determined that a further set of calculations would be undertaken, which allowed for the relative peak power of the two spectral peaks to differ from one another.

SIMULATION (S3)

The additional element of relative peak intensity (RPI), where spectral peaks can essentially be 'dimmed', was added. It was set such that a value of 1 = 100 % or maximum output. Reductions could occur in three levels: 0,7 (70 %), 0,4 (40 %) and 0,1 (10 %). This further complicated the simulation process, as the test SPDs now took into account the RPI variations available. Thus, revisiting the starting points of 435 nm and 566 nm, the simulations were performed as follows – 435 nm SP1, 1 nm BW, 1 RPI, 566 nm SP2, 1 nm BW, 0.1 RPI. This sequence would continue, with the starting points and bandwidths remaining constant

until all RPI combinations were exhausted. The simulations then followed the procedure outlined in S2 whilst taking into account RPI combinations. The starting points for S3 were entered manually, and were based on the best-case scenario SPDs obtained from S2.

The computational simulations for S2 and S3 involved modifying the starting points in 10 nm intervals (± 10 nm) in order to minimise calculation time and optimise the results. Final results were taken once further modification of the starting points resulted in less favourable outcomes than the previous 'best' scenario. This was performed for each of the five paint colours.

7 Results & Discussion

Numerous test SPDs (formulated per S3 methods) were analysed for each test paint colour. The optimal custom SPD test illuminant for each of the paint colours is outlined in table 2, for each of the paint colours assessed.

Table 2 – Custom SPD Test Illuminant

Test SPD	Paint Colour	SP1 (nm)	BW (nm)	RPI	SP2 (nm)	BW (nm)	RPI
Sp-b	Blue	425	7	0.7	572	39	0.4
Sp-g	Green	435	5	0.4	566	75	0.1
Sp-y	Yellow	495	35	1	599	77	0.7
Sp-o	Orange	500	41	1	608	61	0.7
Sp-r	Red	490	29	1	612	101	0.7

The optimal test SPDs are shown in figure 4.

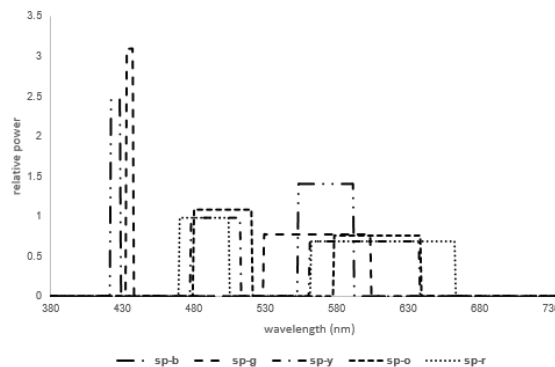


Figure 4 – Power as a function of wavelength for optimised test SPDs.

The increase in chroma, reduction in energy consumption and reduction in absorption of light each of the custom test SPDs, when compared to the reference illuminant, are outlined in table 3. The results indicate that the SPDs of light sources can indeed be customised so that they yield the desired colour appearance of illuminated objects and reduce the damage inflicted on pigments by reducing the amount of light absorbed.

7.1 Optimised SPDs

Part of this research aimed to not only to match the appearance of the paint colours under the reference illuminant, but to also improve it by inducing an increase in chroma.

As shown in figure 5, the spectral reflectance factor of the green paint (r-g) has an incline in reflectance between approximately 450 nm and 550 nm, with a clearly defined peak at 500 nm. In comparison, the SPD of the incandescent reference illuminant shows an increase in radiant power beyond 550 nm. As such, due to the spectral characteristics of both the pigment and the light source, the majority of the power of the reference illuminant is absorbed.

Table 3 – Colorimetric and energy results for optimised test SPDs.

Test SPD	Energy Consumption (%)	ΔE^*_{ab}	dC^*_{ab}	$\Delta E^*_{ab} - dC^*_{ab}$	Light Absorption
Sp-b	44.8	5.49	+5.33	0.16	0.44
Sp-g	45.7	5.42	+5.07	0.35	0.46
Sp-y	54.3	5.49	+5.06	0.43	0.90
Sp-o	56.7	5.97	+5.09	0.88	0.94
Sp-r	60.7	5.98	+5.19	0.79	0.89

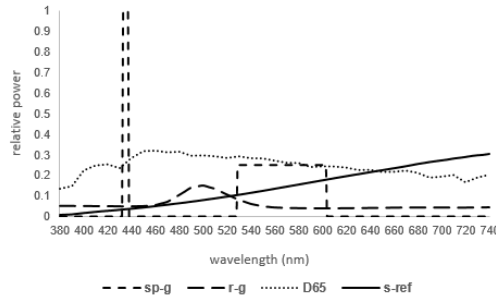


Figure 5 – Reflectance as a function of wavelength for the green (r-g) paint colour (long dashed line). Power as a function of wavelength for the reference incandescent (s-ref) illuminant (solid line), D65 illuminant (dotted line) and optimal test SPD (short dashed line). All three SPDs were normalised to the peak of the test SPD.

In contrast, the D65 illuminant (daylight) is a broad spectrum light source and would render the pigment colour well and increase the sense of colourfulness. However, such a source would prove to be highly damaging. Thus, the custom test SPD for the green paint colour (sp-g) consists of two relatively narrow peaks and is not spectrally broad. It also allows for an increase in chroma ($dC^*_{ab} = +5.07$). Whilst shorter wavelengths have the capacity to impart greater damage, photochemical action is not limited to any one part of the visible spectrum – all wavelengths of light cause damage to artwork. Thus, a narrow band light source, leading to a reduction in overall radiant exposure – as demonstrated by sp-g – provides a distinct conservation advantage in that the net damage is reduced.

7.2 Chroma

Lighting in museum exhibits is currently limited to 50 lx for highly and moderately sensitive artworks. An increase in illuminance would most certainly assist in the appearance of colourfulness in museum artefacts. However, this would result in an increase in damage and is not recommended by conservation guidelines. The customised test SPDs allow for increases in chroma in the appearance of paint colours, without an increase in illuminance. This would provide an increase in perceived brightness, without having to increase illuminance levels. This could be a desirable characteristic in museum environments, as it compensates for the reduced colour discrimination of the human visual system in low light conditions. This also allows for the artwork to appear more as it would under daylight, working towards meeting the artists' original intent.

The CIE 1976 $L^*a^*b^*$ values were determined for the paint colours under both the reference illuminant and test SPD. These values were then used to determine the C^*_{ab} values, and subsequently the dC^*_{ab} , with the desired result being a positive increase in chroma. It is evident from Hunt's results [12] that chromatic saturation increases with illuminance. Further to that, there is considerable difference between the appearance of colour under daylight conditions and when illuminated at 42 lx. This experiment aimed at something in between these two extremes, as demonstrated in figure 6 for the blue paint colour (r-b). Point A in figure 6 shows the CIE 1976 a^*b^* coordinates for the blue paint colour under the reference illuminant ($a^* = 7.40$, $b^* = -49.49$) and point B shows the paint colour under the test SPD sp-b ($a^* = 18.73$, $b^* = -53.52$).

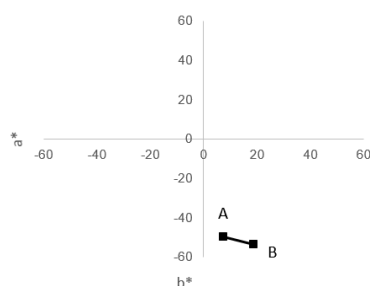


Figure 6 – Two-dimensional CIE 1976 a^*b^* plot for the blue paint colour (r-b). Point A corresponds to illumination by the incandescent reference illuminant and point B corresponds to illumination by the optimised test SPD.

7.3 Energy Consumption

The custom test SPDs simulated in this research, outlined in table 2 and figure 4, each provide considerable energy savings when illuminating their respective paint colours. Savings in energy ranged from 39,3 % to 55,1 %, relative to the incandescent reference illuminant. This can be attributed to the reduction in absorbed light.

7.4 Absorption

The amount of light absorbed by the samples from the test SPDs was measured relative to the amount of light that would be absorbed by the samples when lit by the reference illuminant. Since the reference illuminant absorption was set to a value of 1,0, a value of 0,44 by the test SPD means that the paint colour would absorb only 44 % of the light that it would when illuminated by the reference illuminant, providing a 56 % reduction in light absorption. Absorption values ranged from 44 % to 95 % and are outlined in table 2.

7.5 Practical Applications

The practical application of customised SPDs in museum applications would likely be motivated by the topics discussed thus far – reductions in energy consumption, reductions in absorbed light and enhanced chroma. However, this could lead to further advantages and opportunities for improvement in the display of museum artefacts.

7.5.1 Duration of Exposure

Guidelines set by the CIE recommend a limit on the cumulative lux-hours (lx-hr/yr) that an artwork should be exposed to, based on the principle of reciprocity. When applied to the lx-hr/yr guideline set, an object illuminated at 1000 lx of radiation for one hour is equal to that same object illuminated at 10 lx for 100 hours, provided the SPD of the light source remains constant. This concept provides obvious advantages for museum installations, whereby display times per day can be decreased to allow for more days in a given year that the artwork can be viewed. However, if the light source were to increase the chroma of the pigment – as the custom test SPDs do – this will also result in an increase in apparent brightness, whilst maintaining illuminance. This provides further options. For artworks of high sensitivity, but not in critical condition, the increased chroma and apparent brightness could simply remain as a benefit to the viewer. However, if there is a desire to display the artwork for longer periods of time, the illuminance levels could be reduced to compensate for the increased levels of apparent brightness.

7.5.2 Colour Group SPD

When the custom test SPDs in figure 4 are further analysed, it can be seen that sp-b and sp-g are similar in start points, bandwidths and relative peak values, as are sp-y, sp-o and sp-r. This leads to the conclusion that further research could be conducted to develop custom light sources with SPDs specific for optimising the appearance of an entire colour group. For example, a light source with a specific SPD could be used for pigments in the entire blue and green region family, whilst a different light source would be used for the yellow, orange and red region of the palette.

7.5.3 Improve Appearance of Damaged Artwork

Vienot, Coron & Lavedrine (2011) demonstrated that customised SPDs could be used to enhance faded colours. Although this was accomplished by developing a test illuminant that increased the chroma of the pigment, the damaging effects of the new light source were not discussed. The custom test SPDs presented here increase chroma by at least 5 units. This results in a significant increase in the appearance of chroma of each paint pigment, as shown in figure 6. However, in addition to the increase in chroma, the custom illuminants also allow for a reduction in absorption of light and thus damage.

8 Conclusion

This research aimed to simulate custom SPD light sources, which not only meet current CIE guidelines, but also provide an improvement in the appearance of chroma, reduction of energy consumption and reduction of absorption of light by paint pigments. The results demonstrate that two-peak narrow SPD light sources can be developed that result in improved colour appearance of an artwork by increasing the chroma of a pigment. Furthermore, the custom test SPDs were found to provide a reduction in both energy consumption and absorption of light, when compared to the reference illuminant.

References

- BERNS, R, 2010. Designing white-light LED lighting for the display of art: A feasibility study. *Colour: research and application*, volume 36, issue 5, 324-334.
- CHALMERS, A.N, CUTTLE, C, VAN RYN, R 2006. An experimental illuminator for museum conservation lighting. *Australian Optical Society*, 10, 152.
- CIE 2004. CIE 157:2004. Control of damage to museum objects by optical radiation. *International Commission on Illumination*
- CUTTLE, C, 2000. A proposal to reduce the exposure to light of museum objects without reducing illuminance or the level of visual satisfaction of museum visitors. *JAI*, 39, 229-244
- DELGADO, M, DIRK, D.W, DRUZIK, J, WESTFALL, N 2010. Lighting the world's treasures: Approaches to safer museum lighting. *Color research and application*, volume 36, issue 4, 238-254.
- DORMUS, D, DAVIS, D 2015. Optimising light source spectrum for object reflectance. *Optical society of America*, volume 23, issue 11
- FELLER, R.L, 2009. Control of deteriorating effects of light upon museum objects. *Museum International*, volume 17, issue 2, 57-98
- HUNT, R.W.G, 1977. The specification of colour appearance .II. Effects of changes in viewing conditions, volume 2, issue 3
- SAUNDERS, D, KIRBY, J 1994. Wavelength-dependent fading of artists' pigments. *Maney Online*, volume 39, issue 2, 190-194.
- THOMPSON, G, 1967. Annual exposure to light within museums, volume 12, issue 1, 26-36
- THORNTON, W.A, 1975. The high visual efficiency of prime colour lamps. *Lighting Design Application*, Volume 5, 35-41.
- VIENOT, F, 2009. Kruithof's rule revisited using LED illumination. *Journal of Modern Optics*, volume 56, issue 13, 1433-1446.
- VIENOT, F, CORON, G, BERTRAND, L 2011. LEDs as a tool to enhance faded colours of museum artefacts. *Journal of Cultural Heritage*, volume 12, 431-440.